Sun-Earth-Man

a Mesh of Cosmic Oscillations

HOW PLANETS REGULATE SOLAR ERUPTIONS, GEOMAGNETIC STORMS, CONDITIONS OF LIFE, AND ECONOMIC CYCLES

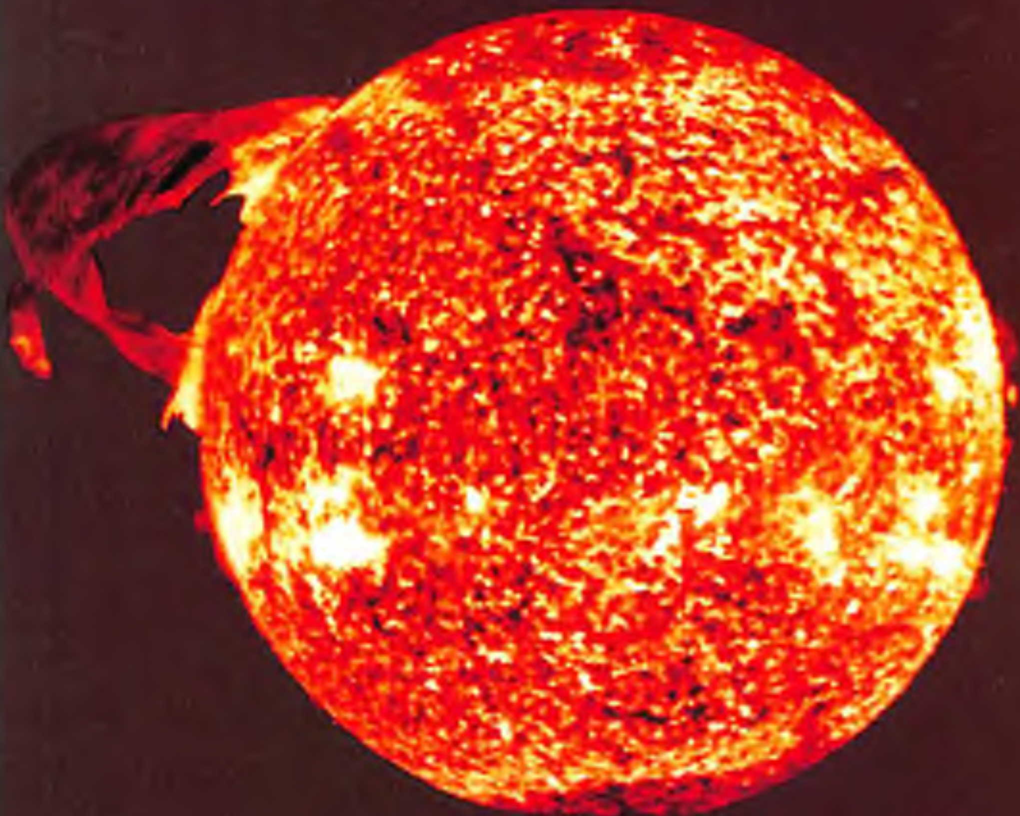

EODOR LANDSCHEIDT

URANIA TRUST

Front Cover shows a gargantuan solar prominence. It is reproduced by kind permission of the Armagh Planetarium and NASA.

Back Cover shows the Mandelbrot set as elaborated by H. O. Peitgen and P. H. Richter in *The Beauty of Fractals – Images of Complex Systems*.

Sun-Earth-Man: a Mesh of Cosmic Oscillations

HOW PLANETS REGULATE SOLAR ERUPTIONS, GEOMAGNETIC STORMS, CONDITIONS OF LIFE, AND ECONOMIC CYCLES

by
THEODOR LANDSCHEIDT
Belle Côte, Nova Scotia, Canada B0E 1C0

URANIA TRUST

First published 1989

Published by the Urania Trust,
396 Caledonian Road, London, N1 1DN England.

Typeset by Mike Kelly Photosetting
Biddestone, Wiltshire.
Printed and Bound by
Butler & Tanner Limited
Frome, Somerset.

ISBN 1–871989–00–0

CONTENTS

VITA THEODOR LANDSCHEIDT

Theodor Landscheidt was born in Bremen in 1927. He studied philosophy, law, and natural sciences at the University of Goettingen where he earned his doctorate. He was, until his recent retirement, a West German High Court judge. He is the Director of the Schroeter Institute for Research in Cycles of Solar Activity, and is on the board of directors of the International Committee for Research in Environmental Factors at the Free University of Brussels. He has been elected a member of various German academies and of the American Geophysical Union.

Since 1974 Landscheidt has made long-range forecasts of energetic solar eruptions and geomagnetic storms. When checked by astronomers and by the Space Environment Services Centre, Boulder, Colorado, his predictions have been shown to have a quality better than 90%. He successfully forcast the end of the Sahelian drought and has correctly identified the turning points in various economic cycles.

Special publictions dealing with research in cycles:

Landscheidt, T. (1976): Beziehungen zwischen der Sonnenaktivitaet und dem Massenzentrum des Sonnensystems, Nachrichten der Olbers-Gesellschaft 100, 2–19

Landscheidt, T. (1980): Saekularer Tiefpunkt der Sonnenaktivitaet, Ursache einer Kaelteperiode um das Jahr 2000?, Jahrb. d. Wittheit zu Bremen 24, 189–220

Landscheidt, T. (1981): Swinging Sun, 79-Year Cycle, and Climatic Change, J. interdisc. Cycle Res. 12, 3–19

Landscheidt, T. (1983): Solar Oscillations, Sunspot Cycles, and Climatic Change, in McCormac, B. M., ed.: Weather and Climate Responses to Solar Variations, Colorado Associated University Press, Boulder, pp. 293–308

Landscheidt, T. (1984): Cycles of Solar Flares and Weather, in Moerner, N. A. and Karlèn, W., eds.: Climatic Changes on a Yearly to Millenial Basis, D. Reidel Publishing Company, Dordrecht, pp. 473–481

Landscheidt, T. (1984): Funktionen kosmischer Organismen: Schwingungen der Sonne und irdische Resonanzen, in Resch, A., ed.: Geheime Mächte, Andreas Resch Verlag, Innsbruck, pp. 37–130

Landscheidt, T. (1986): Long Range Forecast of Energetic X-Ray Bursts Based on Cycles of Flares, in Simon, P. A., Heckman, G., and Shea, M. A., eds.: Solar-Terrestrial Predictions: Proceedings of a Workshop at Meudon, France, June 18–22, 1984, National Oceanic and Atmospheric Adminstration, Boulder, pp. 81–89

Landscheidt, T. (1986): Long Range Forcast of Sunspot Cycles, in Simon, Heckman, and Shea, pp. 48–57

Landscheidt, T. (1986): Cyclic Distribution of Energetic X-Ray Flares, Solar Physics 107, 195-199

Landscheidt, T. (1987): Wir sind Kinder des Lichts – Kosmisches Bewusstsein als Quelle der Lebensbejahung, Verlag Herder Freiburg, Basel, Wien

Landscheidt, T. (1987): Long Range forecasts of Solar Cycles and Climatic Change, in Rampino, M. R., Sanders, J. E., Newman, W. S., and Koenigsson, L. K., eds.: Climate History, Periodicity, and Predictability, van Nostrand Reinhold Company, New York, pp. 421–445

Landscheidt, T. (1988): Solar Rotation, Impulses of the Torque in the Sun's Motion, and Climatic Variation, in press for Climatic Change.

I. INTRODUCTION

The mass-man of our age, so aptly described by José Ortega y Gasset in "The Revolt of the Masses", is dominated by the principles of mechanistic materialism. This anachronistic view of life was au fait with the world view of the exponents of science in the 19th century which looked at the universe as a mechanical device, an assembly of separable parts subject to local effects caused by local interaction. Meanwhile, the avant-garde of scientists has overthrown these local theories that split the world into separated parts which can only be influenced by their immediate environment. The new interpretation of the Einstein-Rosen-Podolsky paradox and the violation of the Bell inequality provide irrefutable evidence of the inseparability and non-locality of the fundamental processes in the universe.[1] This epochal achievement in the history of human knowledge has not yet been valued appropriately. There are even scientists that have never heard of Bell's theorem and those sophisticated experiments that prove its violation. All experts, however, agree on its paramount importance in the history of science.[2]

The unanimous message of mystics of all ages that all entities in the universe are interconnected and constitute an indivisible whole [3] is proven now by unequivocal physical experiments that have been replicated again and again.[4] From this undeniable unity, connectedness, and inseparability follows that any action or configuration in any distant part of the universe can influence processes in the solar system inhabited by man. This is also valid for the interrelations of Sun and planets within the solar system and especially the Earth's connections with other cosmic bodies in the solar system environment.

To look at the solar system and its constituent parts as a whole that embraces a complex web of holistic interrelations, is a premise of traditional astrology, which seemed antiquated, but turns out to be trend-setting. Thus, it appears promising to subject the astrological thesis of an influence of celestial bodies on the Earth and life on its surface to a new test. The quality of the astrological body of theses matches the holistic results of modern research, as it represents the archetype of an integrating science. Astrology of this brand was a historical reality in the era of Kepler, Galileo and Newton. It is well known that Kepler was both an astrologer and one of the creative founders of modern science. Book IV of his principle work "Harmonics Mundi" with the heading "Book on Metaphysics, Psychology, and Astrology" is evidence of this, as well as his papers "De fundamentis astrologiae certioribus" and "De stella nova". Those who pretend that Kepler was not really engaged in astrology should read these writings.

Galileo, the other master scientist, was also an astrologer. Figure 1 from Owen Gingerich[5] shows on top a drawing of the Moon made by Galileo after his construction of an astronomical telescope in 1609. On the same page is the start of a horoscope he cast for Cosimo II di Medici. This concurrence is typical of the holistic approach of Kepler and Galileo. They did not talk about interdisciplinary research,they lived it. Kepler was not only an astronomer and astrologer, but also a meteorologist, mathematician, harmonist, philosopher,

Figure 1: Evidence of Galileo's interdisciplinary work uniting astronomy and astrology: on the same page a drawing of the Moon oberserved by means of Galileo's new astronomical telescope and the start of a horoscope he cast for Cosimo II di Medici.

theologian, and mystic. Newton, last but not least in this trinity of creative scientists, wrote much more papers on alchemy, theology, and metaphysics than on physics and mathematics.[6] In hundreds of nights, spent in his unhealthy alchemic laboratory, he searched for the noumenal light, bearer of life and mind, quite different from the phenomenal light he dealt with in his optics.[7] Kepler, Galileo, and Newton integrated the knowledge of their age. This was a necessary condition of their creativity.

In our days, astrologers and scientists do not live up to their great predecessors who initiated a new age in science. There are few exponents who coalesce astrological views and modern scientific knowledge to create new paradigms. Most scientists do not realize that their findings confirm fundamental astrological ideas, and most astrologers do not see that creative scientists transgress the frontiers of traditional astrological knowledge. In our time, astrology's faculty to integrate diverging fields of knowledge is merely a dormant potentiality. Faint-hearted astrologers timidly defend the old saying "as above, so below" in reducing it to a mere analogy, whereas scientists like the dynamic systems theorist Erich Jantsch[8] and the Nobel-prize recipient Ilya Prigogine[9] boldly claim that there is interdependent coevolution of microcosmic and macrocosmic structures regulated by homologous principles which go back to common cosmic roots that converge in the cosmic-egg phase of our universe. Even Operations research, a rather practical field of knowledge, follows the basic rule that the behaviour of any part of a system has some effect on the system as a whole. The application of such rules, however, is restricted to the narrow limits of human activity in society, technology, and economy. Scientists lack the boldness of astrological imagination that could stimulate a projection of basic insights upon the dimensions of the solar system, the realm of Sun, Earth, and planets that induced creative ideas in Kepler, Galileo, and Newton. The result of the experiments suggested by Bell's theorem begs for a new synthesis that integrates fundamental astrological ideas and modern scientific knowledge.

Thus, let us try such a new kind of genuine interdisciplinary approach. It will yield intriguing results which show that Sun and planets function like an intricate organism regulated by complex feed-back loops. The Sun that makes the planets revolve around its huge body, is again influenced by the giant planets Jupiter, Saturn, Uranus, and Neptune that make it revolve around the common centre of mass of the solar system. This very irregular motion regulates the Sun's varying activity which again influences the planets and so on. This feed-back loop will be revealed by deciphering a kind of Rosetta stone of planetary forcing. We shall come to know how the tidal planets Mercury, Venus, Earth, and Jupiter and the giant planets cooperate in regulating or modulating essential features of the Sun's activity: the former by special effects of tide-generating forces and the latter via the Sun's oscillations about the centre of mass. And Jupiter, this massive planet just below the level of a binary star, is the link between both groups; it is the only planet involved in both functions, thus playing a central part.

Accordingly, special Jupiter configurations, that will be described in detail, prove to be related to variations in the Sun's rotation, the incidence of energetic solar eruptions, geomagnetic storms, variations in the ozone column in the

Earth's atmosphere, rainfall, temperature, rise and fall in animal populations, economic cycles, interest rates, stock prices, variations in the gross national product, phases of general instability, and even historical periods of radical change and revolution. In addition, consecutive Jupiter configurations constitute long-term cycles the harmonics of which point to short-term cycles that appear in various time series of solar-terrestrial events. The most significant harmonics form ratios that reflect consonances and even the major perfect chord in musical harmony. This new precise realization of the Keplerian "music of the spheres" makes it possible to "compose" predictions of the Sun's activity and its terrestrial response. Such forecasts have been checked by scientific institutions and reached a high level of reliability. Details of these data will be presented as well as the foundations on which they are based , so that the reader can judge for himself the dependability of the new results.

II. EXAMPLE AVAILS TEN TIMES MORE THAN PRECEPT

Samuel Smiles was convinced that example is one of the most potent of instructors, though it teaches without a tongue. Here is such an example which demonstrates the fertility of a new kind of multidisciplinary approach that integrates mathematical, physical, astronomical, biological, economical, psychological, sociological, harmonical, and astrological knowledge in a simple, but enlightening way and thus reflects the unity and connectedness of our world as proven by the violation of Bell's inequality therom:

1. FEED-BACK LOOPS, AN ARCHETYPE OF MORHOGENESIS

It has been mentioned already that Sun and planets form complex feed-back loops. Figure 2, the lithograph Drawing Hands by Maurits Cornelis Escher, is a representation of such feed-back systems. A left hand draws a right hand, while at the same time a right hand draws a left hand. Levels which are ordinarily seen as hierarchical – that which draws and that which is drawn – turn back on each other, creating a tangled hierarchy. According to Douglas Hofstadter[10] such strange loops are at the core of creativity. The solar system, too, embodies feed-back loops of this kind: The Sun, the central body and main force in the system, looked at as being in a higher hierarchical position, is in its turn influenced by the seemingly inferior planets that make it oscillate around the common centre of mass and regulate its varying activity, which again influences the planets etc. As the planet Earth and its complex surface features are also involved in this cyclic entanglement of feed-back loops, the yield of these intricate processes is beyond imagination. Even human creativity seems to be involved. Enlightenment in artists, scientists, or mystics that manifests itself in acts of creation concurs with solar light emanations released by energetic solar eruptions.

This may seem inconceivable to some readers, but seemingly simple dynamic systems that comprise loops or cycles do not necessarily possess simple dynamic properties. Even extremely simple mathematical models of non-linear dynamic feed-back systems provide surprising evidence of unfathomable structural complexity. Take an initial number, the seed, square it and add a constant. Feed the result, the output, back into this functional process as new input. Do this over and over again to see if some pattern emerges. The respective output values, when plotted in the plane of complex numbers, reveal the existence of so-called "attractors" that reign over separate domains into which they attract special output. Such attractors at zero and infinity, for instance, could represent the polar tension created by the antagonistic qualities concentration and dissipation. Surprisingly, this discloses a hidden connection between feed-back loops or similar cyclic features and centres of polar tension diametrically opposite in nature. At the boundary between the realms of competing attractors, where their influence approaches zero as a limit, wonders of creativity emerge, patterns delicately poised between order and chaos. Computers can be converted into a kind of microscope for viewing such boundaries. Figure 3 shows an example of a microscopic boundary pattern made visible by H. O. Peitgen and P. H.

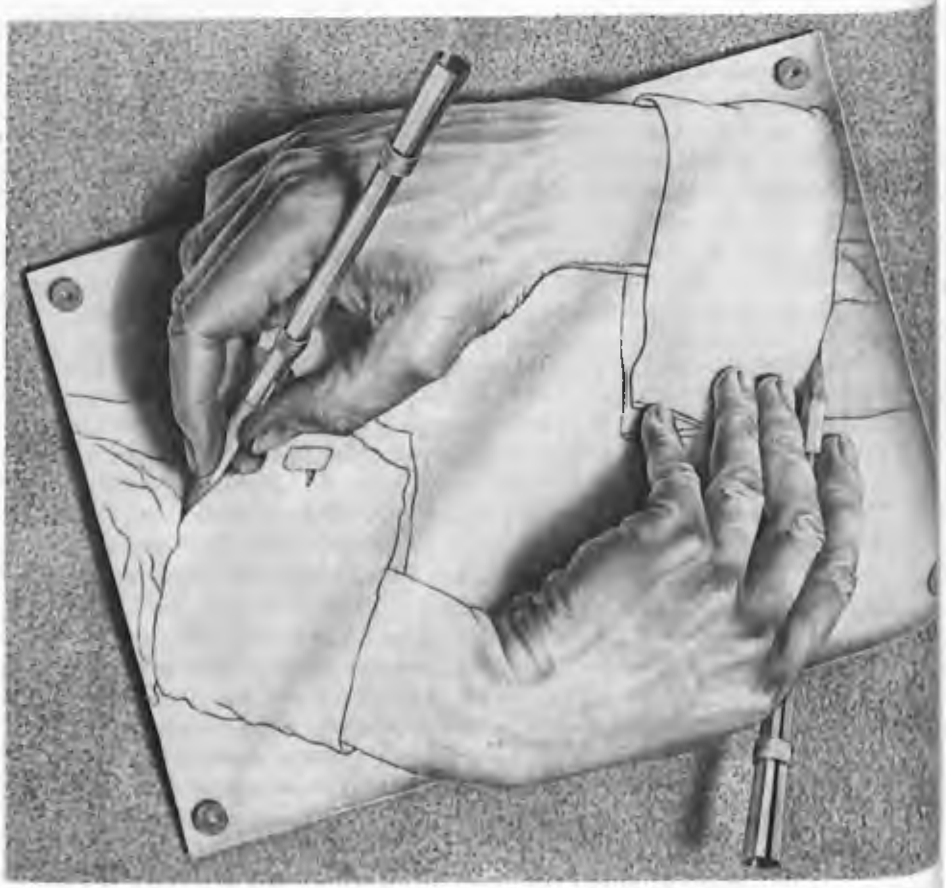

Figure 2: The lithograph "Drawing Hands" by Maurits Cornelis Escher – a representation of "strange loops" which according to D. Hofstadter create a tangled hierarchy. The Sun and the planets embody such a feed-back system.

Richter.[11] Mathematically expressed, it is a Julia set; Peitgen and Richter call it seahorse tail. It winds down and down, going on forever. There is infinite regression of detail. The large tail encompasses complete smaller seahorses that show different features, thus representing a wealth of explicit forms.

One of the peculiar things about the boundary is its self-similarity. If we look at any one of the fractal corners or bays, we notice that the same shape is found at another place in another size. An arbitrary piece of the boundary contains all the essential structure of the whole boundary. The boundary is invariant under this transformation.[12] This mathematical theorem was expressed by Gaston Julia and Pierre Fatou as early as 1919. It supports an astrological thesis, the dictum of the Emerald Tablet: "*Quod est inferius, est sicut quod est superius. Et quod est superius, est sicut quod est inferius, ad perpetranda miracula rei unius*": As below, so above, as above, so below; this accomplishes the wonders of oneness.

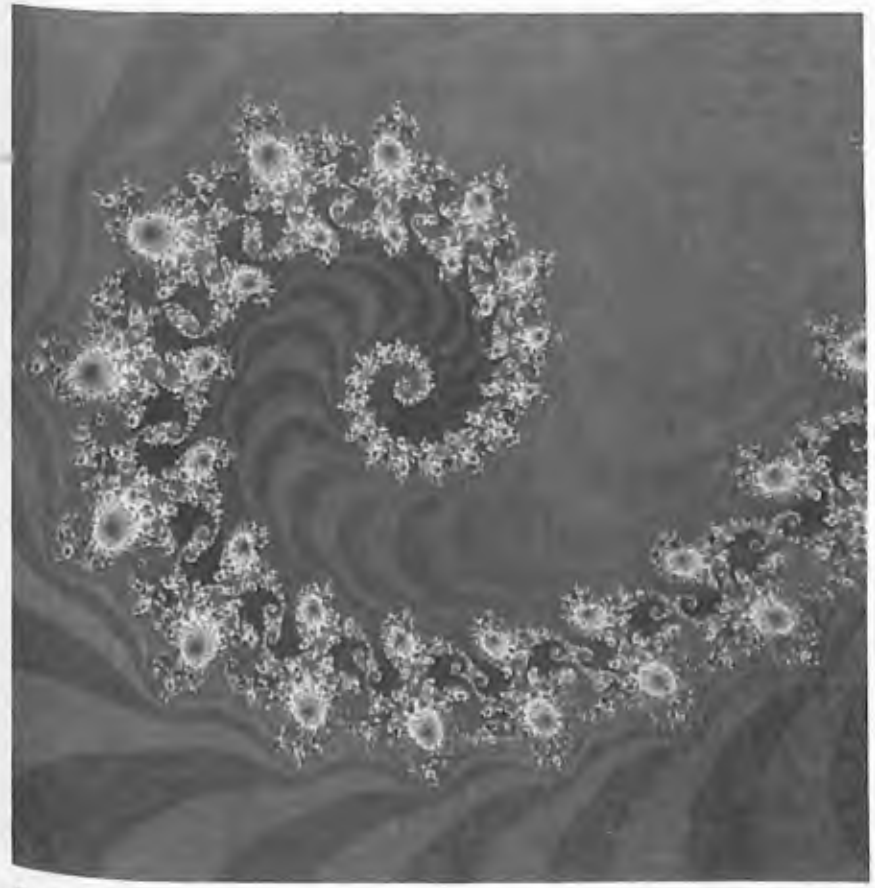

Figure 3: Boundary pattern, called Julia set, elaborated by H. O. Peitgen and P. H. Richter. Julia sets carry incredibly complex dynamics emerging from boundaries between domains of antagonistic attractors that compete for influence. In border regions with polar tension transition from one form of existence to another takes place: from order to disorder, magnetic to non-magnetic state, or however the opposite entities are to be interpreted that meet at the boundary.

At the core of those creative patterns that grow out of the boundary region there exists a central form that represents the implicit order as we find it in cell nuclei. Zooming in for a close computer look discloses it. It is shown in Figure 4 elaborated by Peitgen and Richter.[13] Mathematicians call it Mandelbrot set after its discoverer. It regulates the form of Julia sets and thus may be considered as a pre-image of central regulation. The proportions of the Mandelbrot set provide a wealth of clues to musical harmony including the major perfect chord. It will be shown in a later chapter that even the ratios of harmonics of cosmic cycles are precisely reflected in this core structure. There is mathematical proof that all Mandelbrot sets that emerge in the universe of the complex plane are interconnected, though there is an infinity of them. Everything is held together by extremely thin lines. Thus the infinite set of Mandelbrot sets may viewed as a pre-image of the unity of all core structures in the universe, a special reflection of the wholeness of the universe proved by the violation of the Bell inequality.

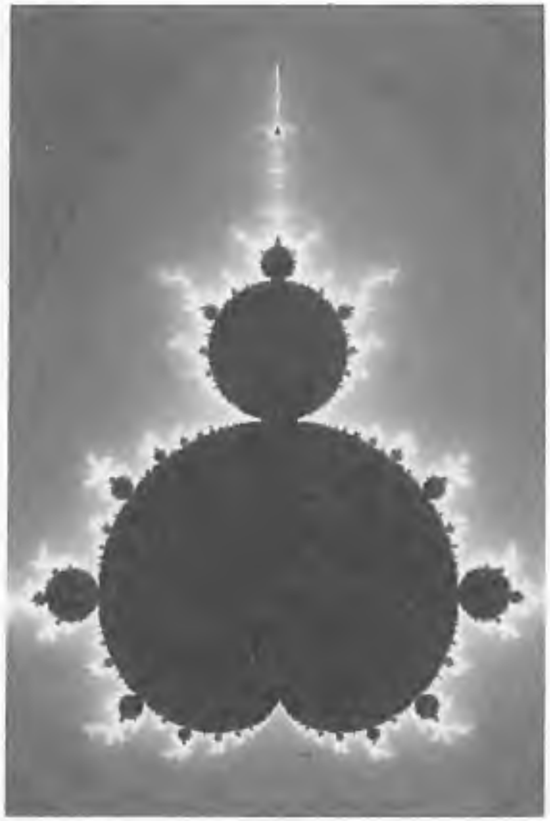

Figure 4: Mandelbrot set, elaborated by H. O. Peitgen and P. H. Richter, which controls the structure of a wealth of diverse Julia sets. According to Peitgen and Richter it reminds of the genetic organisation in higher organisms. Its proportions express consonant intervals in musical harmony and the major perfect chord.

2. THE HALLMARK OF ALL BORDERLINE PHENOMENA: INSTABILITY AND ABUNDANCE OF FORMS

Those boundaries that separate the realms of antagonistic attractors that compete for influence are a model of reality. They represent the qualities of the phase boundary between magnetism and non-magnetism, laminar flow and turbulent flow, cyclicity and non-cyclicity, order and chaos etc. Because of its fractal character the border is infinitely long. By definition, it has infinitesimal width. Thus, its sensitivity is such that the stroke of a butterfly's wing can change the fate of macrocosmic systems, as the meteorologist E. N. Lorenz put it. This is why we do not know whether the solar system will continue to be stable or not. An infinitesimal difference in the initial conditions not accessible to calculation could lead to the dissolution of order in the planetary system. The physicist and mathematician Henri Poincaré provided evidence of this as early as the end of the 19th century.[14] A wealth of boundaries with such qualities is to be found in the solar system. This refutes the often repeated argument against astrology that the energy level of any planetary influence is much too low.

It is inherent in the conditions of emergence of boundaries that their creative potential is irresolvably linked to instability. However, it is just this instability in dissipative systems far from the state of thermodynamical equilibrium which, according to Ilya Prigogine, Hermann Haken,[15] and Erich Jantsch, can lead to a spontaneous formation of new structures out of germs of gestalt or even out of chaos. If there is a boundary transition from one polar quality to the opposite one, instability will arise, but new patterns will emerge too. Our knowledge of the prototypal quality of boundaries can help us to judge the function of special boundary states and transitions properly. This for example, applies to zero phases in cycles, critical days in biorhythms, the boundary between consciousness and subconsciousness, the transition from waking to sleeping with its Kekule-effects, creative acts of artists, eureka moments, mystic experience, birth, death, the balance in mathematical formulae, and interdisciplinary research. Mesocosmic man lives just on the boundary between the realms of the attractors microcosmos and marcrocosmos. This explains man's instability, the dominant quality of all borderlines between chaos and order, but also the unfathomable depths of man's creativity and destructiveness. A crisis in the development of individuals or collectives is again a boundary state. The Swiss writer Max Frisch put it thus: a crisis could be productive if only the tang of catastrophe would be taken from it.

The Earth's surface and the wealth of fractal structures growing out of this small boundary region is a further example. Such spherical surfaces are most interesting. Kepler thought them to be a perfect symbol of God's creative functions. Surfaces of material spheres are phase interfaces where symmetry breaking occurs; the invariance of vertical translation relative to the surface is no longer valid.[16] New structures can emerge. The Sun's surface, too, shows such boundary qualities. It separates the realms of two competing attractors: one that represents contraction and transforms dying suns into neutron stars or even black holes, and another one that represents expansion and dissipating radiation. The borderline between these realms, the Sun's surface, shows the attributes of all boundaries: instability and a wealth of structures. The complex patterns of solar activity – sunspots, faculae, prominences, eruptions, and flares – arise from the Sun's thin, unstable surface layer. As will be shown, this surface activity is linked up with the Earth's surface activity. This is together a connection between two boundary regions in the defined sense.

It has been shown at international conferences of astronomers, geophysicists, and climatologists, but also at astrological research conferences in London, that impulses of the torque (IOT) in the Sun's irregular oscillations about the invisible centre of mass of the solar system, induced by the giant planets, regulate the incidence of energetic solar eruptions and their terrestial response.[17] Details will be given in a later chapter. Strong impulses of the torque occur when the Sun's centre, the centre of mass, and Jupiter, the weighty centre of the world of planets, are in line. These heliocentric conjunctions of Jupiter and the centre of mass again are a boundary phenomenon. They mark a zero phase in the Sun's motion about the centre of mass, in which the torque acting on the Sun reaches zero, changes sign, and shows a more or less sharp increase in the new direction. The Sun changes from approaching the centre of mass to receding from it or vice versa. Just this boundary phenomenon releases instability together with a wealth of new patterns in the Sun's surface that is followed by corresponding effects in the Earth's surface region. These terrestrial responses, that will be dealt with in detail in another chapter, range from geomagnetic storms to abundance in wild life and economic change.

3. VARIATION IN WILD LIFE ABUNDANCE, A PARADIGM OF TERRESTRIAL EFFECTS OF SOLAR SYSTEM BOUNDARY EVENTS

Now we are ready to make an interesting point in our example. Figure 5, after Edward R. Dewey,[18] shows the cyclic variation in Canadian lynx abundance for the years 1735 to 1969. The data are based on records of the offerings of lynx skins by trappers, particularly to the Hudson's Bay Company. As the efforts of trappers to earn a livelihood are fairly constant, biologists feel that the records of skin offerings constitute a rather reliable index of the abundance of lynx. The ordinate axis in Figure 5 indicates the yearly number N of offered lynx skins. Flat triangles mark the epochs of conjunctions of Jupiter with the centre of mass. These epochs show an obvious connection with extrema in the lynx abundance. The pattern, however, is rather complex. There are longer periods with epochs that coincide with peaks, as before 1789, other protracted periods with epochs that concur with troughs, as after 1867, and phase jumps from minima to maxima as before 1823 and 1867. Such phase changes appear in almost all time series of solar and terrestrial data and are thought to pose intricate questions. The first three arrows in the plot point to periods of instability resulting in phase jumps that started about 1789, 1823, and 1867. Even these periods of change show a distinct pattern: the epochs of Jupiter conjunctions on the left of the respective arrows always coincide with a maximum in lynx abundance, whereas the epoch on the right concurs with a minimum. This regular pattern of instabilities yields different results depending on whether the foregoing epochs of Jupiter conjunctions go along with maxima or minima in the time series. Only the instability event starting in 1933 resulted in a different pattern: there was no phase change, but an anomalous period with very small numbers of lynx and poor variations in the abundance.

Fortunately, our knowledge of the fundamental quality of boundaries, derived from mathematical feed-back cycles and physical phase transitions, when combined with astronomical facts and astrological imagination, enables us to explain and predict such instability events. The centre of mass of the solar system is an attractor as defined above. Hermann Haken, the founder of synergetics, a new discipline dealing with nonequilibrium phase transitions and self-organization in physics and biology, has focused attention on profound analogies between completely different systems when they pass through an instability and then build up new macroscopic spatio-temporal patterns. Haken explicitly states that the equations of celestial mechanics follow the rules of synergetics, and he stresses in addition that centres of mass of systems of astronomical bodies play an important part in nonequilibrium

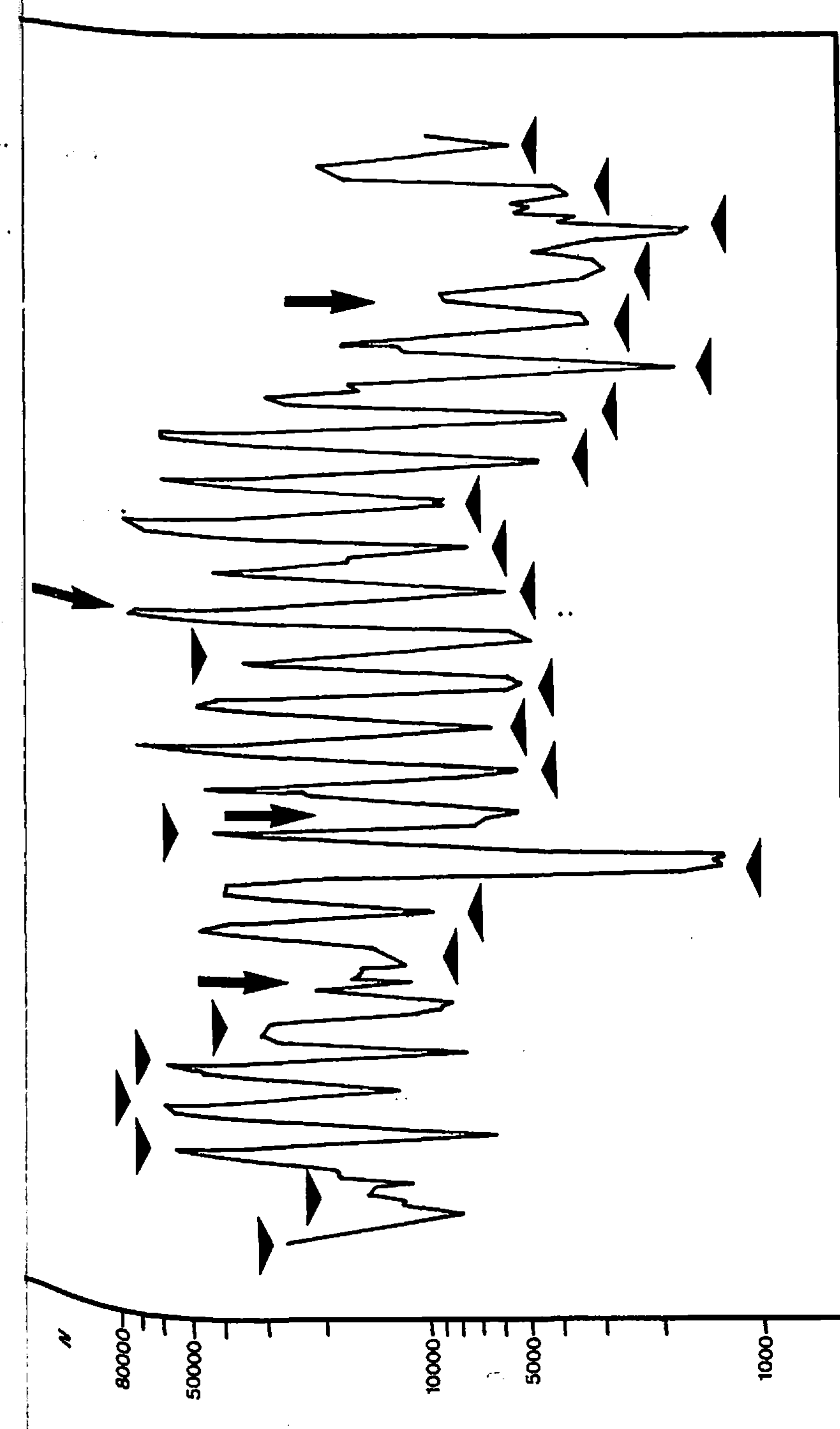

Figure 5: Cyclic variation in Canadian lynx abundance for the years 1735 to 1969. The ordinate axis indicates the yearly number N of offered lynx skins. Flat triangles mark the epochs of special configurations when the Sun's centre, the centre of mass of the solar system (CM) and the giant planet Jupiter are in line (Jupiter-CM conjunctions). These epochs are related to extrema in the lynx abundance. The phase pattern of this relationship or major anomalies in the distribution depend on major solar instability events the starting epochs of which (1789, 1823, 1867, and 1933) are designated by arrows. Major instability events occur when the centre of mass, an attractor, remains for years in or near the Sun's surface, a boundary region.

phase transitions as they act as order parameters that function like attractors.[19] As has been shown already, the Sun's surface is a boundary in terms of the morphology of nonlinear dynamic systems. Thus, it makes sense that the major instability events starting about 1789, 1823, and 1867, and later about 1933 and 1968, occurred just when the centre of mass remained in or near the Sun's surface for several years.

When the Sun approaches the centre of mass (CM), or recedes from it, there is a phase when CM passes through the Sun's surface. Usually, this is a fast passage, as the line of motion is steeply inclined to the surface. There are rare instances, however, when the inclination is very weak, CM runs nearly parallel with the Sun's surface, or oscillates about it so that CM remains near the surface for several years. Fixing the epochs of start and end of such periods involves some arbitrariness. The following definition is in accordance with observation and meets all requirements of practice: major solar instability events occur when the centre of mass remains continually within the range 0.9 — 1.1 solar radii for 2.5 to 8.5 years, and additionally within the range 0.8 — 1.2 solar radii for 5.5 to 10 years. The giant planet Jupiter is again involved. In most cases major instability events are released when Jupiter is stationary near CM.

The first, sharper criterion yields the following periods:

1789.7 — 1793.1	(3.4 yr)
1823.6 — 1828.4	(4.8 yr)
1867.6 — 1870.2	(2.6 yr)
1933.8 — 1937.3	(3.5 yr)
1968.4 — 1972.6	(4.2 yr)
2002.8 — 2011.0	(8.3 yr)

The first decimal is only given to relate the results rather exactly to the criterion. The epochs of the onset and the end of the phenomenon cannot be assessed with such precision. The second, weaker criterion yields periods which begin earlier:

1784.7 — 1794.0	(9.3 yr)
1823.0 — 1832.8	(9.8 yr)
1864.5 — 1870.9	(6.4 yr)
1932.5 — 1938.3	(5.8 yr)
1967.3 — 1973.3	(6.0 yr)
2002.2 — 2011.8	(9.6 yr)

Henceforth, the starting periods 1789, 1823 etc. of the first criterion will be quoted.

In case of major instability events that affect the Sun's surface and the incidence of features of solar activity displaying in this thin, sensitive layer, the instability seems to spread out in the planetary system and seize all events in time series that are connected with the Sun's activity. The instability pattern in the abundance of lynx is only one example of this effect. The rhythm induced by Jupiter conjunctions with the centre of mass, however, does not

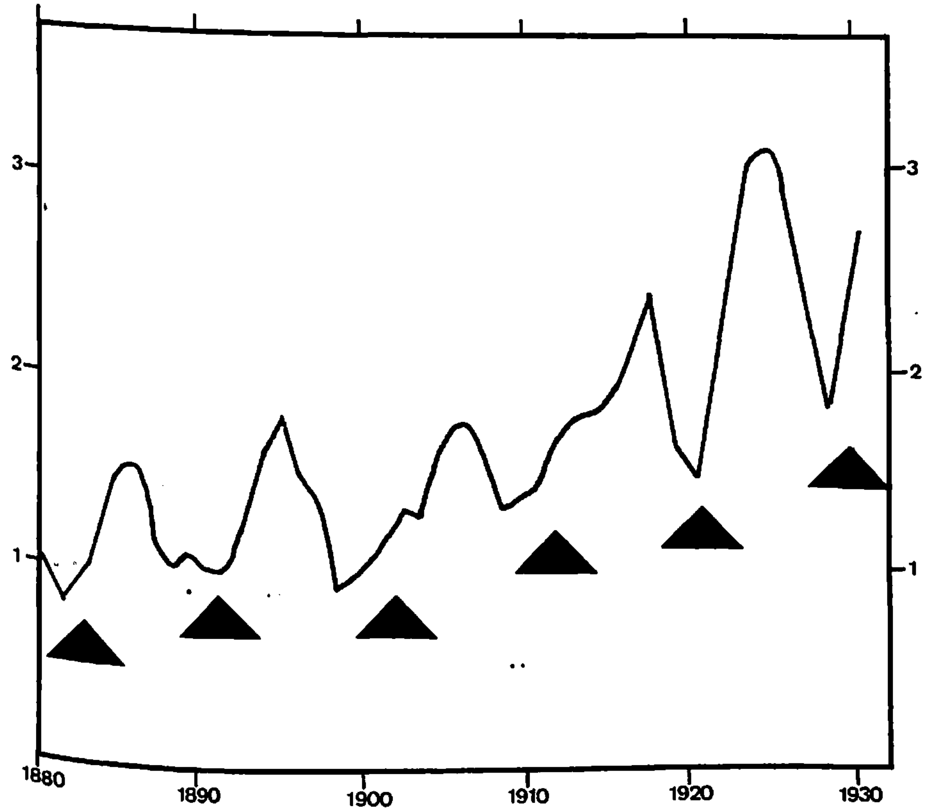

Figure 6: Cycle of Atlantic salmon abundance after E. R. Dewey. The ordinate axis indicates the catch of salmon per rod per day in the Canadian Restigouche Salmon Club 1880 to 1930. Flat triangles mark epochs of Jupiter-CM conjunctions. Their consistent connection with minima in the abundance is in phase with that of the Canadian lynx. This relationship was not disturbed by phase anomalies, as there were no major solar system instability events during the period of observation.

show any disturbances if there are no major instability events. Figure 6, after Edward R. Dewey,[20] presents a cycle in Atlantic salmon abundance. The ordinate axis indicates the catch of salmon per rod per day in the Canadian Restigouche Salmon Club covering the years 1880 to 1929. Flat triangles indicate the epochs of Jupiter conjunctions. The consistent connection with minima in the abundance is in phase with that of the Canadian lynx and the Chinch bug in Illinois. Calculations show that there was no major instability event between 1880 and 1929.

Major instability events seem to affect nearly everything in the solar system. They do not only mark turning points in long-term solar activity, but also influence planets as a whole. Figure 7, after Malcolm G. McLeod,[21] shows the response of the secular variation in the Earth's magnetic field. The upper curve presents the time rate of change of the northern component of the field. The triangles mark the starting epochs of periods of major instability in the Sun's surface about 1933 and 1968. The geophysical literature is replete with papers on the geomagnetic jerk around 1968.

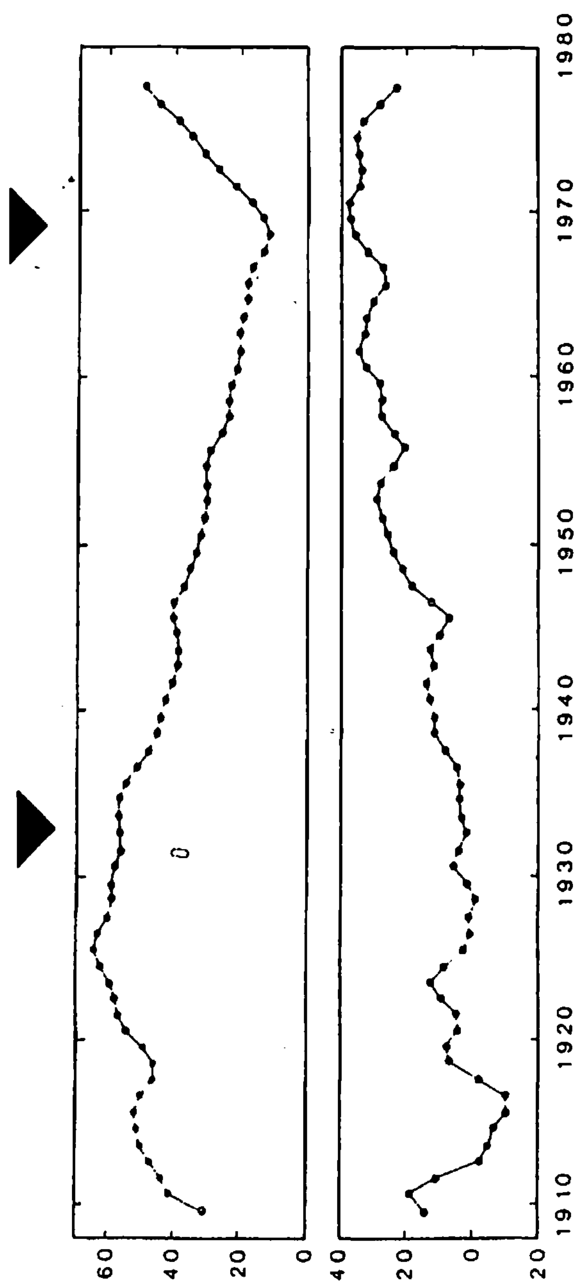

Figure 7: The curve in the top graph after M. G. McLeod presents the time rate of change of the northern component of the Earth's magnetic field. Triangles mark the starting epochs 1933 and 1968 of major instability events in the solar system. They seem to have left their mark in the secular variation of the geomagnetic field.

4. CONJUNCTIONS OF JUPITER WITH THE CENTRE OF MASS, A COSMIC INDICATOR OF TURNING POINTS IN ECONOMIC CYCLES

Human activity is involved too. Economy is an expression of such activity. Figure 8, after Samuel Benner and Edward R. Dewey,[22] shows the ups and downs in the U.S. pig-iron prices from 1834 to 1900. Flat triangles mark Jupiter conjunctions with the centre of mass. The fat arrow points to the boundary event that began in 1867 and resulted in a phase jump from minima to maxima. Epochs of Jupiter conjunctions that before had been connected with troughs in the prices shifted to a connection with peaks. Incidentally, since 1954 all peaks in U.S. long government bond yields have coincided with epochs of Jupiter conjunctions and all valleys with phases in the middle between such epochs. The next peak is to be expected about 1990–91.

Figure 9 presents the yearly percental variation in the gross national product of West Germany. Flat black triangles designate epochs of Jupiter conjunctions with the centre of mass, while white triangles indicate second harmonics of cycles formed by consecutive conjunctions. The fat arrow points to the epoch of the major instability event initiated in 1968 when the center of mass began to stay in or near the Sun's surface for years. The corresponding change in the pattern of the percental variation is obvious. Before this boundary event all epochs of Jupiter conjunctions and second harmonics were related to sharp single-peaked maxima, whereas after the event Jupiter conjunctions were connected with minima in the variation of the gross national product, and second harmonics with broad maxima forming a double peaked plateau. The white triangles that mark the epochs of second harmonics always point to the same position in the plateau, just before the second peak. The next major instability event will not begin before the year 2002. Thus it is to be expected that the pattern will be permanent in the current millenium.

A forecast can be read from the plot. In 1988 the growth will probably be less than 2%, in 1989 it could be negative, and in 1990, the epoch of a Jupiter conjunction, it will reach a minimum. The first, higher peak is to be expected in 1992, and the position on the plateau near the second, lower peak, indicated by a white triangle, will be reached in 1994. The plots of the gross national products of other countries might display somewhat different details. They should be, however, in conformity with the basic pattern: connection of the extrema with the epochs of Jupiter conjunctions and phase jump around 1968. The relation to the epochs of Jupiter conjunctions might be masked by lags that may be different for different countries. The respective lags, however, should show a consistent pattern with a change after 1968. A list of the epochs of Jupiter conjunctions with the centre of mass, the only prerequisite for such studies, is given in Table 1.

5. MULTIDISCIPLINARY FORECAST OF STOCK PRICES

Variations in stock prices, another very complex expression of man's activity, are also influenced by solar instability events. This seems incredible at first sight. But if the violation of Bell's inequality and the resulting oneness of all features of reality are taken seriously, there is no inconsistency in the

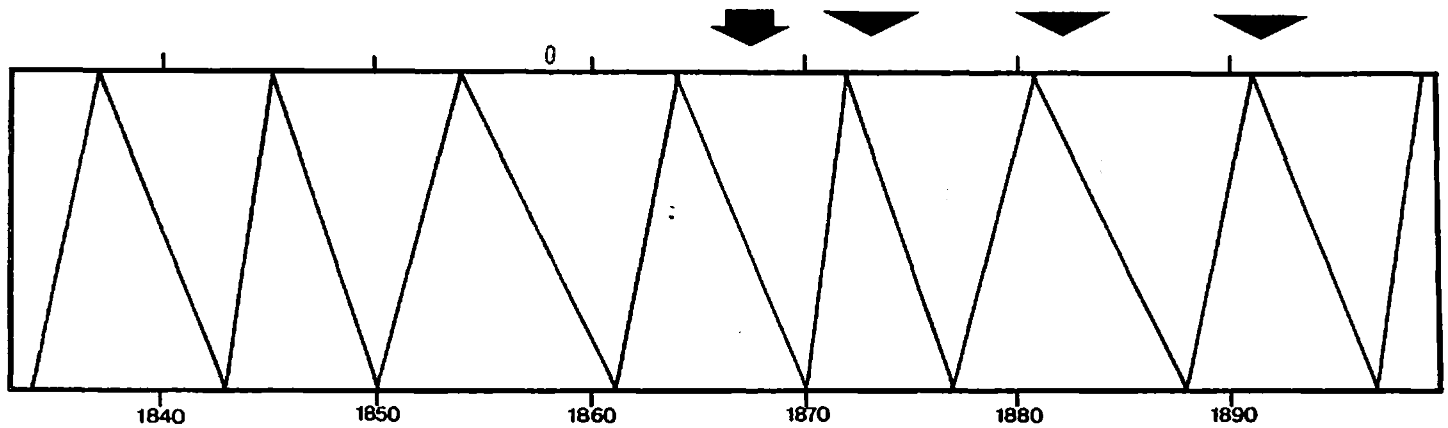

Figure 8: Cycle in U.S. pig-iron prices 1834 to 1900 after E. R. Dewey. Flat triangles indicate the epochs of Jupiter-CM conjunctions. The fat arrow points to the starting epoch 1867 of a major instability event that resulted in a phase jump in the time series. Before 1867 the epochs of Jupiter conjunctions were consistently connected with minima and afterwards with maxima.

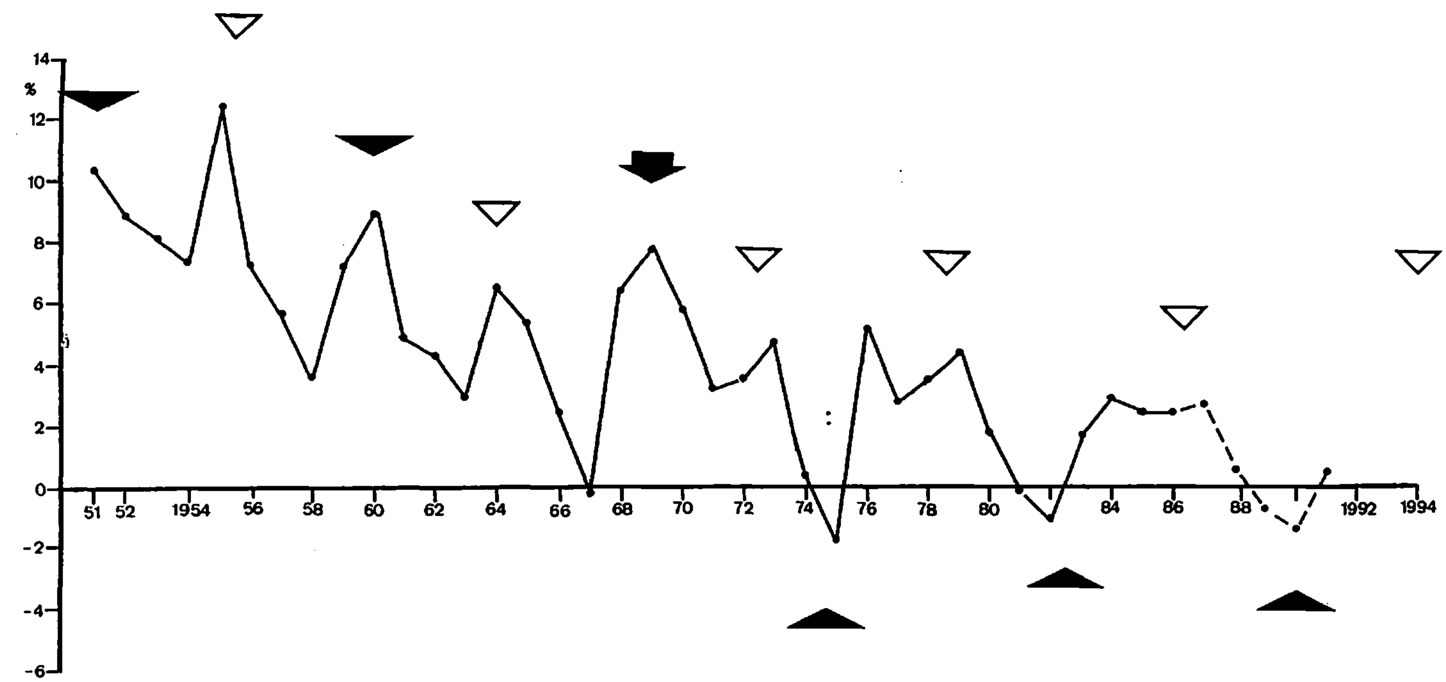

Figure 9: Yearly percental variation in the gross national product of the Federal Republic of Germany 1951 to 1986. Flat black triangles designate epochs of Jupiter-CM conjunctions. White triangles indicate second harmonics of cycles formed by consecutive conjunctions. The fat arrow points to the starting epoch of the major instability event 1968 that changed the pattern of the relationship of Jupiter-CM constellations with extrema in the gross national product. The next minimum in this economic time series is to be expected in 1990.

hypothesis that enhanced instability in the unstable boundary region of the Sun, the center of energy display and regulation, releases instability, too, in a peripheral feature in the Earth's unstable surface like man. It is imaginable that people involved in the sale and purchase in the stock market who are psychologically unsteady and plagued by unstable autonomous nervous systems or hormones, might act differently from well-balanced, optimistic people. Experts acknowledge that a large part of variations in share prices cannot be explained by economic laws and facts.

Figure 10 after Edward R. Dewey[23] presents percental deviations of U.S. stock prices from the 9-year moving average trend for the years 1830 to 1942. Triangles point to epochs of Jupiter conjunctions. The fat arrows mark the epochs of major instability events beginning in 1867 and 1933. The same pattern emerges as in other time series: before 1867 the Jupiter conjunctions coincided with negative extrema in the deviations, whereas after the major instability event they concurred with positive extrema. After 1933, the starting epoch of the next boundary event, the pattern changed again, as was to be expected. The Jupiter conjunction in 1942 indicated a negative extremum instead of a positive one as before.

The turning points of stock prices after World War II continued to match the Sun's phases of instability. Figure 11 is an illustration of this. It presents the German share index published by the Frankfurter Allgemeine Zeitung (F.A.Z.). The rather complex connection with solar instability events requires some explanation. The patterns that emerge from instability and concomitant processes of dynamic self-organisation may be quite different, as they can be influenced by infinitesimal differences in the initial conditions. Thus, it seems natural that different time series that follow identical cyclic periods regulated by Jupiter conjunctions with the centre of mass, may show different phases when they have passed through an instability event. Even within the same time series it may occur that the ups and downs in the data show unexpected responses after periods of major instability. This depends on how many different phases can be realized in the cycle of a special time series. In most cases there are only two. The cycle of stock-prices, formed by consecutive Jupiter conjunctions, is more complex. It shows three different phase states: coincidence of epochs of Jupiter conjunctions with maxima, minima, or mean values in between, just in the middle of the curve ascending from minimum to maximum.

Such mean phases are designated in Figure 11 by small horizontal arrow heads. Before the start of the major instability event in 1968, marked by a large short pointer, the epochs of Jupiter conjunctions in 1951, 1959, and 1967, indicated by arrows, consistently coincided with respective mean phases in the ascending branch of the curve. This pattern changed after 1968. From then on the epochs of Jupiter conjunctions coincided with bottoms in stock prices. The respective epochs in 1970, 1974, and 1982 are again indicated by arrows. This pattern will be preserved until 2002, the epoch of the start of the next major instability event. Thus, the epoch of the next minor instability event, the conjunction of Jupiter with the centre of mass in 1990.3 (April 20, 1990), points to the coming turning point where stock prices reach their bottom and begin to rise again. Such turning points indicate a global trend that affects all

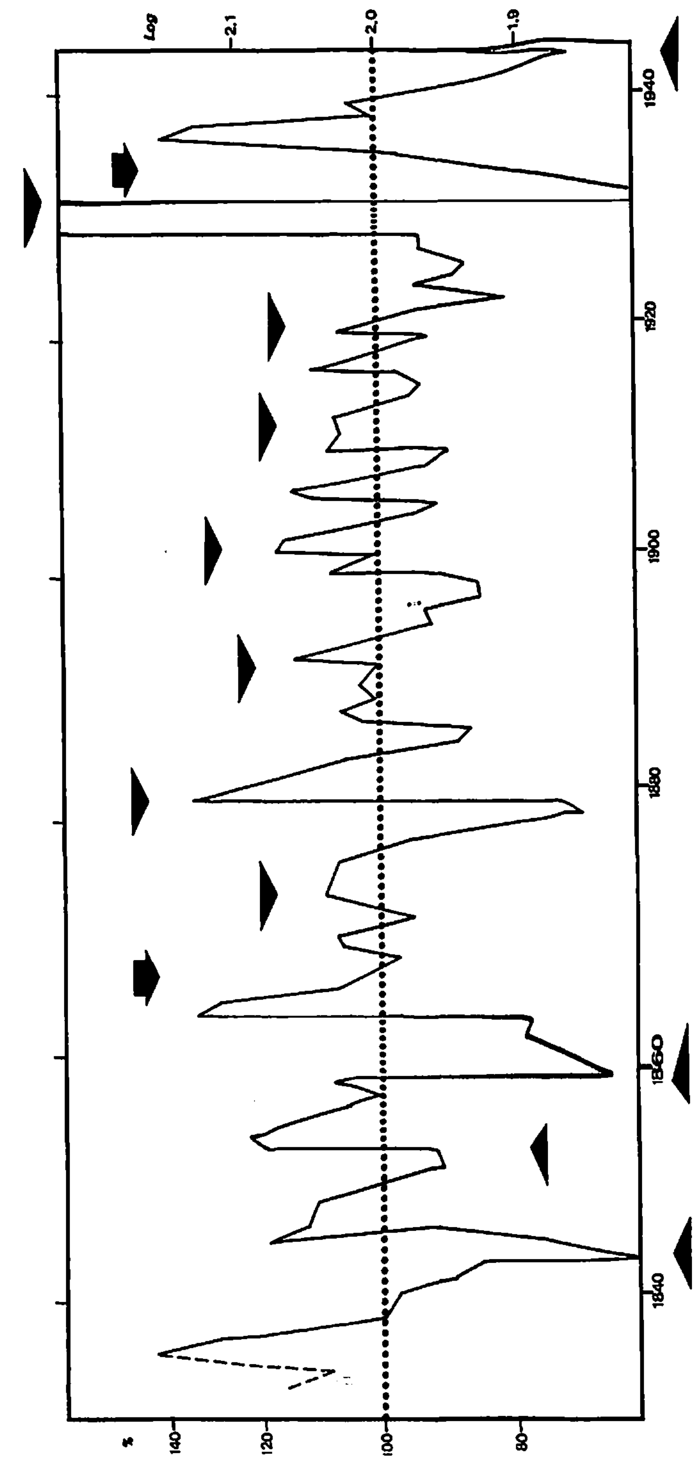

Figure 10: Percental deviations of U.S. stock prices from the 9-year moving average trend for 1830 to 1942 after E. R. Dewey. Triangles point to epochs of Jupiter-CM conjunctions that are related to extrema in the deviations. Fat arrows mark the beginning of predictable major instability events in 1867 and 1933 that changed the pattern of the relationship.

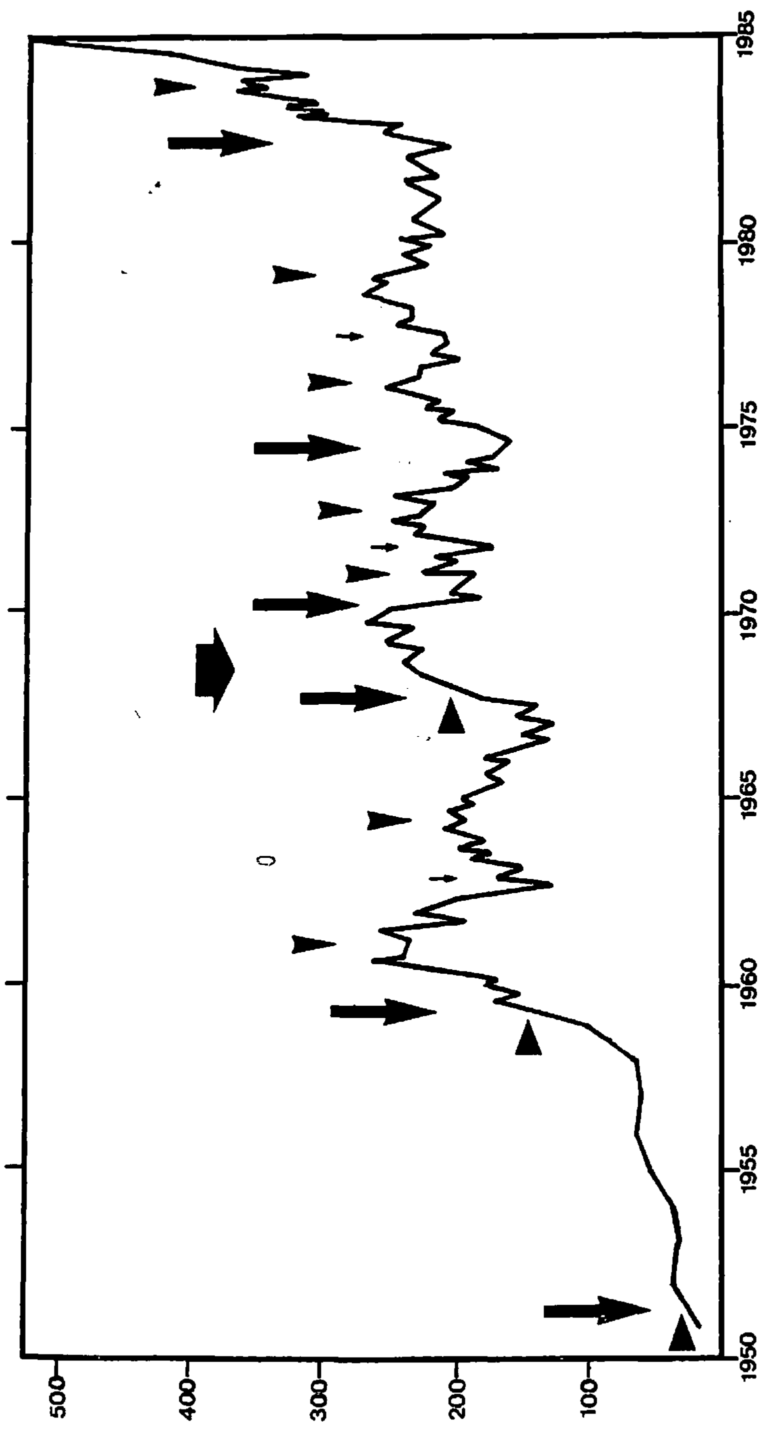

Figure 11: German index of share prices published by the Frankfurter Allgemeine Zeitung (F.A.Z) since 1951. Epochs of Jupiter-CM conjunctions are marked by large arrows. The starting epoch of the major instability event 1968 is indicated by a large fat pointer. The relationship of Jupiter-CM conjunctions with main phases in the course of stock prices shows a different pattern before and after 1968. Before this major instability event the epochs of conjunctions coincided with index ordinates just on the trendline, as marked by small horizontal pointers, whereas after 1968 the conjunctions met bottoms and will continue to do so until the beginning of the next major instability event about 2002. Arrow heads and small pointers indicate secondary tops and [illegible]

important stock exchanges such that the average of their indices is a good match. The indices of individual stock markets may fall several months behind the exact date of the turning point or show a premature release. Thorough knowledge of the state of the special market of interest remains a necessary condition for making appropriate use of the fundamentalist tool offered here. Chart techniques alone are not sufficient to foresee major change. Black Monday, the stock market crash on October 19, 1987, is evidence of this. A combination of expertise, chart techniques, and a general survey of the fundamental turning points will yield more satisfying results than less holistic attempts in the past.

Further analysis of the data in Figure 11 reveals that the fifth harmonic of the cycles formed by consecutive conjunctions of Jupiter and the centre of mass plays an important part with respect to the detailed pattern of cycles in stock prices. There are two subcycles in the respective cycle that comprise two maxima, marked in Figure 11 by vertical arrow heads, and an intermittent minimum, indicated by a small arrow. The epoch of the first peak is at 1/5 of the respective length of the cycle of Jupiter conjunctions, the intermittent trough at 2/5, and the second peak before the final bottom phase at 3/5. The epochs can be calculated by means of a simple formula: first peak: epoch of preceding Jupiter conjunction + 1/5 length of cycle; intermediate valley: epoch of conjunction + 2/5 length of cycle; second peak: epoch of conjunction + 3/5 length of cycle. For the years 1959 to 1982 the mean deviation from this pattern was 0.22 years; the standard deviation reached $\sigma = 0.18$ yr.

The current cycle was initiated by the conjunction of Jupiter with the centre of mass on October 31, 1982 (1982.83), and will be terminated by the conjunction on April 20, 1990 (1990.3). The length of the cycle is 7.5 years. One fifth of this length is 1.5 years. Accordingly, the first peak in the international average of stock indices was to be expected in 1984.3, the intermittent valley in 1985.8, and the second peak in 1987.3. In the case of vigorous hausses like that in the roaring twenties and again after 1982, the two peaks grow together in forming one ascending branch that reaches its top at the epoch of the second peak. The intermittent valley becomes apparent only by a temporary reduction in the pace of rising. On this basis, a forecast was published in January 1986 that pinned down the turning point in the recent boom to 1987.3.[26a] It was explicitly stated that after this date the average of international indices would fall down to a bottom around 1990.3. Recommendation was given to sell before 1987.3 (end of April 1987). The mean of the indices of ten of the most important stock exchanges reached the turning point in 1987.25. Those that walked beyond this cliff in the bull market were shaken by the crash initiated on Black Monday.

The third phase state that emerges in cycles of stock prices is by no means restricted to indices of shares. Figure 12, after Edward R. Dewey,[24] presents another example, the rate of immigration into the U.S.A. from 1824 to 1950. The ordinate axis indicates smoothed percental deviations from trend. Large pointers mark the starting epochs of major instability phases in 1867 and 1933. Before 1867 the epochs of Jupiter conjunctions, designated by arrow heads, coincided with extrema in the immigration rate. After 1867 this relation was subjected to a change: the epochs went along with zero phases, intersections

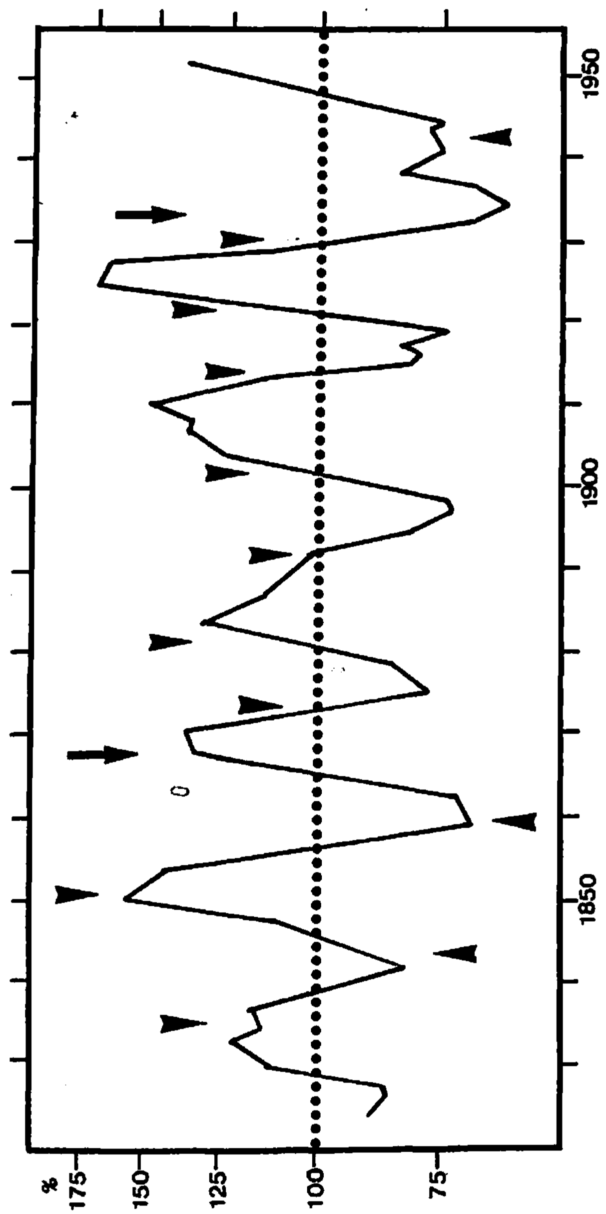

Figure 12: Variations in the rate of immigration into U.S.A from 1824 to 1950 after E. R. Dewey. The ordinate axis indicates smoothed percental deviations from the trend. The major instability events beginning about 1867 and 1933 are marked by arrows. Arrow heads designate the epochs of Jupiter-CM conjunctions. Before 1867 these conjunctions matched extrema in the immigration rate. After 1867 this pattern changed; epochs of Jupiter-CM conjunctions met zero phases on the 100 % trend line. The next major instability event about 1933 initiated a further change.

of the curve with the x-axis that represents time. This pattern changed again after the major instability event starting about 1933.

6. BORDERLINE PHENOMENA IN HISTORY, ART, AND SCIENCE

The special constellation of Sun and planets that makes the centre of mass and the Sun's surface coalesce, is also reflected in the fields of sociology, art, and science. The years that followed 1789, 1823, 1867, 1933, and 1968 were periods of radical change and revolution, a break-down of old structures and the emergence of new forms and ideas. The following examples give an impression of the turning-point function of these epochs, a proper expression of the basic quality of boundary effects as explained in the beginning:

About 1789 to 1793: Great French revolution; spread of modern democracy; first modern constitution in U.S.A.; invention of lighting gas; Mozart, The Magic Flute.

About 1823 to 1828: Monroe doctrine; end of the Spanish empire in South America, Simon Bolivar; Greek war of independence against the Turkish rule; Decembrist conspiracy in Russia; non-Euclidian geometry; foundation of thermodynamic theory; Ohm's law in electricity; Brownian movement; first synthesis of an organic compound (urea) from inorganic substance; invention of steam locomotive, electromagnet, sewing machine, ship's propeller, and aniline dye; Beethoven, Ninth Symphony, Missa Solemnis; Schubert, Seventh Symphony.

About 1867 to 1870: Alaska bought by U.S.A.; nihilism in Russia; Karl Marx, The Capital; foundation of first Social Democratic Party; Maxwell's equation describing the interrelation of electric and magnetic fields; concept of periodic table of chemical elements; Kekulé's concept of six-carbon benzene ring; invention of dynamo, spark-ignition engine, type-writer, rotary press printing, reinforced concrete; dynamite; impressionism in art.

About 1933 to 1937: Great economic depression, collapse of the world market; Stalin's dictatorship, forced collectivisation of agriculture; start of Japan's Far Eastern expansion; breakthrough of Hitler's national socialism; Goedels revolution in logic; discovery of neutron, positron, meson, and heavy hydrogen; creation of electron-positron pairs from energy and vice versa; discovery of nucleic acid in cell nuclei; invention of television, jet engine, and electron microscope.

About 1968 to 1972: Upheavals and rebellions of students all over the world; spread of hippies; Cultural revolution in China; six day Arab-Israeli war; new economic structures in Czechoslovakia, suppressed by Russian invasion; turning point in Vietnam; space travel; astronauts on the Moon; Glomar Challenger expedition, plate tectonics; first Aids infections; ecological movement; Gnostics of Princeton; Pop art.

The next major instability event will start about 2002 and last till 2011. This is an exceptionally long period. It is impossible to predict the details of its historic effects. But the basic quality of all boundary functions will be evident: the years past 2002 will prove to be another turning point, a period of instability, upheaval, agitation, and revolution, that ruins traditional structures, but favours the emergence of new patterns in society, economy, art, and science. Furthermore, the rhythm in terrestrial time series that shows a connection with the Sun's activity will change again. Perhaps people at the beginning of the third millenium will be better prepared to realize the dangers and chances of cosmic periods of change like these. Possibly, the holistic results presented here will contribute to such awareness.

7. SOLAR TORQUE CYCLES, PRECAMBRIAN CLIMATE, AND CLASSICAL ASTROLOGICAL CONJUNCTIONS

This is the end of our comprehensive example which demonstrates the fertility of a genuine holistic approach that integrates basic astrological ideas with modern scientific knowledge. A single notion taken from the fields of mathematics and physics, a simple model of feed-back loops or cycles, seemingly infinitely apart from astrological views, when looked at in an unbiased multidisciplinary way, has been shown to yield new results that profoundly change our perspective. Critics may object that impulses of the torque (IOT), even if initiated by conjunctions of Jupiter and the centre of mass, show no relation to traditional astrological constellations. But actually conjunctions and oppositions of the giant planets play a vital part in the Sun's irregular motion about the centre of mass (CM). The Sun reaches extreme positions relative to CM when traditional constellations are formed by Jupiter, Saturn, Uranus, and Neptune. When Jupiter on one side of the Sun is in opposition to Saturn, Uranus and Neptune on the other side, the Sun's centre and the centre of mass CM come together, whereas the two centres reach their greatest distance when all of the four giant planets are in conjunction. The synodic cycle of Jupiter and Saturn with a period of 19.86 years and cycles of double (39.72 yr), fourfold (79.44 yr), eightfold (158.9 yr), and 16-fold (317.8 yr) length are of paramount importance in solar torque cycles. They even appear in the solar cycle in Precambrian time, 680 million years ago, derived from records covering more than 16.000 years. According to G. E. Williams[25] the so-called "Elatina cycle" of solar activity, that shows a strong relation, too, with climatic cyclicity, has an average duration of 314 years. This is near to the 16th subharmonic (317 yr) of Jupiter's and Saturn's conjunction cycle. The

harmonics of 79 and 157 years in the "Elatina cycle" match the fourth (79 yr) and 8th (158 yr) subharmonic of the synodic cycle of Jupiter and Saturn.

A further classical constellation, the triple conjunction of Jupiter, Saturn, and Uranus, the period of which is 317.7 years, is immediately related to the "Elatina cycle" and together to torque cycles. As will be shown, one of the most important torque cycles has a mean period of 13.3 years. It can be derived from the conjunction cycles of Jupiter and Neptune (12.8 yr) and Jupiter and Uranus (13.8 yr). The mean of both synodic cycles (13.3 yr) matches just the torque cycle of this length. Interestingly, the remaining harmonics of the "Elatina cycle" of 52, 63, and 105 years can be derived from the 13.3-year torque cycle. They are near its 4th (53 yr), 5th (66 yr), and 8th (106 yr) subharmonic. There are many other relations that connect traditional astrological constellations with torque cycles, solar activity, and terrestrial effects. This shows that traditional astrology had hands on something, the precise contours of which, however, can only be worked out by unprejudiced investigations that make interdisciplinary use of modern means of research. Astrologers should follow the respective pieces of advice given by H. Eysenck.[25a]

III. PREDICTIONS OF SOLAR ERUPTIONS BASED ON PLANETARY CONSTELLATIONS

The extensive example presented in the initial part of this monograph was intended to give a first survey of the advantages of a holistic approach and the new kind of multidisciplinary techniques that integrate basic astrological views and modern scientific knowledge. In the following part, a body of evidence will be presented that supports the fundamental astrological concept of the influence of planetary constellations on terrestrial phenomena. It is shown how planets modulate the Sun's variable activity and thus indirectly influence diverse effects of solar-terrestrial interaction. These connections were tested by long-range predictions of solar activity and related terrestrial events checked by astronomical and geophysical institutes. John Addey's dictum "that astrological effects can be best understood in terms of cosmic periods and their harmonics", is substantiated by cyclic patterns formed by consecutive conjunctions of Jupiter with the centre of mass of the solar system. Such cycles and their harmonics emerge in time series of the Sun's rotation, energetic solar eruptions, geomagnetic storms, and weather. The abundance of wild life and economic cycles have already been dealt with in the introductory part.

The dependability of the forecasts in question, that were based on planetary configurations in the solar system, forms a sharp contrast to what scientists think of predictions based on planetary constellations. At the Fifth Astrological Research Conference, "Exploring Astrology", held in London on November 22 – 23, 1986, the critic Geoffrey Dean was engaged in spreading "bad news for astrologers", as he put it. In his paper "Does Astrology Need To Be True?" he covered the same topic. He especially dealt with surveys of astrological predictions that proved spurious: "What most surely appears . . . is the perfect inanity of the astrological undertaking . . . what was announced did not happen, what happened was not announced." Geoffrey Dean, too, reviewed his own analysis of J. H. Nelson's daily forecasts of shortwave radio quality based on heliocentric planetary positions. With respect to his evidence that Nelson's relatively simple technique did not work he concluded: "Yet for 30 years Nelson was convinced he saw a correlation that in fact did not exist. So we should not be surprised that astrologers, working with generally vaguer events and far more complicated techniques, can see correlations even if none actually exist." Eventually, Geoffrey Dean stated: "The astrologers' response to these five surveys, which are the only ones I know of, has not been to generate surveys of their own. Instead there has been either silence or brusque dismissal. . . "[26]

This statement is not true, and Geoffrey Dean knew well that it was not in accordance with facts. He was present at the Second Astrological Research Conference, London, November 28/29, 1981, when the positive yield of long range forecasts of energetic solar eruptions and their terrestrial effects was presented that was based on constellations of planets. These results were reviewed in a conference report in *Correlation*[26a] and thoroughly explained in papers published in proceedings of international science conferences and

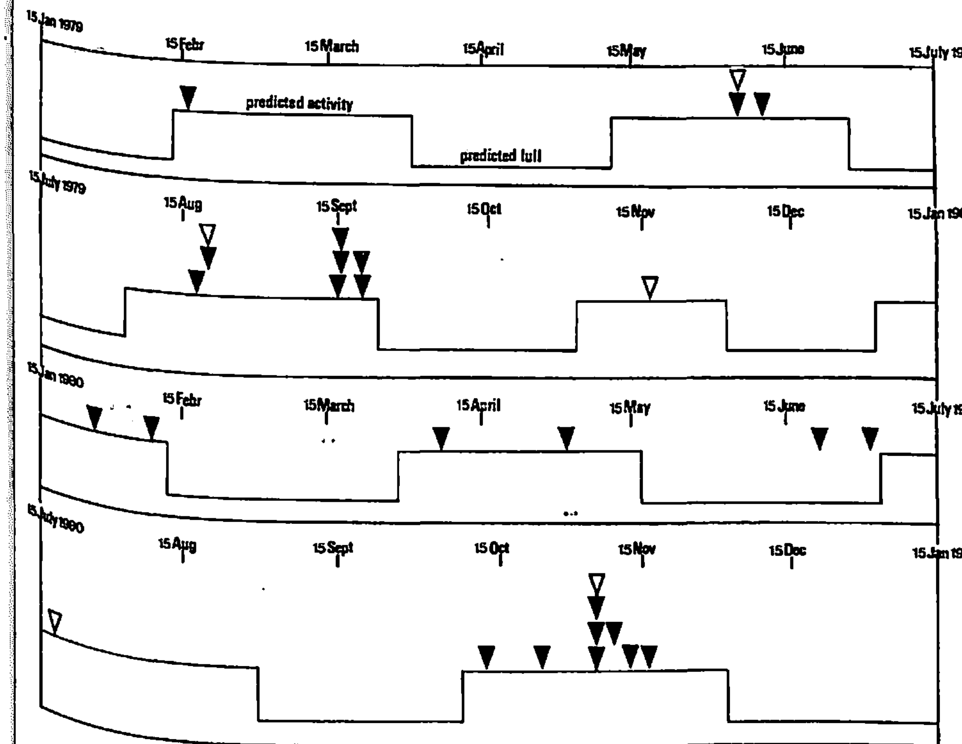

Figure 13: Result of yearly forecasts of energetic solar X-ray bursts equal to or greater than class X2 (black triangles) and proton events (white triangles) for 1979 to 1981. Out of 29 events observed, 27 fit the periods of predicted activity.

scientific and astrological journals.[27] Geoffrey Dean cannot argue that predictions of solar activity, even if based on planetary constellations, have nothing to do with astrology. He explicitly holds that the hypothesis of a planetary modulation of the Sun's activity and an indirect influence on life on Earth would be entirely compatible with astrological tradition.[28] This is why he thought it worthwhile to write a critical analysis of the forecasts of shortwave radio quality by John H. Nelson.[29]

Figure 13 shows the result presented at the Second Astrological Research Conference. The forecasts in question, covering the years 1979 to 1981, were published one year in advance respectively and checked by the astronomers W. Gleissberg, J. Pfleiderer and H. Wöhl, as well as by the Space Environment Services Center, Boulder, U.S.A.[30] Each of the four frames presents the data for half a year. Elevated rectangles mark periods of predicted eruptional activity in a quantitatively defined range, whereas troughs indicate predicted lulls. Epochs of observed energetic eruptions of the defined classes are marked by triangles. Black triangles point to flares accompanied by X-ray bursts equal

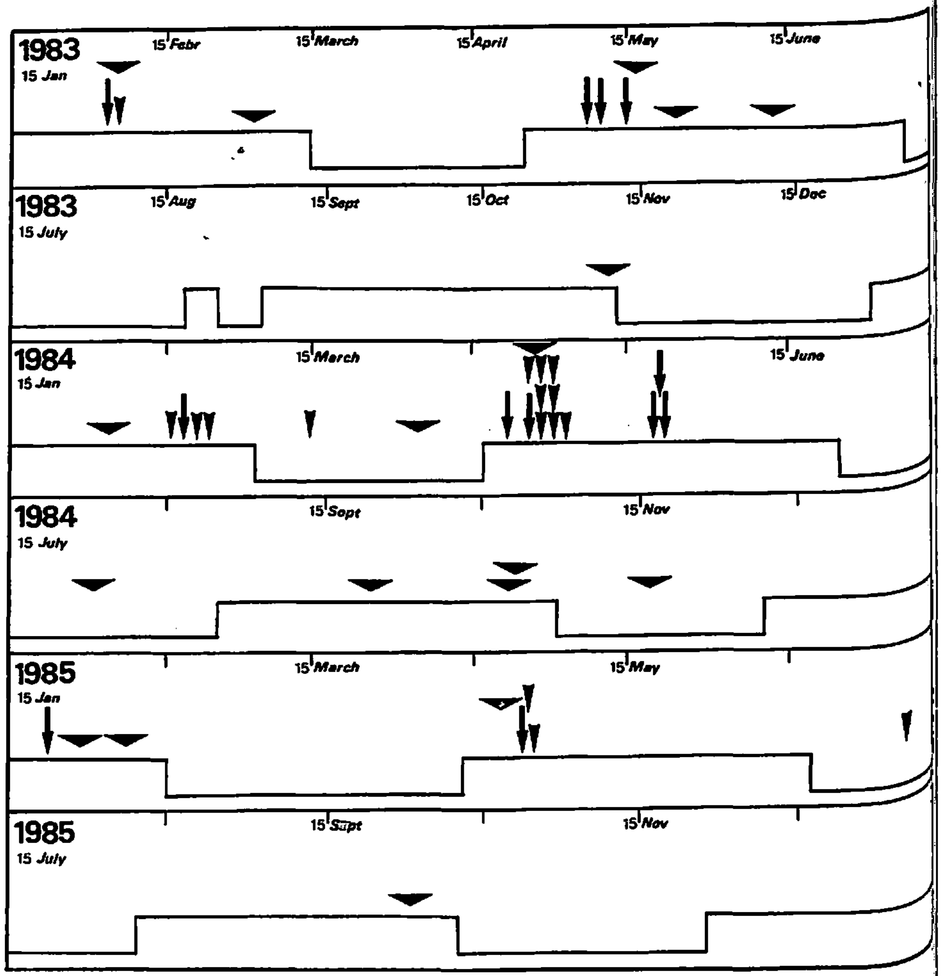

Figure 14: Outcome of a long-range forecast of energetic solar-terrestrial events covering the 3-year period 1983 to 1986. Out of 46 events observed, 41 match the periods of predicted activity: all of 12 X-ray bursts equal to or greater than class X2 (marked by arrows), 14 of 16 proton- and polar cap absorption events (indicated by arrow heads), and 15 of 18 geomagnetic storms (marked by flat triangles).

to or greater than (≤) class X2, and white triangles designate proton events ≤ 50 particles at 10 MeV. Out of 29 energetic events observed in the forecast period January 1979 to January 1981, 27 met the predicted periods of enhanced activity. It can be seen without any statistical evaluation that this is a good fit. A Pearson-test yields χ^2 (1 degree of freedom) = 20.9; $P < 0.00001$.

Some of the terms used in this part might seem rather technical. This should not deter the reader from going on, the thread of the argument will prove easy to follow. Technical details, which are necessary to convince experts, may be neglected by readers who only want to grasp the essential connections. (There is an extensive glossary in the appendix that explains most of the technical terms.)

In January 1983 a new long-range forecast was issued that covered a period of three years. Besides energetic X-ray flares and proton events, strong geomagnetic storms were included in the prediction. The data were again checked by astronomers and the Space Environment Services Center. Figure 14 shows the result of the forecast. Out of 46 energetic events observed January 1983 to January 1986, 41 fit the periods of predicted activity. These include all of 12 observed X-ray bursts ≤X2, marked by arrows, 12 of 14 proton events ≤ 50 particles at 10 MeV, and both polar cap absorption events ≤ 2 dB, indicated by arrow heads, as well as 15 of 18 magnetic disturbances $A\kappa \leq 50$, marked by flat triangles. A Pearson-test yields $\chi^2 = 16.3$ (1 degree of freedom); $P < 0.00006$). The astronomer Hubertus Wöhl, member of the Fraunhofer Institute for Solar Physics, Freiburg, who checked the forecast, published the result of his evaluation, commenting that the 3-year forecast was "very successful".[31]

A replication of the evaluation of the prediction experiment by means of observed events of less eminent categories again yields a good fit. Out of 62 observed events, 55 hit the periods of predicted activity. A Pearson-test reaches $\chi^2 = 21.3$; $P < 0.00001$. Events whose distribution is subjected to a χ^2-test should be quite independent. This condition is not fulfilled within the time series under consideration, as energetic solar events form clusters. The chance, however, that such clusters coincide with periods of predicted lulls is as good as that of accumulations in periods of predicted activity, if the pattern, the forecast is based upon, is not valid. Thus, the Pearson-test may nevertheless give useful evaluations of the goodness of fit of predicted and observed events. If not, it can be seen quite without tests of statistical significance that the prediction was successful.

The forecast for the year 1982 ran a special risk as it dealt with very rare events, namely energetic flares accompanied by X-ray bursts greater than class X9. Since 1970 only two such events had been observed when, according to the January 1982 forecast, events greater than X9 were to be expected January 15, 1982, to January 14, 1983. Highest probability was assigned to the period from the end of September to the middle of December 1982, and second highest probability to the period from April 29 to June 24, especially April 29 to May 5, and May 22 to June 9, 1982. The observations fit this prediction. X-ray bursts X12, X12.9, and X10 occurred on June 6, December 15, and December 17, 1982. The foregoing X10 event, observed on July 5, 1974, was also predicted in a forecast issued February 20, 1974, and checked by the Space Environment Services Center, Boulder.

IV. CYCLES OF SOLAR ERUPTIONS

1. SOLAR-TERRESTRIAL EFFECTS OF FLARES

The set of checked predictions, presented above, is based on a body of connections that go back to constellations of planets. The controversial thesis that events on Earth are influenced by planets would get substantiation if there were evidence that even the huge Sun and its varying activity are subject to planetary regulation. As to solar activity, attention is usually focused on sunspots; they are spectacular and well documented. But the magnetic energy stored in or above sunspot groups solely constitutes a potential for solar-terrestrial interaction, which is actually released if there are solar eruptions. Thus, energetic solar eruptions are a sharper criterion of immediate solar-terrestrial relations than sunspots.

Flares are the most powerful and explosive of all forms of solar eruptions, and the most important in terrestrial effect. Large flares release energy equivalent to the explosion of more than 200 million hydrogen bombs in a few minutes' time, sufficient to meet mankind's energy demands for a 100 million years. Momentary temperatures exceed 20 million ° K, which is hotter than in the searing interior of the Sun. Ultraviolet and X-ray radiation increases dramatically and causes multiple geophysical effects in the upper atmosphere. Flare effects include corpuscular emission, cosmic ray events, Forbush decreases, aurorae, sudden ionospheric disturbances, radio noise storms, disturbance of navigation on the terrestrial surface and of satellite operation in space, geomagnetic disturbances, short-wave fade out, polar blackout, disruption of telephone connections, power-line failures, computer malfunctions by "mad electrons", and ionization of the atmosphere. Coronal holes, that also contribute to such ionization, are again released by energetic flares.[32]

Geomagnetic storms, another effect of energetic solar eruptions, have caused extensive power blackouts in cities, states, and provinces of the United States and Canada. There are records of baby booms, especially for New York, that occurred nine months after these events. Besides strong power surges on long lines, telephone and microwave relay circuits can seriously be impaired. In Canada there is current legal as well as scientific interest in the possible effects of the large magnetic storm on February 8, 1986, caused by solar eruptions that were initiated by an X-ray burst of class X3. Just at this time a head-on collision between a freight train and a passenger train occurred, and scientists question whether potentials induced by magnetic disturbances could have affected operation of a microwave device that was supposed to control the red light that should have stopped the freight train.[33] Magnetic storms also curtail geophysical exploration studies, destroy vital communication links and can produce significant radiation hazards to both astronauts and airline passengers. Further terrestrial flare effects are increased incidence of lightnings and atmospherics, changes in weather, variations in chemical reactions, increase of electric potentials in the atmosphere as well as in trees and in man, coagulation of colloids, increase in myocardial infarction, leucopenia, psychic instability and traffic accidents.[34]

2. SOLAR ERUPTIONS AND HUMAN CREATIVITY

Flares also seem to stimulate human creativity. There are intriguing examples of scientific discoveries, creative intuition of artists, and mystic vision that concurred with highly energetic flares. The recently published book "Children of the Cosmic Light" [35] deals with this facet of the Sun's boundary creativity. Here are some examples. The trappist monk Thomas Merton, author of "The Seven Storey Mountain", had a mystic experience on December 3, 1968, as described in his diary.[36] Figure 15, after Armstrong *et al*,[36a] shows the incidence of solar eruptions in 1968 that emitted energetic particles. The arrow points to the date that relates strong surface activity of the Sun to a human boundary event. Unfortunately, direct measurements of the intensity of energetic effects of solar eruptions, as presented in Figure 15, are merely available for a few decades after World War II. As to observations of flares themselves, the situation is not much better. Observations of flares in white light are very rare. The vast majority of flares can only be observed in a selected region of the spectrum. Not until the invention of the spectroheliosceope by Hale in 1926 was there any hope of studying flares systematically. Since this instrument was not fully developed until 1931, the 17th solar cycle of the late thirties was the first during which flares could be studied systematically. Even then flare lists were not complete.

In addition, the recorded optical intensity of flares has meanwhile proved to be a poor indicator of the actual energy involved and of its terrestrial effect.[37] Energetic X-ray bursts emitted by flares are a sharper criterion, but they can only be observed by satellite instrumentation available since the late sixties. There is, however, a proxy means that points to energetic solar eruptions: major geomagnetic storms that have been recorded for more than 120 years. If such major storms occur, there must have been a preceding energetic solar eruption, a strong ejection of solar plasma. There may sometimes be energetic solar eruptions that do not release strong magnetic storms due to the solar system geometry; eruptions near the Sun's limb, especially east of the central meridian, produce only small storms or none at all, no matter how large. But the actual incidence of a major magnetic storm is a dependable indicator of corresponding energetic eruptions that eject fast solar plasma. There is a host of indices to measure geomagnetic disturbances. The indices *aa* published by P. N. Mayaud[38] form a time series, the quantitative homogeneity of which is acknowledged to be good. It begins with the year 1868.

Exact dates of mystic experience are rare; real mystics do not talk much. All dates, however, that have become known show coincidence with *aa*-indices far above the level of the annual mean (*am*). Gopi Krishna, who practised Tantric Yoga, had his first mystic experience at Christmas 1937.[39] During deep meditation he was overwhelmed by a wave of fluid light and ineffable blissfulness. This did not only occur at sunrise, but also at the time of strong solar boundary activity that released a strong magnetic storm on Earth (*aa* = 75; *am* = 19.1). In the same year, but under quite different circumstances, Arthur Koestler had a mystic experience, aptly described in his autobiography, when he was under sentence of death during the Spanish Civil War. His experience was released when he was meditating in his prison cell on the

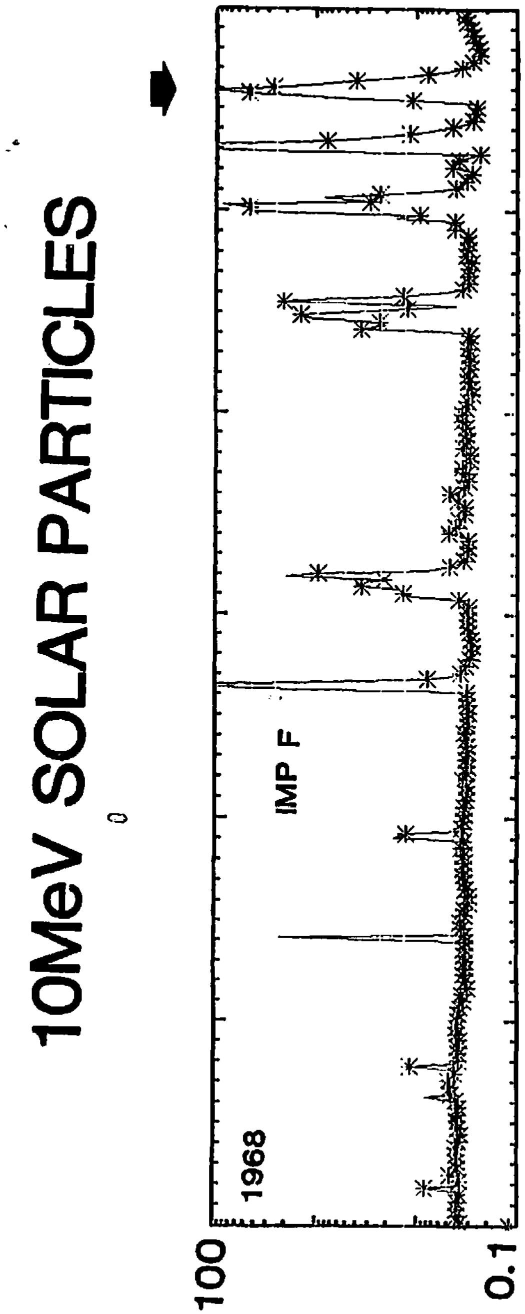

Figure 15: Incidence of solar eruptions in 1968 that emitted energetic particles, after Armstrong (1983). The arrow points to the date of December 3, when the trappist monk Thomas Merton had the mystic experience as described in his diary. This is an example of links between energetic surface activity of the Sun and human boundary events.

nature of prime numbers and Euclid's proof of the infinity of the sequence of prime numbers. Koestler's report is of great importance as he was well respected as a critic, writer, journalist, and scientist. His experience occurred on February 17, 1937, when there were solar eruptions pointed to by a strong magnetic storm (*aa* = 55; *am* = 19.1). Richard Maurice Bucke, [40] who coined the term Cosmic consciousness, has recorded two other data of mystic experience: J. W. W., January 20, 1885, and Paul Tyner, May 11, 1895. The respective geomagnetic indices are: aa = 74; *am* = 15.5 and *aa* = 64; *am* = 18.2. Three persons that did not want their names published gave the following dates of their mystic experience: June 4, 1950 (*aa* = 59; *am* = 24.4); July 19, 1959 (*aa* = 241; *am* = 30.2); June 26, 1963 (*aa* = 67; *am* = 21.3).

This is a rather eclectic sample; it is very difficult, however, to find such rare events at all that in addition are exactly dated and occurred after 1868, the beginning of the *aa*-record. Fortunately, Nicholas Kollerstrom has gathered another sample of acts of creation, though for another purpose. At the 5th International Astrological Research Conference, held in London, on November 22–23, 1986, he presented a sample of 17 eminent discoveries of scientists, aptly called Eureka moments.[41] Eleven of these data lie after the beginning of Mayaud's *aa*-index. Two were cancelled. Fermi's direction of the first controlled nuclear chain reaction in 1942 was no real act of creativity; it was only a phase in a technical development the mental basis of which was founded earlier. And Shockley's invention of the transistor, dated as 1947, is given as 1948 by several other sources. The remaining nine cases confirm the connection between boundary events on the Sun and human acts of creativity. Particles that are ejected by solar eruptions can reach the Earth within a few hours to four days. Thus, if it is assumed that Eureka moments concur with energetic solar eruptions that in most cases release strong geomagnetic storms, it seems reasonable to expect such storms on the Eureka day or one of the three following days. The observations confirm this working hypothesis:

Mendeleyev: 1 March 1869; concept of periodic table of chemical elements; *aa* = 64; *am* = 20.9

Edison: 7 November 1877; invention of phonograph; *aa* = 57; *am* = 9.3

Roentgen: 8 November 1895; discovery of X-rays; *aa* = 100; *am* = 18.2

Becquerel: 1 March 1896; discovery of radioactivity; *aa* = 89; *am* = 18

Loewi: 28 March 1921; discovery of chemical transmission of nerve impulses; *aa* = 42; *am* = 16.6

Fleming: 3 September 1928; discovery of Penicillin; *aa* = 54; *am* = 17.7

Tombaugh: 18 February 1930; discovery of the planet Pluto; *aa* = 50; *am* = 28.6)

Szilard: 12 September 1933; concept of atomic fission theory; *aa* = 71; *am* = 16.4

Watson: 28 February 1953; discovery of the molecular structure of gene substance; *aa* = 92; *am* = 22.2.

This result can be subjected to a statistical test, though the sample is rather small. Mayaud gives two half-daily values of the *aa* index for each Greenwich day. For the range of four days after the nine Eureka events the number of *aa* values thus amounts to 72. Statistically, the mean of these *aa* values, $\bar{x}_1 = 29.13$, and the standard deviation of their distribution, $\sigma_1 = 21.56$, are characteristic parameters of this first group. They set off against the parameters of the second group formed by the nine annual means of geomagnetic activity related to the years of the Eureka events: $\bar{x}_2 = 18.66$; $\sigma_2 = 4.89$. The statistical t-test evaluates whether the difference between the means of both groups is significant. The test yields $t = 3.47$ for 63 degrees of freedom (df). As the first group is known and expected to have a higher mean than the second group, the rules valid for single-sided distributions apply: $P < 0.0007$. The probability P that this result has been produced by random sampling is smaller than 1 in 1400. This points to a highly significant difference between the *aa* indices in both groups in accordance with the working hypothesis proposed above. When monthly means are chosen instead of yearly means, the difference between both groups continues to show highly significant results.

This example shows that significant results can emerge in very small samples. If so, this indicates strong relations that are of practical importance. Connections that only become visible when thousands of cases are investigated may be of theoretical interest; in practice, however, they are often of negligible weight. Naturally, the relation between solar boundary events and human creativity has to be corroborated by replications making use of new data. In this respect, it is a significant that Suitbert Ertel has established a relation between human acts of creation in various fields of art and science, and sunspot cycles of different length.[42] His highly significant results, corroborated by many replications, are based on a quite different, independent approach and careful statistical analysis of large bodies of data. Unfortunately, Ertel's voluminous work has not yet been published.

As has been stated in the beginning, instability indicative of boundary states is a pre-condition of creativity. Heavy geomagnetic storms that are linked to solar instability events are themselves an expression of strong instability in the Earth's magnetic field. It is not out of the question that this magnetic instability may induce instability in the electric activity of the brain cells, evidenced in electroencephalograms, or of the autonomous nervous system.[42a] Certainly, such instability cannot produce a creative potential other conditions of which are not fulfilled. But if there is a creative potential, it may be stimulated or triggered by instability.

According to Arthur Koestler[43] there is a remarkable form of blindness which often prevents even an original thinker from perceiving the meaning and significance of his own discovery. It resembles an "anti-body reaction" directed against new ideas irrespective of whether it is a new pattern created by others or oneself. Kepler nearly threw away the elliptic orbits of planets; for nearly three years he held the solution in his hands without seeing it. After the breakthrough of the new concept Kepler confessed: "The truth of Nature, which I had rejected and chased away, returned by stealth through the backdoor, disguising itself to be accepted. Ah, what a foolish bird I have been."

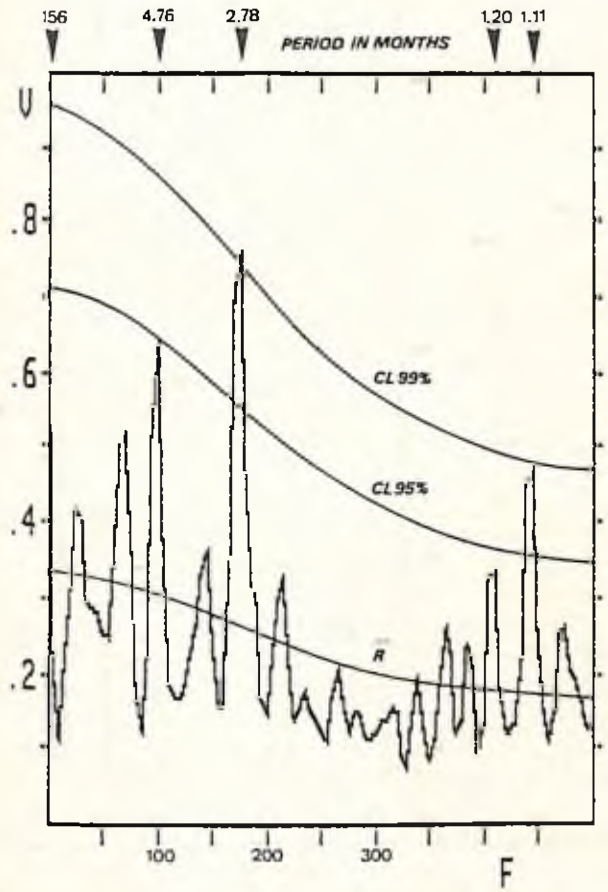

Figure 16: Blackman-Tukey power spectrum of flare-generated X-ray bursts equal to or greater than class X1 observed 1970 to 1982 by means of satellite instrumentation. The frequency f of investigated cycles is measured in millicycles per sampling interval of half a month. The ordinate axis represents the relative variance V of the respective frequencies. Periods of outstanding peaks, pointing to cycles of flares, are indicated on top of the figure. The significance of the deviation of prominent peaks from the Markov red noise (R) can be evaluated by means of the confidence level curves CL. The result provides evidence of cyclic features in the distribution of energetic solar flares

Koestler aptly remarks that the defence mechanisms which protect habits against the intrusion of novelty account both for our mental inertia and mental stability. It seems plausible that strong instability in the Earth's magnetic field, that affects the basic electric conditions of brain functions, may release mental instability which makes it easier to overcome mental inertia.

Inversely, unshaken inertia would prevail when the geomagnetic field keeps quiet. There are examples that seem to point to such effects. Irene Curie and Frédéric Joliot were talented physicists; they were awarded the Nobel prize for the synthesis of new radioactive elements. On January 18, 1932, they made an observation the significance of which they did not grasp. Thus, they missed the discovery of the neutron, a fundamental subatomic particle. When the young physicist Ettore Majorana, a disciple of James Chadwick, read the report of the Joliot-Curies, he remarked sarcastically: "These fools, they have

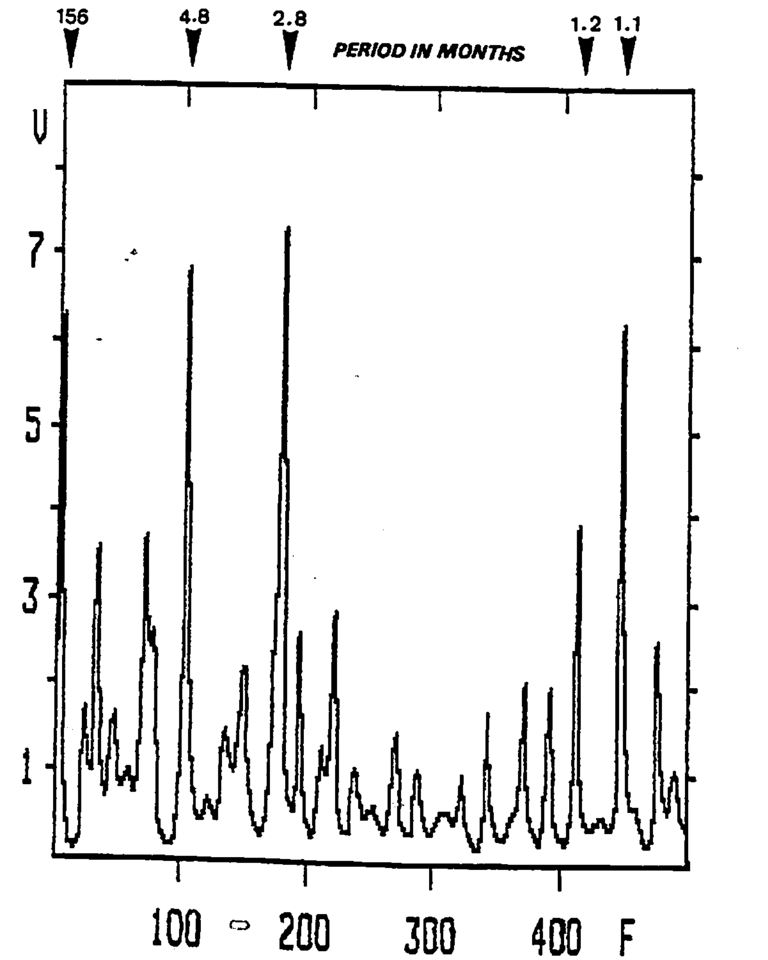

Figure 17: Maximum entropy spectrum of the same sample of X-ray bursts equal to or greater than class X1 as presented in Figure 16. The analysis based on the Burg-algorithm includes 312 data points and has a filter length of 82 coefficients. The frequency f is measured in millicycles per sampling interval of half a month. The ordinate axis indicates the relative variance of the respective frequencies. The outstanding peaks conform with those in the spectrum of Figure 16. This points to a cyclic pattern in the investigated sample of X-ray flares.

discovered the neutral proton and do not see that."[44] The Earth's magnetic field was unusually quiet at that time. The mean value of the Mayaud index for January 18 to 22, 1932, was $aa = 5$ and the standard deviation $\sigma = 0.8$, wheras the annual mean reached $am = 19$. However, when the physicist Klaus von Klitzing on February 5, 1980, observed facts that pointed to a quantized Hall effect, he at once fully realized the theoretical meaning of his finding;[45] it was a genuine Eureka moment that won him the Nobel prize. This time there was strong geomagnetic activity around the date of observation. The Mayaud index reached $aa = 67$ on February 6, 1980 ($am = 18.1$). As energetic flares were continually monitored by means of satellite instrumentation, there is confirmation that the strong geomagnetic activity around the date of discovery coincided with an X-ray burst of class X2 and a proton event.

3. SUCCESSFUL SEARCH FOR CYCLES OF FLARES

With respect to the multiple effects of energetic solar events, there is urgent need to develop a dependable flare forecast. Cycles of flares, if they existed, could be a help in this endeavour. But the general opinion of astronomers is that flares show a stochastic distribution. Research in solar eruptions seems to follow the same type of history as that of sunspots. It took more than 200 years to find out that they form a cycle of 11 years. Credit for this discovery has to be given to the pharmacist Schwabe; professional astronomers thought that sunspots were stochastically distributed. Fortunately, the delay with flares will be shorter. It has been shown that there are distinct cycles of energetic flares.[46] Energetic X-ray bursts below 12 Å are the hallmark of highly energetic X-ray flares and proton flares. They are a good general indicator of the geophysical significance of flares. X-ray bursts can only be observed by satellite instrumentation (SOLRAD/SMS/GOES). Such data in the 1 to 8 Å range are available from 1970. They beg for an analysis of their distribution over time.

Accordingly, all X-ray events $\geqslant$ X1 reported 1970 to 1982 in the Ursigrams of IUWDS and the prompt reports of Solar-Geophysical Data have been subjected to spectral analysis. Figure 16 presents the Blackman-Tukey power spectrum [47] of these flare-generated X-ray bursts. The weighted numbers of the observed bursts were summed within equidistant sampling intervals of half a month. The weights were derived from the X-ray class of the respective bursts. Thus, for example, the value 9 was assigned to a sampling interval comprising one burst X5 and two bursts X2. The resulting time series includes 312 data points. The frequency f is measured in millicycles per sampling interval of half a month. The ordinate axis designates the relative variance V of the respective frequencies. The spectrum shows prominent peaks at 156, 4.8, 1.2, and 1.1 months. The amplitudes around 1.1 months are near the highest resolvable frequency, though not beyond the limit defined by the Nyquist frequency. Yet an analysis based on a sampling interval of ¼ month yields the same result.

There are indications that the most pronounced peaks are real. R in Figure 16 designates the adopted Markov red noise, an appropriate model of random variability in spectra based on the Fourier cosine transform of estimates of the autocorrelation function.[48] The significance of the deviation of prominent peaks from the Markov red noise level can be evaluated by means of a special χ^2-test.[49] The resulting confidence levels CL are marked in Figure 16. The peaks at 2.8 and 1.1 months are significant at the 99% level while the peak at 4.8 months reaches the 95% level. Two further peaks approach this zone of significance. The peak around 156 months is at 83%, and the peak at 1.2 months at 90%.

These results are replicated by another approach. J. P. Burg [50] has developed a new form of spectral variance analysis, the maximum entropy spectral method (MEM), which shows much higher resolution than earlier methods, especially at lower frequencies. The new method reaches an exactness and sharpness that matches the optical spectra. Meanwhile, the MEM is practised in several scientific fields including astronomy and geophysics. Figure 17 shows the result of the maximum entropy spectral analysis applied to the same time series of X-ray bursts comprising the same sampling intervals of half a month. The calculation based on the Burg-algorithm covers 312 data points and 301 frequencies. The filter length of 82 coefficients is in accord with the suggestion of most authors not to go beyond 30% of the number of data points.[51] The extreme sensitivity of the MEM can lead to spectral shifts or spectrum instability, especially when the filter length is extended beyond 30 to 40% of the length of the time series. Experiments with different filter lengths up to 40% show that the spectrum presented in Figure 17 is stable. There is no shift in the outstanding frequencies. The MEM spectrum shows the same prominent peaks at the same frequencies as in the Blackman-Tukey power spectrum. A narrower sampling interval of ¼ month does not change the result.

It is a disadvantage of the MEM that an acknowledged reliability test of spectral peaks does not yet exist. According to the simple and useful "rule of thumb" expressed by Stuart *et al.*,[52] a spectral peak is regarded to be significant if it contains at least three computed points which deviate from the noise and has a maximum two or three times greater than the surrounding noise level. According to this standard the peaks in Figure 17 marked by period pointers deviate significantly from the noise. As these are the same peaks as in the Blackman-Tukey spectrum of Figure 16 that proved to be significant at confidence levels going up to 99%, there is sufficient evidence supporting their reality. A further replication is contributed by dividing the data set in half. The maximum entropy spectra for each half again set off the peaks around 4.8, 2.8, 1.2, and 1.1 months; only the 156 months period is lost, as was to be expected.

V. PLANETARY CONTROL OF THE SUN'S MOTION ABOUT THE CENTRE OF MASS OF THE SOLAR SYSTEM

The prominent cyclic features are consistently present in all spectra examined. Thus, there are sufficient reasons to propose the working hypothesis that the incidence of X-ray flares in the 1 to 8 Å range shows a cyclic pattern. Where do these flare cycles come from? As to predictions, this is a crucial question because the analysis is based on the rather small time-span of 13 years. If there are strong variations in the actual period of cycles, forecasts of flares and connected terrestrial events will go astray if it is not clear which changes will occur. It will be shown that the prominent amplitudes in the spectra indeed represent quasi-cycles with wide variations in their periods. The knowledge of the mean period of such quasicycles is no real help in predictions. The 11-year sunspot cycle with a range of variation from 7 to 17 years is an example of this. As long as it is not known how the cycle is regulated, there will be no solid basis for predictions. Without a reasoned physical background to guide selection, there is a severe risk of finding accidental patterns in diverse and varied data sets. The statistical analysis of past data does not constitute a reliable means to foresee future change in the data pattern. Thus, it is of both practical and theoretical importance that the spectrum can be exactly related to the variation in astrophysical quantities and to calculable planetary configurations by an approach following the fundamental rule of Operations research that the behaviour of any part of a system has some effect on the behaviour of the system as a whole. The results were tested by extended forecast experiments described above.

The first process involved are impulses of the torque (IOT) in the Sun's motion about the centre of mass of the solar system (CM) that were mentioned already. They are induced by special heliocentric constellations of the giant planets Jupiter, Saturn, Uranus, and Neptune. Figure 18 shows the ecliptic positions of CM relative to the Sun's centre for 1945 to 1995. The heliocentric representation and the line marking the limb of the Sun make it easy to see whether CM is to be found above or below the Sun's surface; most of the time it is on the outside of the Sun's body. The distance of both centres varies from 0.01 to 2.19 solar radii. It takes 9 to 14 years to complete one revolution. In relation to the galactic centre only CM follows an elliptic path around the centre of mass of the Milky Way system, whereas the Sun describes a very irregular helix around the elliptic line of motion of CM. The planets' paths are still more complicated. There is mutual interdependence. While the planets make the Sun oscillate around CM, the Sun induces a still more intricate dance of the planets about the centre of mass of the solar system. Newton was the first to see this: "Since that centre of gravity is continually at rest, the Sun, according to the various positions of the planets, must continually move every way, but will never recede far from that centre."[53] In 1928 Ludwig Zehnder [54] suspected a connection of the Sun's motion with the 11-year sunspot cycle. Paul D. Jose [55] made a thorough computer analysis of this special relation in 1965. Unfortunately, his predictions for the 11- year sunspot cycle No. 21, based on his analysis, failed to be accurate.

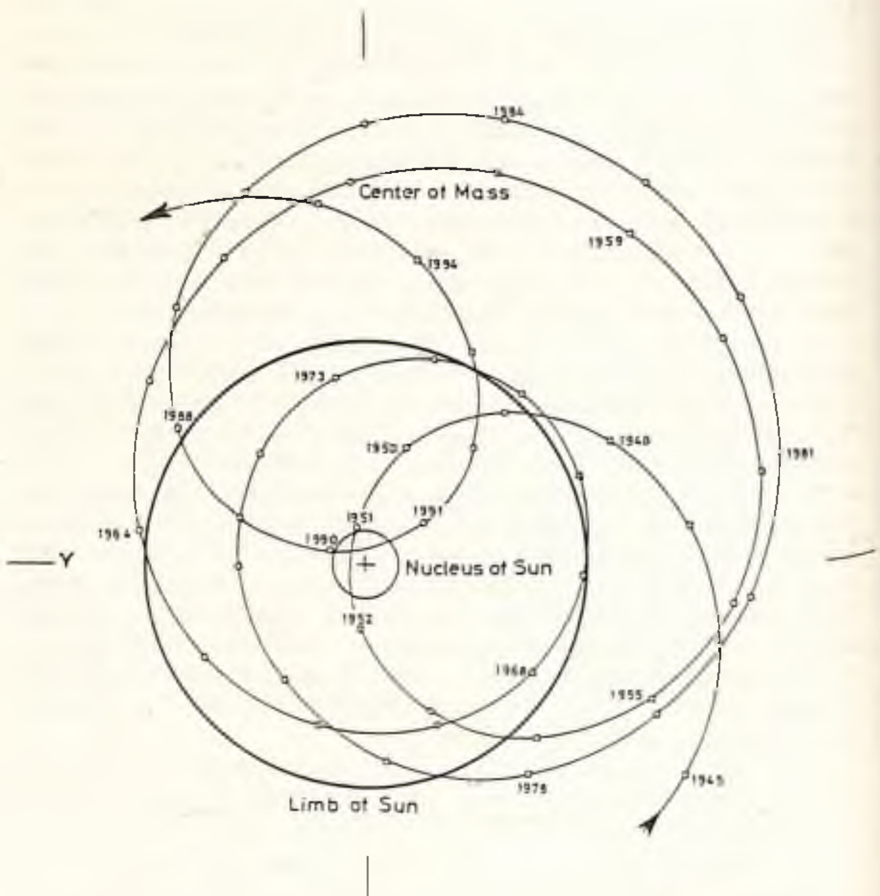

Figure 18: Position of the centre of mass of the solar system CM in the ecliptic plane relative to the Sun's centre CS for the years 1945 to 1995. Heliocentric representation and marking the limb of Sun make it easy to see whether CM is above or below the Sun's surface. The distance of both centres varies from 0.01 to 2.19 solar radii.

VI. PLANETARY REGULATION OF SECULAR AND SUPERSECULAR SUNSPOT CYCLES

Since the middle seventies attention has been focused on special phases in the Sun's revolution about CM that proved to be the hallmark of all kinds of cycles of solar activity.[56] The Sun reaches extreme positions relative to CM when the giant planets form special constellations. The Sun's centre (CS) and CM come very near to each other when Jupiter on one side of the Sun is in opposition to Saturn, Uranus, and Neptune on the other side, whereas CS and CM reach their greatest distance when all of the giant planets form a conjunction. Conspicuously, just in 1951, when the Sun's centre CS was very near CM and the Sun changed from approaching it to receding from it, the secular sunspot cycle of about 80 years reached a maximum. This was no fortuitous fit. Further analysis showed that such phases of spectacular change in the Sun's orbital motion coincide with relatively strong impulses of the torque (IOT).[57]

The torque T acting on the Sun is defined by $T = dL/dt$, which is the first derivative of the angular momentum L of the Sun's orbital motion. Impulses of the torque, measured by the time integral $\Delta L = \int_{t_0}^{t_1} T(t)dt$, occur when T approaches zero, changes sign, and shows a more or less sharp increase in the new direction measured in the relatively short time interval $t_1 - t_0 = 300$ days. L, the Sun's orbital momentum, can vary from about -0.1×10^{47} g cm^2 s^{-1} to about 4.3×10^{47} g cm^2 s^{-1}, which is an increase by a factor of up to 40 and more. The maximum value of the Sun's orbital momentum reaches 25% of the Sun's rotational momentum which is 1.7×10^{48} g cm^2 s^{-1}. If there were spin-orbit coupling, a transfer of angular momentum from the Sun's orbit to the Sun's spin on its axis or vice versa, this could make a difference of more than 5% in the Sun's equatorial rotational velocity,[58] which is actually observed.

When consecutive IOT are taken and smoothed to constitute a new time series, a wave pattern emerges that bears information as to the epochs of extrema in the secular Gleissberg-cycle. Figure 19 shows this wave for the years 1100 to 2100 A.D. It has a mean length of 166 years, but each extremum, whether positive or negative, is correlated to a maximum in the secular sunspot cycle, while minima occur when the curve reaches zero values. The mean interval between consecutive extrema is 83 years and varies within 47 to 118 years. Wolfgang Gleissberg found corresponding variations in the secular cycle that range from 40 to 120 years. The cycle length of 83 years conforms with results elaborated by G. W. Brier. He found a prominent period of 83 years in the unsmoothed cosine transform of 2148 autocorrelations of 2628 monthly sunspot numbers.[59] The assessment of the mean length of the secular torque cycle of 83 years is based on calculations covering the period 5259 B.C. to 2347 A.D.[60] The fat arrows in Figure 19 indicate the epochs of maxima in the secular sunspot cycle assessed by Wolfgang Gleissberg making use of data by D. J. Schove.[61] These epochs are in phase with the computed secular torque cycle. The wave in Figure 19 reveals that there is an excess of positive or negative impulses of the torque for many decades. This is an indication of a cumulative effect.

The plot in Figure 20 covers the years 300 to 1100 A.D. The smoothed curve, elaborated by W. Gleissberg, is based on detailed data by J. D. Schove.[62] D_M

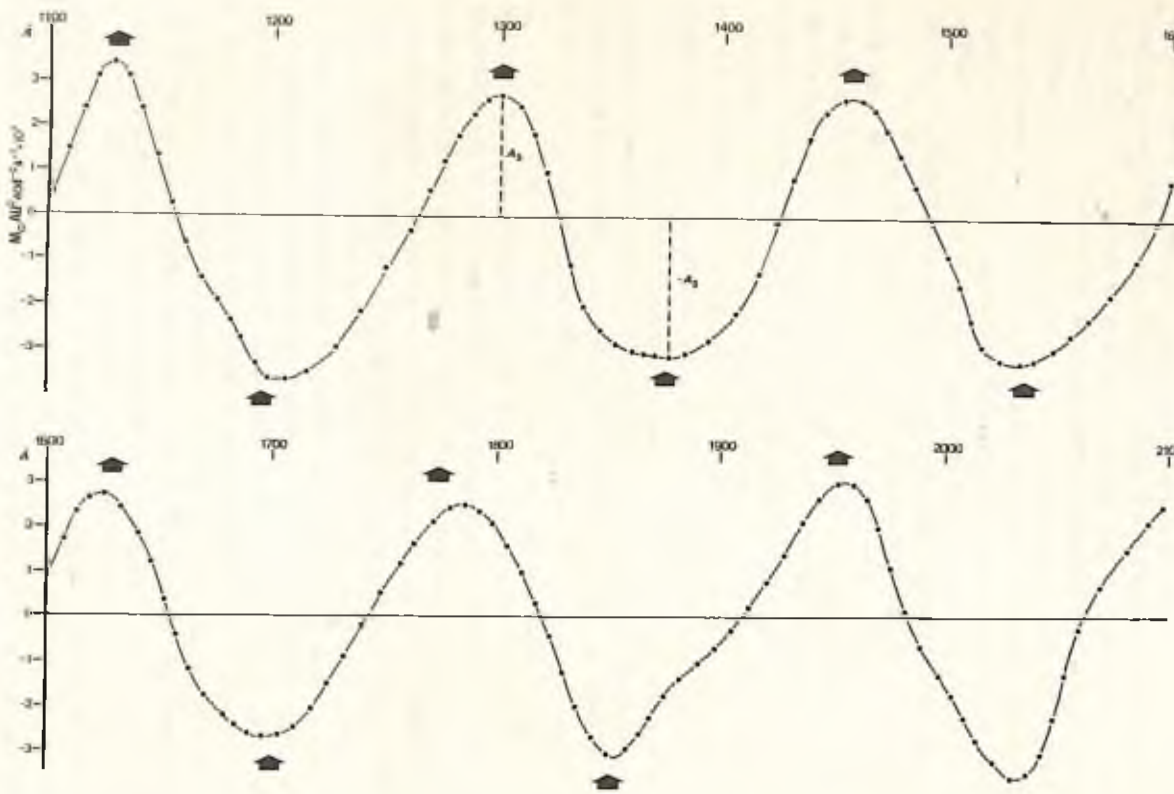

Figure 19: Smoothed time series of consecutive impulses of the torque (IOT), the epochs of which are indicated by dots. The resulting wave pattern is related to the secular cycle of sunspot activity. The average wave-length is 166 years. Each extremum at mean intervals of 83 years is connected with a maximum in the secular sunspot cycle. These maxima, as assessed by W. Gleissberg, are marked by fat arrows. Minima occur when the wave is near zero values. The wave reflects the effect of solar system configurations that cause impulses of the torque.

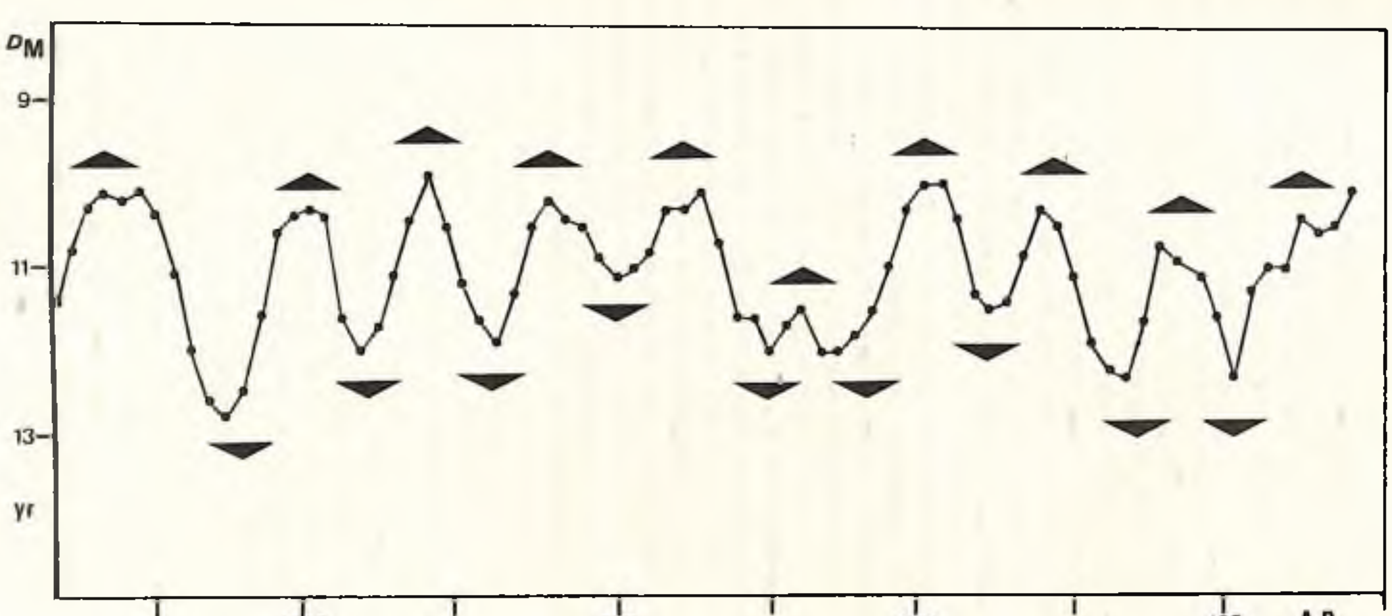

Figure 20: Secular cycle of sunspots for 300 to 1100 A.D. after W. Gleissberg and D. J. Schove. Flat triangles indicate epochs of secular maxima and minima derived from calculated IOT-data. The extrema of the two data sets are in phase.

represents intervals between consecutive 11-year maxima that reflect the secular cycle. Minima of D_M correspond to strong sunspot maxima and inversely. The flat triangles indicate the calculated epochs of secular maxima and minima based on the secular torque cycle. The data sets are in phase. An evaluation of the total result for the years 300 to 1980 confirms the high degree of synchronism of the Gleissberg-data and the calculated torque epochs. A Pearson-test yields the value 54.5 (1 degree of freedom; $P \ll 0.00001$) for the maxima, and 22.3 (1 degree of freedom; $P < 0.00001$) for the minima. When subsets are formed, the results prove to be homogeneous. The torque wave points to a secular sunspot minimum past 1990.

The extrema in the secular wave of IOT can be taken to constitute a smoothed supersecular wave with a quasi-period of 391 years. This long wave points to an imminent supersecular sunspot minimum about 2030.[63] There are indications that secular and supersecular sunspot minima are related to variations in climate. Thus a prolonged period of colder climate is about to be initiated by the secular minimum past 1990, will reach its deepest point around the supersecular minimum in 2030, and come to an end about 2070. A shorter torque cycle of 31 years, based on an analysis of a cross-correlation function of sunspots and IOT, made it possible to predict the end of the Sahelian drought three years in advance. The forecast: "The next drought maximum is to be expected about 2010. A humid period should already begin within 2 yr and reach a first maximum about 1986", was published in 1983.[64] There was enough rain in the Sahelian countries in 1985 and still more in 1986. Geoffrey Dean, whose negative review of forecasts based on planetary constellations has been mentioned above, had received a preprint of this paper that also contained the evaluation of the positive result of the forecasts of energetic flares for the years 1979 to 1981 as well as the successful prediction of X-ray bursts > X9 in 1982. He nevertheless declared that successful predictions based on planetary configurations did not exist.

VII. PLANETARY FORCING AND FLARE CYCLES

Cycles of solar activity of medium wavelength, like the 11-year sunspot cycle, are also related to IOT.[65] But even such short cycles as those that emerged from the spectral analysis of the distribution of energetic flares are connected with IOT. Strong impulses of the torque are initiated when the planet Jupiter, the centre of mass CM, and the Sun's centre CS are in line (JU-CM-CS). There are two types of JU-CM-CS events: those that are accompanied by a sharp increase in orbital momentum and centrifugal motion of the Sun away from CM (JU-CM-CSc), and those that coincide with a decrease in orbital momentum and centripetal motion of the Sun toward CM due to prevailing gravitation (JU-CM-CSg). These two different types can have different effects on the Sun and solar-terrestrial interaction. JU-CM-CSg events that can be related to the investigated time series of energetic flares, covering the period 1970 to 1982, occurred during 1970.02 and 1982.83. They formed a cycle with a period of 153.7 months.

Just this cycle and harmonics of it represent most of the variance in the flare spectra discussed above.[66] The most prominent amplitudes in Figures 16 and 17 point to the torque cycle itself, to the exact harmonics 4.8 months and 1.2 months with a neighbouring peak at 1.1 months, and to a strong amplitude at 2.8 months, that seems out of sequence, since 2.4 months would be the fitting harmonic between 4.8 and 1.2 months. But the shift to 2.8 months seems to be the result of the interference with another flare cycle in this range, regulated by tidal planets. Its mean period is 3.36 months. This value, when combined with the 2.4 month harmonic of the torque cycle, yields a mean value of 2.88 months which properly matches the strong amplitude at 2.8 months in the flare spectrum.[67]

This combination is consistent in so far as the torque harmonic of 2.4 months is nearer to the interfering period of 3.36 months than the torque harmonic of 4.8 months. But this latter harmonic is also connected with the interfering cycle. Calculation shows that the period of the 3.36-month cycle has a range of variation of ± 1.6 months. If it gets in phase with the torque harmonic of 4.8 months, which occurs at irregular intervals, as a rule highly energetic X-ray bursts are released. This connection is of practical importance in assessing the category of expected X-ray bursts in predictions. There is a gap between the prominent amplitude related to the torque cycle of 154 months itself and its higher harmonics of 4.8 months and beyond. This could be due to resonance with the interfering oscillator, the period of which varies about 3.36 months. Only the higher harmonics of the torque cycle are then expected to respond.

There is a wealth of papers that try to establish a relation between tidal planets and sunspots. Critical authors stress that all tidal planets, when in conjunction, could only raise a tide of a few millimeters on the Sun. But it should be taken into consideration that the horizontal component of the tidal forces could be of interest, as the Sun's gravity acceleration is 28 times that of the Earth's. E. Oepik[68] has shown that the mean velocity of tidal currents on the Sun can reach about one-third of tidal currents generated by the Moon on Earth. This is not negligible as the plasma in the Sun is subject to magnetohydrodynamic instabilities and turbulence. There are only few papers

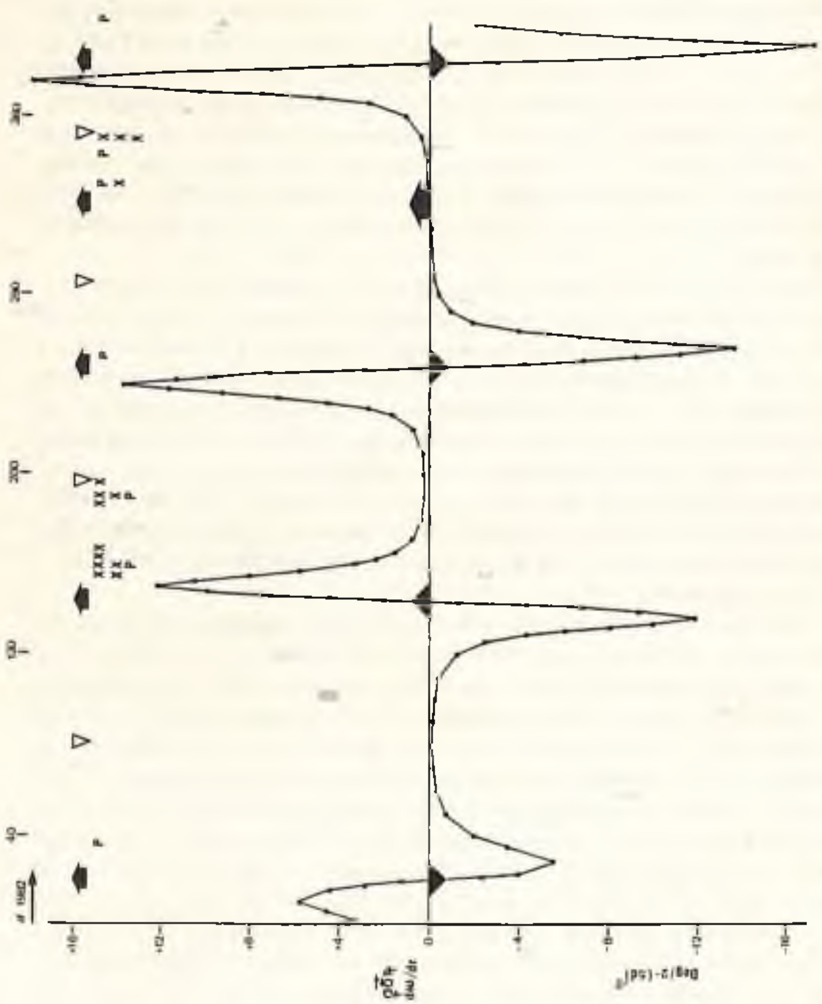

Figure 21: The angular acceleration $d\omega/dt$ of the composed vector of the tidal forces of Venus, Earth, and Jupiter, plotted for 1982, forms a cyclic pattern that correlates with observed proton events (P) and X-ray burst equal to or greater than class X3 (X). Active phases in the related flare cycle, displayed on top, begin when $d\omega/dt$ changes from positive to negative values, or inversely. These crucial zero phases that coincide with a boundary transition are indicated by fat marks. Lulls in flare activity begin in the middle between consecutive zero phases; these lull starts are [illegible]

that deal with relations of tidal planets with flares.[69] This is difficult to understand, as it is known from Skylab observations that flares are set off by initial disruptions in hot coronal loops over active regions. It is easier to imagine that weak tidal disturbances may trigger such events in an unstable zone of the Sun's atmosphere than to concede that the tide-generating forces could act on the strong magnetic fields that are contained in sunspots.

Calculations of the relative tidal forces of the planets Mercury to Saturn show that the latter is as negligible as that of Mars. Comparison of the composed vector of the tidal forces of Venus, Earth, and Jupiter, excluding or including Mercury, shows that the vector including Mercury oscillates around the vector of Venus, Earth, and Jupiter. Therefore, only the latter was investigated in its relation to energetic flares marked by X-ray bursts equal to or greater than class X2 ($\geqslant$X2). Figure 21 presents the result. Unexpectedly, no cardinal correlations with the magnitude of the vector emerged. But the change in direction proved to be crucial. The angular acceleration $d\omega/dt = d^2\varphi/dt^2$ of the vector forms a cyclic pattern which shows a strong relation with X-ray bursts observed since 1970. Figure 21 reflects the course of the cycle in 1982. The abscissa axis designates the days of 1982. The ordinate represents the time rate of change of the angular velocity of the vector. The active phase of the related flare cycle begins when the curve crosses the time axis. This is again a boundary phenomenon, a transition from the domain of one quality into the realm of the opposite quality, which is together the transgression of a borderline; $d\omega/dt$ changes from positive to negative acceleration, or inversely. These crucial zero phases are indicated in Figure 21 by fat triangles, and in one case by a fat arrow. The effect on flares is stronger when the curve ascends then when it descends. Furthermore, the strength of the effect is inversely proportional to the steepness of the ascent or descent. Slow ascent releases prolonged flare activity reaching a high level of energy display. Cases of less steep ascent occur when the magnitude of the vector reaches maximum values. The fat arrow on the time axis designates such a situation.

Lull phases in the flare cycle always begin in the middle between two zero values of $d\omega/dt$. Their start is marked by the second harmonic of the respective cycle. On top of Figure 21 the active and the lull phases of the tidal flare cycle are marked by arrows pointing upwards, and by white triangles pointing downwards. Observed proton events and X-ray bursts $\geqslant$ X3 are indicated by P and X. They match the phases of activity without exception. In 1982 the steep ascent marked by a triangle pointing upwards had as strong effects as the slow ascent marked by a fat arrow; but the latter category showed a stronger overall effect since 1970. When all 118 X-ray bursts $\geqslant$ X2 observed since 1970 are tested, 96 of them fit active phases in the tidal cycle, and only 22 inactive ones. A Pearson-test yields the value 47 for 1 degree of freedom ($P < 0.00001$). All events $\geqslant$ X6 fell into the active periods. As the sample covers more than 40 cycles, the result seems to indicate a dependable relationship.

In the spectra of energetic X-ray flares presented in Figures 16 and 17, the two prominent peaks in the range of higher frequencies at 1.1 and 1.2 months are clearly set off though they are close together. The 1.2-month amplitude has been explained to be a harmonic of the torque cycle. The tidal cycle is involved too. The exact period of the neighbouring amplitude in the spectra is 1.12 months, precisely the third harmonic of the period 3.36 of the tidal cycle.

The change in the length of the tidal cycle and the torque cycle is very irregular. The length of the $d\omega/dt$ cycle varies between 40 and 134 days. The current torque cycle marked by JU-CM-CSg events 1982.83 and 1998.56 will have a length of 15.7 years, compared with 12.8 years of the former cycle. So the former 4.8-month cycle changes to 5.9 months, the former harmonic at 2.4 months will be at 2.9 months, and the combined cycle at 2.8 months will shift to 3.2 months. These variations affect forecast techniques that make use of the interference effects of the torque cycle and the tidal cycle. The complex results show how difficult it would be to predict solar flares and their terrestrial effects without knowledge of the intricate regulation of solar activity by both the giant planets and the tidal planets, the effects of which are coupled by Jupiter, the main factor in both groups. The new forecast issued in January 1983, discussed in the beginning, was based on the current torque cycle with a period of 15.7 years. The strongly varied periods of its harmonics in comparison with those of the former cycle and the tidal cycle were allowed for. The change in the pattern offered a chance to test the reliability of the connections in question. As has been shown above, this test yielded a distinct confirmation.

VIII. MODULATION OF THE SUN'S ROTATION BY PLANETARY CONFIGURATIONS

The successful forecast of highly energetic events greater than class X9 in 1982 was directly founded on the JU- CM-CS event in 1982.83. Such constellations are nearly always accompanied by very energetic eruptional activity.[70] They seem to affect such activity via the Sun's rotation rate. The Sun, rotating on its axis, and the Sun, revolving around CM, could be looked at as coupled oscillators capable of internal resonance resulting in slight positive or negative accelerations in the Sun's spin. Such accelerations are actually observed. Speeding up or slowing down of the Sun's rotation rate is liable to influence the Sun's activity. Slower rotation seems to be linked to enhanced activity and faster rotation to weak activity. According to investigations by John E. Eddy,[71] based on historical observations by Scheiner and Hevelius, the rotation of the Sun's equator sped up just before the Maunder Minimum, a protracted period of very weak sunspot activity in the 17th century, whereas its rotation rate about 1620, near a secular maximum of sunspots, was much the same as it is today. Modern data confirm this relation. Mt. Wilson observations[72] show two striking jumps in the Sun's rate of rotation in 1967 and in 1970. These jumps into deceleration concurred with the epochs of IOT, as can be seen in Fig. 22. The arrows indicate heliocentric conjunctions of Jupiter and CM (JU-CM-CS) that initiate IOT. A further deceleration was observed in 1974, the epoch of the following JU-CM-CS event.

The planet Jupiter that is involved in these constellations plays a dominant role even among the giant planets that regulate the Sun's oscillations about CM. Jupiter holds 71% of the total mass of the planets and 61% of the total angular momentum of the system, whereas the Sun governs less than 1% of the angular momentum. This seems to be indicative of a case of spin-orbit coupling of the spinning Sun and the Sun revolving about CM, involving transfer of angular momentum from Jupiter to the revolving Sun and eventually to the spinning Sun. With respect to the angular momentum conservation law it makes sense that the observed slowing down in the Sun's spin coincides with an increase in the Sun's orbital angular momentum. Coupling could result from the Sun's motion through its own electric and magnetic fields that are relatively strong near the Sun's body. Even at a height of one solar diameter above the Sun's surface the electron density is still about 1 million electrons per cm^3. The Sun's average distance from CM is 1.1 solar radii. Thus, the low corona can act as a brake on the Sun's surface.[73]

The older Mount Wilson data were not corrected for scattered light. Meanwhile corrected rotation data are available that are based on a single reduction method for the entire interval 1967 to 1982. This time series elaborated by R. Howard[74] covers Carrington rotation numbers 1516 to 1726. They are displayed on the x-axis of Figure 23 and correspond to the period December 29, 1966, to September 4, 1982. The rotation values represent the equatorial angular sidereal rotation rate averaged over respective rotations. The plot is based on the running variance of these data. Running means are a well known feature in statistics. Variance, the square of the standard deviation, can be subjected to a similar process. The respective moving values

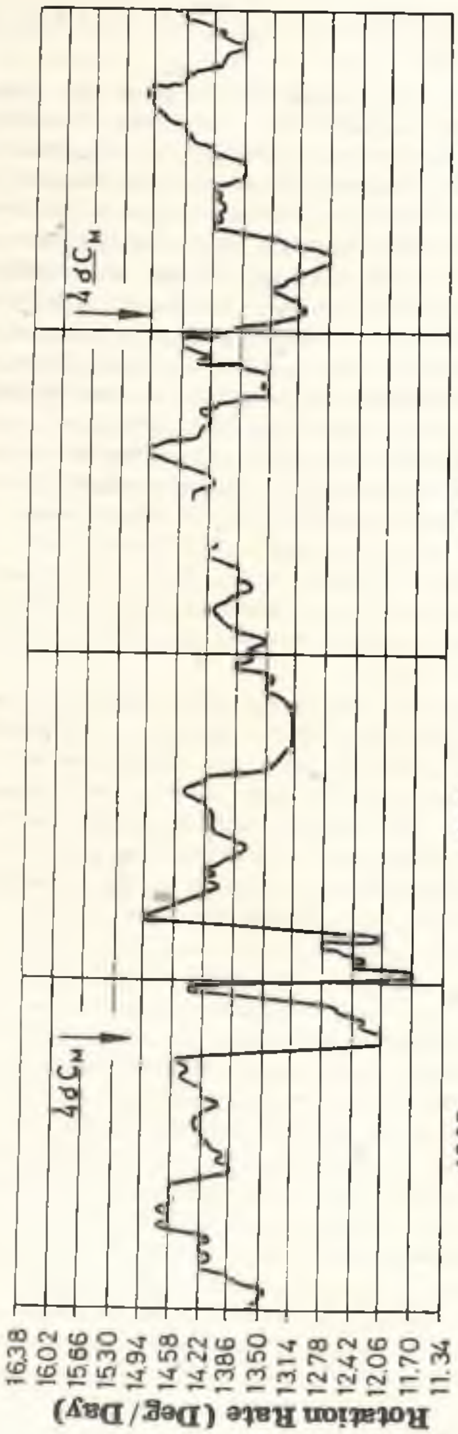

Figure 22: Sudden decrease in the Sun's rate of rotation (Mount Wilson data) related to heliocentric conjunctions of Jupiter with the centre of mass CM.

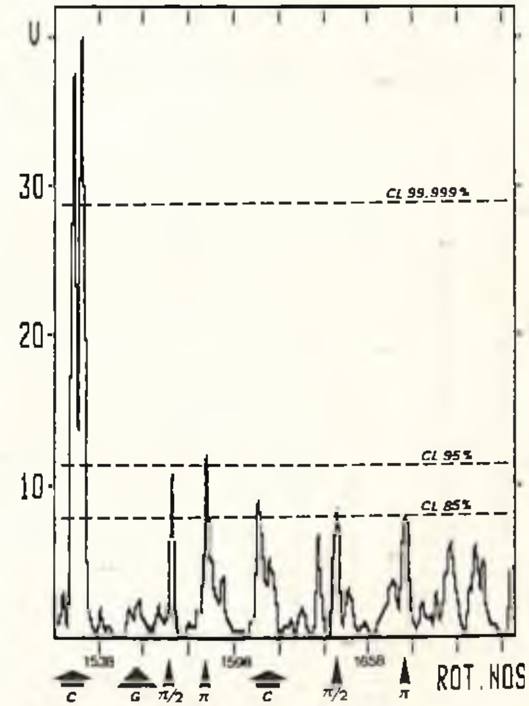

Figure 23: Smoothed running variance V of the Sun's equatorial angular sidereal rotation rate (Mount Wilson data) covering Carrington rotations 1516 (December 29, 1966) to 1726 (September 4, 1982). Fat arrows point to JU-CM-CSc epochs (C), while a triangle marks the epoch of a JU-CM-CSg event (G). Arrow-heads designate harmonics of quasi-cycles formed by consecutive JU-CM-CS events.

of the variance cover two consecutive rotations, thus measuring the variation in variability from one rotation to the next one. These results have been subjected to a Gaussian low-pass filter eliminating short range features covering less than five rotations. The ordinate axis measures this smoothed running variance. The epochs of JU-CM-CS events in 1967.8 and 1974.48 are marked by fat arrows and the letter C, whereas the epoch of the event in 1970.02 is indicated by a fat triangle and the letter G. This makes allowance for the two types of JU-CM-CS events mentioned already: those that go along with an increase in orbital momentum and resulting centrifugal motion of the Sun (C), and those that initiate a decrease in orbital momentum and centripetal motion due to prevailing gravitation (G).

The two C-conjunctions are related to prominent variance peaks significant at the 85% confidence level (CL) and far beyond. If the running variance is not subjected to smoothing, the second C-peak in 1974 reaches the 95% confidence level. There is only a relatively small variance peak connected with the G-conjunction in 1970. This points to a different quality of this kind of events, which was to be expected, as the orbital momentum does not increase, but is diminished. Nevertheless, G-conjunctions, too, have an impact on the Sun's differential rotation. The Mount Wilson rotation data do not cover the following G-conjunction in 1982.8. It is beyond the frame of the plot. If consecutive conjunctions are thought to form quasi-cycles initiated by the

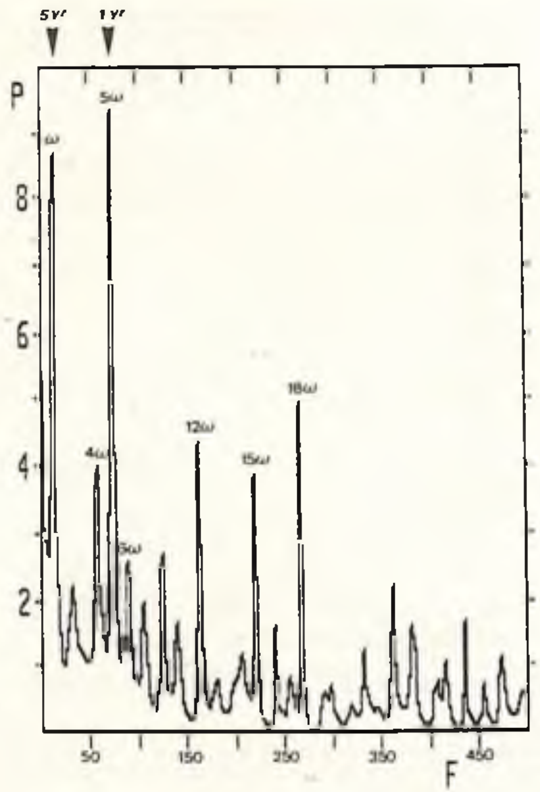

Figure 24: Maximum entropy spectrum of the running variance of the Sun's equatorial rotation rate (Mount Wilson data). The prominent peaks represent the mean period (ω) of the JU-CM-CS cycles involved and its harmonics 4ω, 5ω, 6ω, or simple multiples of these frequencies.

respective foregoing event, there should emerge subcyclic effects in the rotation data, provided that these are connected with the fundamental cycle. The quasi-cycle initiated by the second C-conjunction in 1974.5 had a period of 8.3 years as the following conjunction occurred in 1982.8. It can be seen in Figure 23 that the phases π/2 and π radians (90° and 180°), indicated by small pointers, coincide with variance peaks that are significant at the 85% confidence level. In the unsmoothed data these peaks reach the 95% level. The corresponding phases are outstanding, too, in the foregoing quasicycle initiated by the G-event indicated by a triangle. The peaks reach the 99% confidence level in the unsmoothed data. So far only the equatorial rotation rate has been investigated. As the Sun's differential rotation is rather complex, decelerations or accelerations in other latitudes may be involved.

As shown in Figure 23, subcyclic features like the second and fourth harmonic of cycles of JU-CM-CS events can be identified by their mark on the Sun's rotation. Fig. 24 is a confirmation of this connection. It presents the maximum entropy spectrum of the rotation data. It covers 211 data points (Carrington rotations No. 1516 – 29 December 1966 – to No. 1727 – 4 September 1982) and is based on 70 filter coefficients. The frequency *f* is measured in millicycles per sampling interval of a Carrington rotation. The ordinate axis

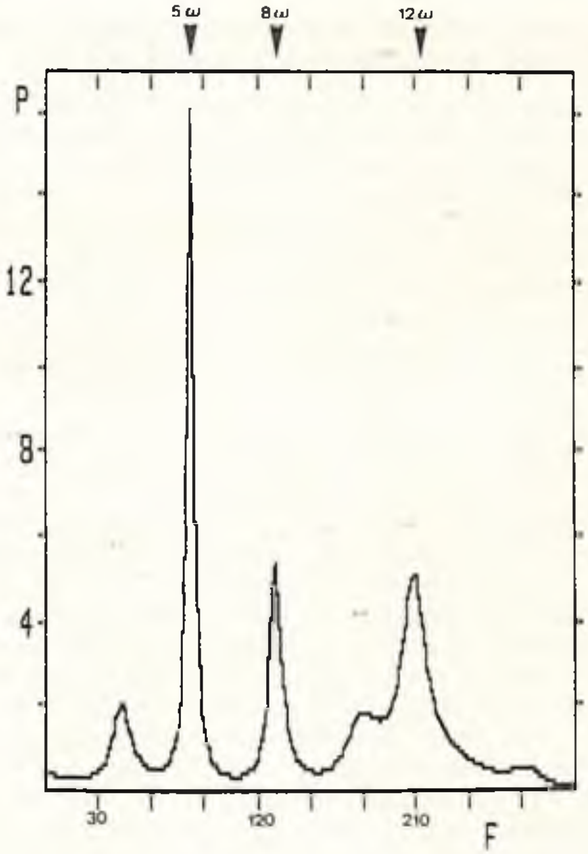

Figure 25: Maximum entropy spectrum of the running variance of Mount Wilson rotation data covering the JU-CM-CS quasi-cycle 1970 to 1974.5. The prominent peaks point to the frequency 5ω and the double value of 4ω and 6ω.

designates the relative power *P* of the respective frequencies. The spectrum is stable. A change in the number of filter coefficients does not generate spectral shifts. The prominent low frequency peak, the fundamental ω, has a period of 66.67 Carrington rotations or 5 years. This is exactly the mean interval of the JU-CM-CS events involved (1967.8, 1970, 1974.5, 1982.8; (2.2yr + 4.45yr + 8.35yr)/3 = 5yr). The outstanding harmonic is 5ω with the period 1 year. It is known in the physics of vibrating systems, especially that of vibrating strings, that the 5th harmonic is in a central position. An indication of this is the fact that in musical harmony the three major chords F-A-C, C-E-G, and G-B-D each represent fundamental tone sequences with the frequency ratio 4 : 5 : 6.[75] The neighbouring harmonics 4ω and 6ω are exactly represented in the spectrum, too, and in addition the peaks 12ω, 15ω, and 18ω, which are simple multiples of the 4th, 5th, and 6th harmonic. Figure 25 corroborates the weight of these harmonics. It shows the maximum entropy spectrum of the rotation data of the single JU-CM-CS-cycle 1970 to 1974.5. The 5th harmonic again stands out from the other frequencies, and the prominent peaks 8ω and 12ω are simple multiples of the 4th and 6th harmonic.

IX. HARMONICS OF SOLAR SYSTEM CYCLES, THE MAJOR PERFECT CHORD, AND HIGHLY ENERGETIC SOLAR ACTIVITY

These results beg for an experimental synthesis of the 4th, 5th, and 6th harmonic such that corresponding cosine waves are superimposed to form a resultant wave with the frequency of the fundamental which is the cycle of JU-CM-CS events. The amplitudes of the single cosine waves were chosen to form the inverse ratio 6 : 5 : 4. Figure 26 presents the prototypal pattern of the composite wave. The time units 0 to 100 on the x-axis represent normalized centesimal fractions of the period of JU-CM-CS cycles of any length. Thus events that occur in the same phase of cycles of different periods coincide in the prototypal pattern. Phase coincidence becomes immediately apparent. This is important as JU-CM- CS cycles show very different periods from 2 to 16 years.

Solar cosmic ray events, that are accompanied by very energetic X-ray bursts, were observed since 1942. As they are rare events, only 21 of them were listed through 1969. The epochs of these highly energetic proton events are marked in Figure 26 by the letter P. Out of 21 events, 17 match positive phases of the composite wave that are marked at the top by lines bounded by bars. The two phases that show a less steep descent, cycle fractions 20/100 to 26/100 and 50/100 to 55/100, seem to show a prolonged effect; thus three negative percentiles were added to the respective positive phases as indicated by those lines bounded by bars. A Pearson-test of the distribution of these 21 solar cosmic ray events yields $\chi^2 = 8.1$ for 1 degree of freedom ($P < 0.005$).

Since 1970 X-ray bursts have been continually observed by satellite instrumentation and listed in Ursigrams of IUWDS and in Solar- Geophysical Data, published by the National Oceanic and Atmospheric Administratrion (NOAA), in Boulder, Colorado. From 1970 through 1986 altogether 46 flare-generated X-ray bursts $\geqslant X4$ were recorded. The epochs of these bursts are indicated in Figure 26 by a.row heads. Out of 46 bursts 41 fit the defined positive phases of the composite wave; only 5 hit negative phases. A Pearson-test yields $\chi^2 = 28.2$ for 1 degree of freedom; $P = 1.1 \times 10^{-7}$. When only very energetic X-ray bursts $\geqslant X7$ are selected, all of 18 observed events fit the positive phases. A combination of cosmic ray events and bursts $\geqslant X4$ gives a sample of 67 events, 58 of which meet the positive phases of the superposition. A Pearson-test yields $\chi^2 = 35.8$ for 1 degree of freedom; $P = 7 \times 10^{-10}$.

This highly significant result was tested by predictions. According to a long-range forecast issued January 15, 1983, during respective positive phases of the JU- CM-CS cycle 1982.83 to 1990.3 – 15 Jan. to 1 April 1983, 1 Jan. 1984 to 1 Febr. 1985, and 1 Jan. 1986 to 9 Jan. 1987 – the incidence and weight of energetic X-ray bursts, proton flares, and geomagnetic storms were expected to reach 2.5 times that of less active intervening periods. Meanwhile, this forecast has turned out to be correct. All bursts $\geqslant$ X4, the most energetic proton events, and all severe magnetic disturbances fit the predicted phases of stronger activity: 3 Febr. 1983: $X4$; 4 Febr. 1983: proton event 340 particles $(\mathrm{cm}^{2}$ ster s$)^{-1}$ at 10 MeV; 5 Febr. 1983: $A\kappa = 110$; 16 Febr. 1984: proton event 660 particles; 24 April 1984: X13; 26 April 1984: proton event 2500 particles; 19 May 1984: $X4$; 20 May 1984: $X10$; 11 Nov. 1984: $A\kappa = 87$; 22 Jan. 1985: $X4$; 8 Febr.

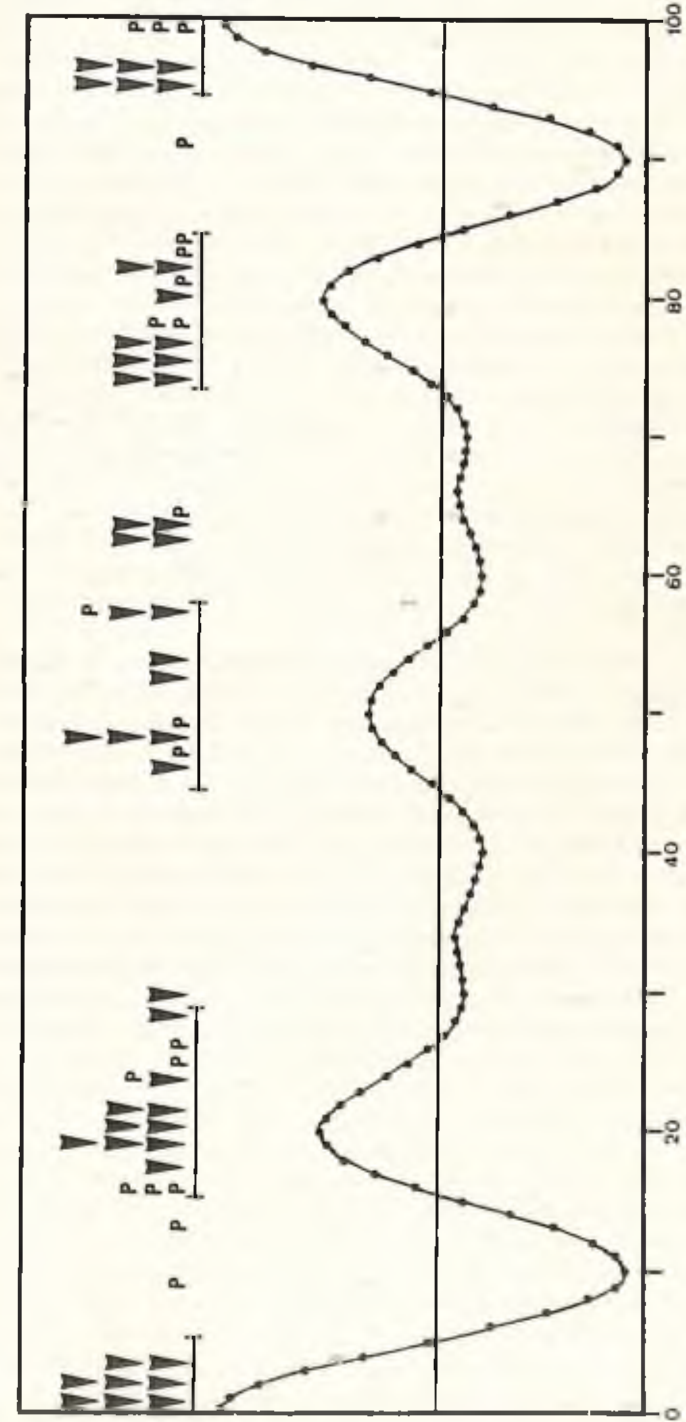

Figure 26: Prototypal pattern of a composite wave formed by the superimposition of harmonics with the frequency ratio 4 : 5 : 6. The time units 0 to 100 represent normalized centesimal fractions of JU-CM-CS cycles of any length. The positive phases of the composite wave coincide with clusters of solar cosmic ray events (P) observed from 1942 to 1969 and flare-generated X-ray bursts equal to or greater than class X4 (marked by pointers) registered 1970 through 1986.

1986: $A_K = 230$. These successful forecasts were again checked by astronomers and the Space Environment Services Center, Boulder.

The periods of predicted events > X9 in 1982 met a positive phase in the preceding JU-CM-CS cycle; this was one of the clues pointing to eruptional activity rising above the usual level. This shows how different cycles, that can all be derived from impulses of the torque initiated by JU-CM-CS events, can be used to develop a long range forecast of solar activity that covers most of the energetic events which are important in solar-terrestrial interaction. The cycles involved are often related to all kinds of JU-CM-CS events, and sometimes only to JU-CM-CSc or JU-CM-CSg events. It will be a difficult task to find out in detail how special IOT events are connected with special time series of solar-terrestrial data. The results presented here are only a first step in a new direction. It is intriguing that the ratio of the superimposed harmonics 4 : 5 : 6 is that of the major perfect chord in musical harmony. Kepler had found just this chord C – E – G when he analyzed the ratios of the velocities of different planets at aphelion and perihelion. Kepler's finding is also valid for the outer planets Uranus to Pluto.[76] Thus, the major perfect chord turns out to be a fundamental structural element of the planetary system. The results presented here are a new substantiation of the Pythagorean harmony of the spheres at a complex level that relates planetary configurations to the Sun's oscillations about CM, solar rotation, the Sun's activity, and solar-terrestrial interaction.

There is still another confirmation of harmonical relations. In Figure 26 one larger aggregation of 5 events at 63/100 on the horizontal axis is outside the positive phases. This position represents exactly the ratio 5 : 8 of the minor sixth in musical harmony, and together that of the golden section (61.8 : 38.2), key to aesthetic proportions in art. When allowance is made for this ratio, too, 63 out of 67 very energetic solar eruptions of the last 4 decades could have been forecast by means of JU-CM-CS cycles, their harmonics, and harmonical and aesthetic ratios. As has been shown, an actual forecast covering a period of seven years has proved successful since 1983. Such "composition" of dependable predictions based on key chords of the Sun's energetic music of the spheres is by no means an isolated feature. It will be shown in the final chapters that cosmic harmony expressed in precise consonant ratios is a paramount phenomenon that regulates the most important cycles of the Sun's energy display and their terrestrial response.

X. SOLAR SYSTEM CONSTELLATIONS AND GEOMAGNETIC DISTURBANCES

Geomagnetic storms, which are released by energetic solar eruptions, are important geophysical events. Newer results indicate that there is a connection with weather. Figure 27, after V. Bucha,[77] shows zonal type of atmospheric circulation (at top) as a result of geomagnetic disturbances caused by the Sun's eruptional activity, and meridional circulation (at the bottom) related to a lull in geomagnetic activity. This is a permanent feature that regulates the prevalence of warm westerly flow or cool arctic air over Europe and North America. A statistical analysis covering the years 1955 to 1974 yields a correlation coefficient $r = 0.65$. Bucha has tried to give a geophysical explanation of this correlation.

The bulk flow speed of the solar wind, that is indicative of the energy of eruptional mass ejections and resultant shock waves caused by solar eruptions, is strongly coupled to geomagnetic activity,[78] which in turn seems to be the common factor of a wide variety of terrestrial phenomena. Many authors including Sazonov,[79] Mustel,[80] Beynon and Winstanley,[81] Stolov and Shapiro,[82] and Sidorenkov,[83] have reported various connections between geomagnetic disturbances and features of the troposphere. Cobb[84] has shown that the monthly variation of the air- earth current from mean values at Mauna Loa, Hawaii, is correlated with Bartel's magnetic character index *Cp*.

According to Mustel[85] surface pressure increases in anticyclones and decreases in cyclones after isolated geomagnetic storms. King[86] has reported similar results. In a study that covers the years 1964 to 1971, Roberts and Olson[87] have found that troughs that enter the Gulf of Alaska or are formed there two to four days after a sharp increase in geomagnetic activity, tend to be larger than average size. Prohaska and Willett[88] applied Eigen-analysis technique to a matrix of cross-correlation coefficients between the geomagnetic *aa*-index and the monthly mean temperature at 32 United States stations, and isolated temperature anomaly patterns that are highly correlated with the *aa*-index. As this index is considered to be a strong descriptor of the solar wind, Prohaska and Willett hold that the source of the effect influencing the local temperature field through the atmospheric circulation is also driving the solar wind and disturbing the geomagnetic field.

Sazonov[89] and King[90] have drawn attention to the similarity between meteorological and geomagnetic contour maps. Neubauer[91] has discovered that sudden commencements of geomagnetic storms, released by solar eruptions, are related to displacements in the 70 mb polar vortex in the lower stratosphere which in turn influence the polar vortex in the troposphere. The shift in the 70 mb polar vortex is caused by a localized sudden stratospheric warming. Of 66 magnetic storms observed during the winters 1978/1979 and 1979/1980, as much as 61 were accompanied by such stratospheric warming. According to Neubauer this effect can be explained in detail by geophysical processes. There are indications that explosive volcanic activity is related to changes in weather and climate.[92] It is not out of the question that variations in the torque exerted by the solar wind on the Earth's magnetosphere have an

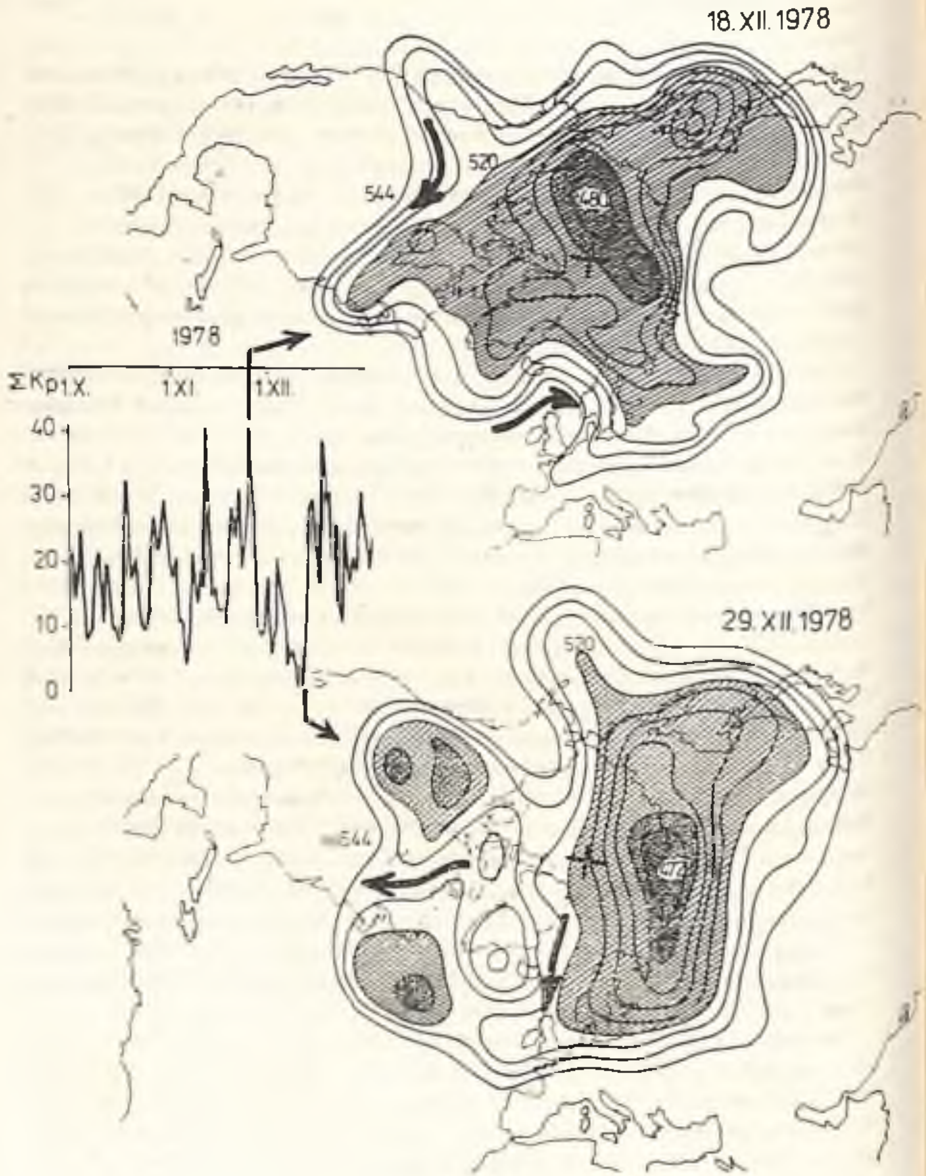

Figure 27: The plot by V. Bucha shows zonal type of atmospheric circulation, parallel to the equator (at top) as a result of geomagnetic disturbances caused by the Sun's eruptional activity, and meridional circulation (at the bottom) related to a lull in geomagnetic activity. The *Kp*-scale (in the middle) measures the degree of geomagnetic activity.

influence on volcanic activity via changes in the Earth's rotational velocity and the motion of continental plates with respect to one another.[93]

Some of these results may be spurious. Nevertheless, one of the few common threads that appear so widely in the otherwise disparate literature as to suggest that they probably have some validity, is the link between geomagnetic storms and meteorological or geophysical responses.[94] The Executive Committee of the International Working Group on Magnetic Field Satellites holds that there is an apparent relationship in the geomagnetic secular change to the length of the day and average global temperature on a decade time scale, suggesting that several of the major physical forces on the Earth may be interrelated[95]. Thus, long-term prediction of geomagnetic activity seems to be important, both for space mission planning and testing empirical understanding of the impact of the fast solar wind on the Earth's magnetosphere and possible meteorological responses.

Long range forecasts of geomagnetic activity were thought to be impossible, though there is a general correlation with the sunspot number *R*. In detail, however, the data do not correspond as well. This can be seen in Figure 28 after P. N. Mayaud[96] which presents yearly means of the Mayaud-index *aa* that measures the observed geomagnetic activity. The data run from 1868 to 1984. Upward arrow heads at the bottom of the plot mark the epochs of 11-year sunspot maxima. They do not match the highest peaks in the plot and sometimes even coincide with minima, as for instance in 1979. The arrows pointing downwards, however, fit the most prominent peaks in geomagnetic activity in nearly all cases. They mark the epochs of JU-CM-CS events that occurred 1868 to 1984.

There were only two striking exceptions to the fit: the conjunctions in 1901 and 1912. But they coincided with deep protracted 11-year sunspot minima; there was no potential of activity to draw on. No other such coincidence occurred in the investigated period. The deficit in conjunction effects seems to have depressed the general level of activity in the decades from 1900 to 1920; it reached the deepest point in the period of observation of more than a hundred years. In 1967 and 1970 the related peaks were low. This could be due to a disturbance of the rhythm in the pattern. The interval between the two JU-CM-CS events involved was unusually short, only 2.2 years. The depression in geomagnetic activity, however, could also be a special expression of the major solar instability event in 1968.

A Pearson-test of the goodness of fit of outstanding *aa*-peaks, going beyond defined thresholds, and JU-CM-CS epochs yields the value 17.1 for 1 degree of freedom ($P = 0.00004$). The strong enhancement of geomagnetic activity in 1982 was forecast with regard to these results in January 1982. The prediction was controlled by the astronomers W. Gleissberg, J. Pfleiderer, and H. Woehl. A new peak in geomagnetic activity is to be expected around the next conjunction in 1990.3. Its height depends on the activity potential of the 11-year cycle No. 22.

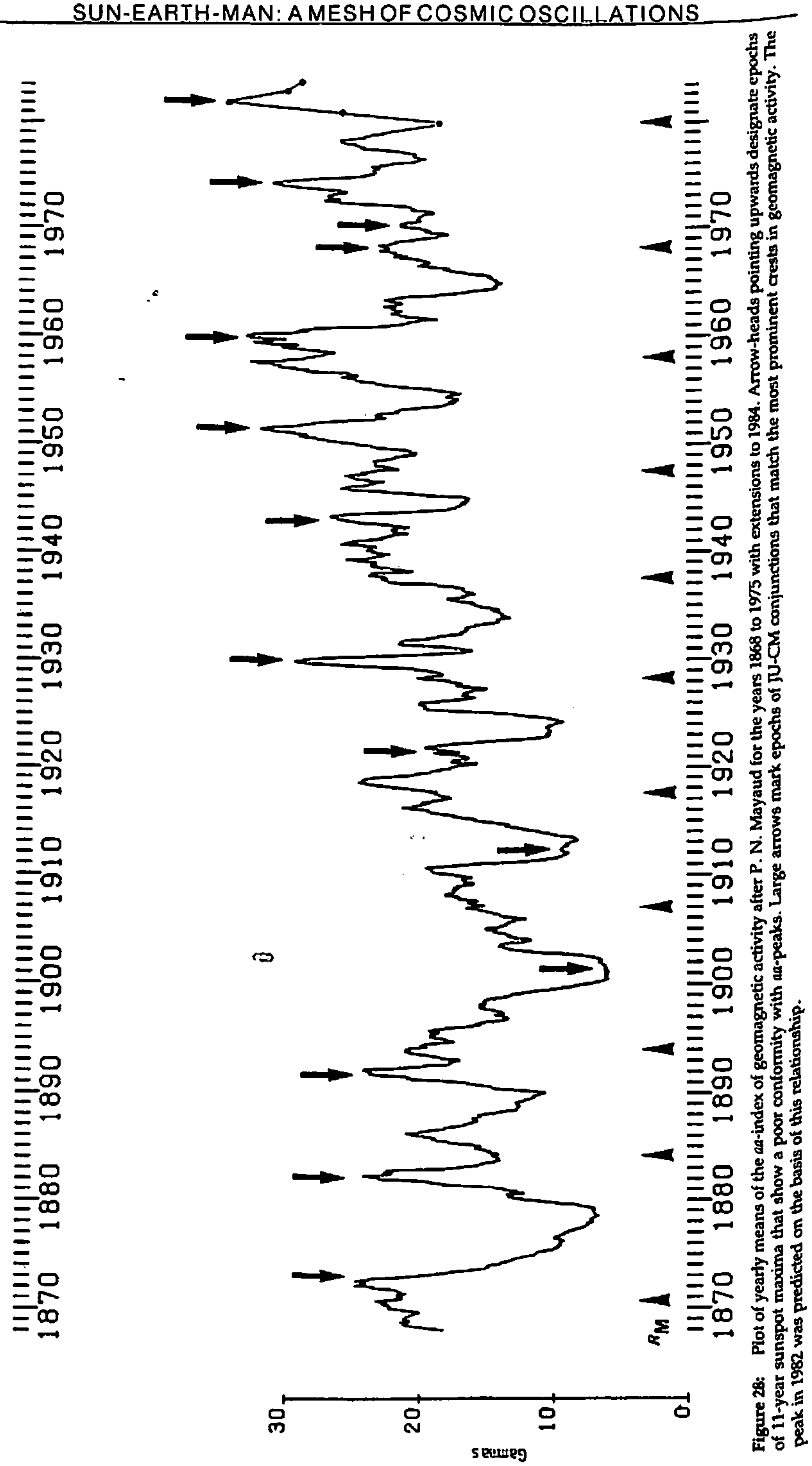

Figure 28: Plot of yearly means of the *aa*-index of geomagnetic activity after P. N. Mayaud for the years 1868 to 1975 with extensions to 1984. Arrow-heads pointing upwards designate epochs of 11-year sunspot maxima that show a poor conformity with *aa*-peaks. Large arrows mark epochs of JU-CM conjunctions that match the most prominent crests in geomagnetic activity. The peak in 1982 was predicted on the basis of this relationship.

XI. JUPITER, CENTER OF MASS, AND THE OZONE COLUMN

There is an abundance of papers speculating about the response of atmospheric ozone to solar activity and its effects on tropospheric climate. R. Reiter[97] has launched a series of radiosonde flights immediately after energetic solar flares. These observations revealed lowering of the tropopause, intrusion of warm stratospheric air from higher levels, formation of a sharply defined secondary ozone maximum immediately above the tropopause, perforation of the tropopause, emerging of jet streams, and change from zonal to meridional circulation. This development, involving ozone profile, was observed to occur within a few days after energetic flares. Intriguingly, JU-CM-CS events seem also to be related to variations in the ozone concentration. Modern U.S. and Canadian records of such data extend back only to about 1960. But continuous ozone monitoring at Arosa in the Swiss Alps since 1926 provides a rare long-term record of ozone levels.[98]

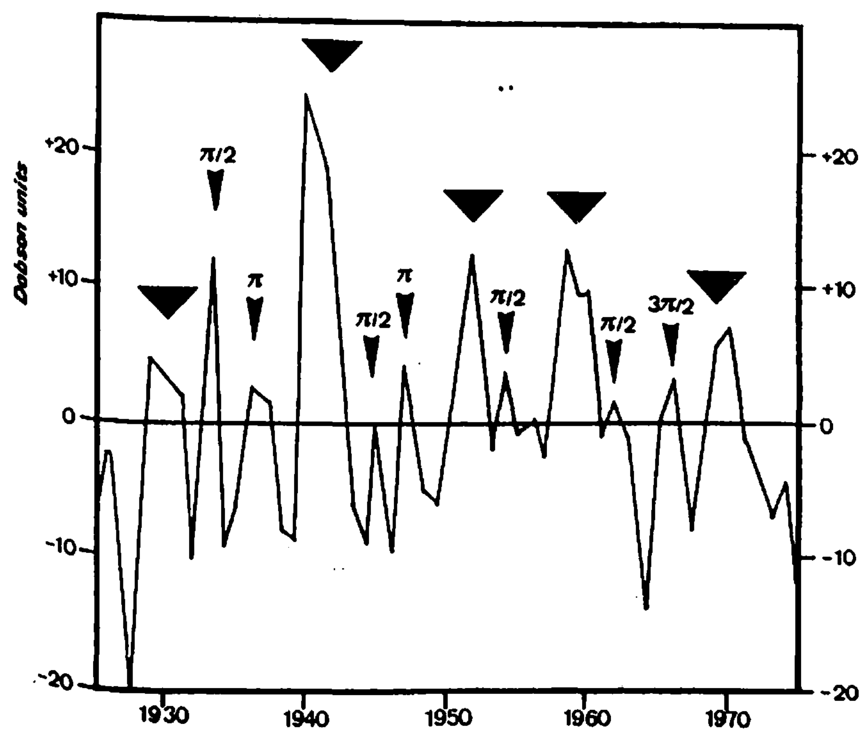

Figure 29: Arosa record of ozone levels since 1926 after H. U. Duetsch. The curve plots the deviation of annual mean values from the 50-year mean of 337 Dobson units. Triangles mark epochs of JU-CM-CS events. Arrow heads point to harmonics of cycles formed by consecutive Jupiter-CM conjunctions. The respective epochs meet peaks in the ozone column.

Figure 29 presents the deviation of annual mean values from the 50- year mean of 337 Dobson units. A change of about 17 Dobson units corresponds to a 5% change in ozone concentration. The epochs of JU-CM-CS constellations are marked by flat triangles. As to the events 1967.8 and 1970, which are only separated by an interval of 2.2 years, the mean of both epochs is indicated. It is together the epoch of the major solar instability event that started in 1968. The JU-CM-CS epochs, which are related to periods of energetic flare activity, also fit the strongest ozone deviations, as can be seen in Figure 29. In addition, the phases $\pi/2$ and π radians (90° and 180°), that were conspicuous in the Sun's rotation data, concur with secondary peaks. Small arrow heads point to these phases. After the instability event starting in 1968 the pattern seems to have changed. The epoch of JU-CM-CS in 1974 coincided with a minimum. If the new pattern proves to be stable, the next minimum is to be expected in 1990.

XII. COSMIC INFLUENCE ON WEATHER

There has been a lot of controversy over whether or not the Sun's activity influences weather on Earth. Simple relationships discovered in the 1870's and 1880's vanished when examined more critically, or faded in the light of longer records. A classical example is a marked correlation between the 11-year sunspot cycle and the water level in Lake Victoria that seemed to imply a direct connection between solar activity and rainfall in Africa. After the middle 1920's, however, the pattern that included two sunspot cycles vanished and did not appear again. In addition, such ephemeral relationships were limited to special regions and did not cover larger areas subjected to the same or a similar climate. These discussions will perhaps enter a new stage now. The following results cover more than a century and large parts of the Northern Hemisphere in a consistent way.

Figure 30 provides evidence of a strong connection of rainfall over central Europe with JU-CM-CS epochs. The investigation is based on the mean of yearly rainfall totals in mm derived from observations of 14 German stations by Baur.[99] This homogeneous time series, supplemented by data from "Berliner Wetterkarte", published by the Meteorological Institute of the Free University of Berlin, covers the period 1851 to 1983. The 2-year running variance s^2 of these data was subjected to a Gaussian low-pass filter. Peaks in the plot point to a strong contrast in the rainfall of consecutive years. Very wet years are followed by very dry years or very dry years by very wet years, whereas minima go along with little contrast in this respect. The x-axis indicates the years of observation and the y-axis the smoothed variance $v = s^2$. It is obvious that the epochs of JU-CM-CS events marked by pointers show a good correlation with peaks in the plot, whereas minima, designated by open circles, coincide with phases π radians (180°) in the middle between two epochs that also can be looked at as second harmonics of cycles of consecutive JU-CM-CS events. Only at the secular minimum in sunspot activity around 1900 the respective maxima are quite weak or even disappear.

This correlation is corroborated by a statistical analysis of the unsmoothed 2-year running variance of the German rainfall data presented in Figure 31. The JU-CM-CS epochs are marked by flat triangles and the phases π radians (180°), the second harmonics, by open circles. The analysis evaluates the significance of the difference between means of the running variance of two groups: Group 1 composed of the variance of years coinciding with JU-CM-CS epochs and of the respective preceding year and following year; Group 2 comprising the variance of the years that concur with phases π radians (180°) and the respective preceding year and following year. The rainfall distribution is Gaussian and free from Markov type persistence. Daily or monthly data show some persistence patterns. These were eliminated, however, by the formation of yearly means. Thus, the t-test may be applied. The Fisher-Behrens formula, described in the glossary, is to be used, as the variance in the test groups shows a significant difference.

Group 1 yielded: number of data points $n_1 = 46$; mean $\bar{x}_1 = 13.46$; standard deviation $s_1 = 15.25$. The corresponding values in Group 2 are: $n_2 = 48$, $\bar{x}_2 =$

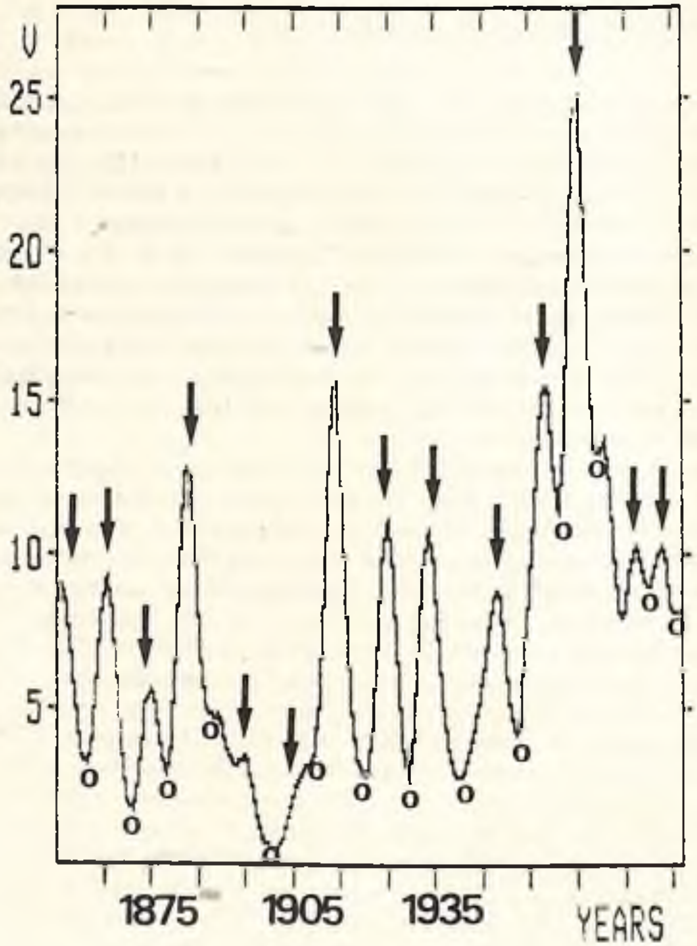

Figure 30: Smoothed running variance of yearly rainfall totals (mm) derived from observations of 14 German stations by F. Baur. The time series covers the period 1851 to 1983. Arrows mark epochs of Jupiter- CM conjunctions which coincide with maxima in the running variance. Open circles designate second harmonics of respective cycles created by consecutive heliocentric conjunctions of Jupiter and the centre of mass CM that match minima in the variance of rainfall.

3.48; s_2 = 7.65. The corresponding test value t (df=67) = 3.98. Considering that the variance generates positive values only and Group 1 is known to have a higher mean than Group 2, the rules valid for single-sided distributions apply: $P < 0.0002$. The null hypothesis of no significant difference between the means involved can be rejected at a high level of significance. The same procedure applied to the same data set, but based on a 3-year running variance, gives the results: $n_1 = 46$; $\bar{x}_1 = 12.19$; $s_1 = 8.76$. $n_2 = 48$; $\bar{x}_2 = 4.38$; $s_2 = 6.8$. t (df=87) = 4.82; $P < 0.00003$. 4-year and higher running variance shows deteriorating results. Nonparametric tests confirm the established connections. The Mann-Whitney-test yields: $z = 3.84$; $P < 0.0001$.

Another approach contributes to these corroborations. The complete data set is characterized by $n = 132$; $x = 7.5$; $s = 11.85$. In a group that comprises only the variance data of the years of phases π radians (180°), the corresponding values are $n_3 = 16$; $\bar{x}_3 = 1.15$; $s_3 = 1.3$. The t-test yields t (df=147) = 5.87; $P < 0.000002$. This connection relating the phase π radians (180°) in the middle between consecutive JU-CM-CS events, the second harmonics, to low variance values, seems to be rather dependable. This means in practice that around phases π radians (180°) there is little contrast as to wetness and drought in consecutive years, whereas change of flood years to drought years or inversely occurs frequently around JU-CM-CS events, at least in central Europe since the middle of the 19th century.

A replication was made by means of yearly rainfall averages in England and Wales for the years 1850 – 1976.[100] The same procedure based on 2-year running means yielded: $n_1 = 47$; $\bar{x}_1 = 2.67$; $s_1 = 3.55$. $n_2 = 45$; $\bar{x}_2 = 1.06$; $s_2 = 1.62$. t (df=66) = 2.83; $P < 0.004$. The null hypothesis of no real difference between the means of the two groups is disproved again.

When the groups of three years each around the epochs in question are replaced by groups allotted to a sine wave that comprises all data available, the tests continue to indicate highly significant results. The JU-CM-CS epoch is assigned to the sine wave such that it coincides with the phase $\pi/2$ radians (90°) at the crest, while the epoch in the middle between JU-CM-CS concurs with the phase 3/2 π radians (270°) at the trough. All years matching positive phases of the sine wave including the phases 0 and π radians (180°) fall in Group 1, and all years coinciding with negative phases are assigned to Group 2. As to the rainfall over Germany, this new procedure, when based on a 2-year running variance, yields t (df=109) = 3.9. The corresponding probability $P <$ 0.0002 justifies the dismissal of the null hypothesis at a high level of significance. The rainfall averages in England and Wales subjected to the new procedure give t (df=104) = 3; $P < 0.002$. Another replication makes use of the yearly total rainfall (mm) in the eastern United States, reduced to Philadelphia equivalent values, covering the period 1850 – 1967.[101] The sine wave procedure yields: $n_1 = 66$; $\bar{x}_1 = 1.72$; $s_1 = 1.91$. $n_2 = 51$. $\bar{x}_2 = 1.01$; $s_2 = 1.14$. t (df=110) = 2.48; $P = 0.009$. The null hypothesis can be rejected. This points to a real difference of the two groups as to rainfall in the northern hemisphere, but so far only as to mid- latitudes.

The next replication makes use of data from the equatorial region: yearly monsoon season (June – September) rainfall (mm) at Bombay for the years 1850 to 1960.[102] The difference of both groups is still evident, but the sine wave procedure reveals a phase shift: the effect begins and ends $\pi/2$ radians (90°) earlier. If allowance is made for this shift, the results are: $n_1 = 65$; $\bar{x}_1 = 2.54$; $s_1 = 3.09$. $n_2 = 45$; $\bar{x}_2 = 1.45$; $s_2 = 2$. t (df=109) = 2.24; $P = 0.014$. The phase shift by $\pi/2$ (90°) emerging in low latitudes is no ephemeral feature. It is confirmed by the analysis of All-India summer monsoon (June to September) rainfall (mm) for the period 1871 – 1978.[103] Sine wave processing yields: $n_1 = 68$; $\bar{x}_1 = 9.84$; $s_1 = 13.4$. $n_2 = 44$; $\bar{x}_2 = 4.88$; $s_2 = 6.47$. t (df=104) = 2.62; $P = 0.005$. This result is again a dismission of the null hypothesis at a high level of significance. Therefore, a two-phase system with relation to the geographic latitude seems to be a promising approach.

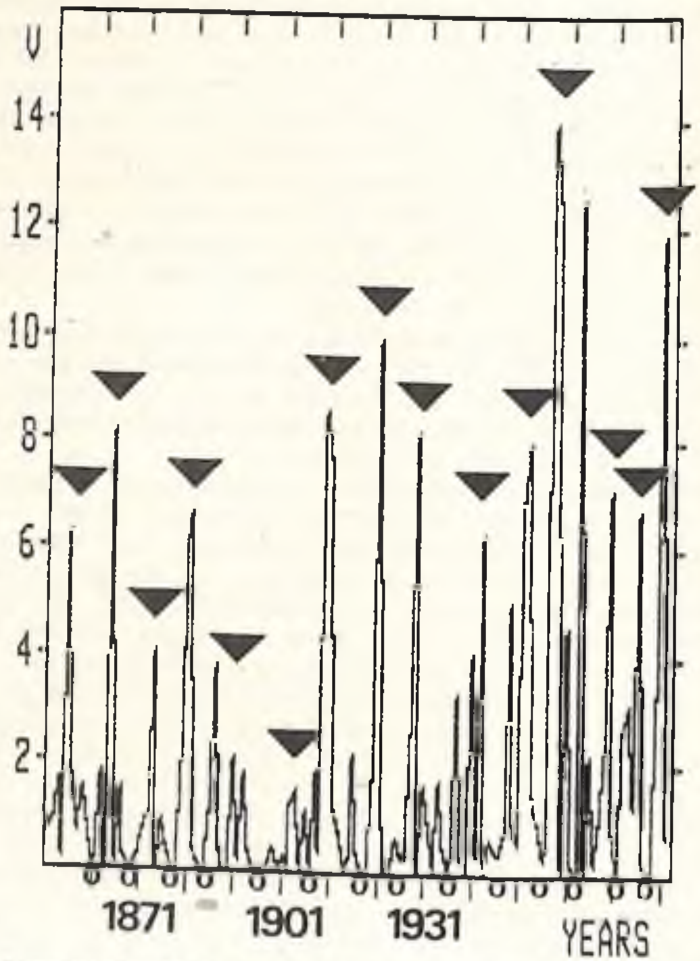

Figure 31: Unsmoothed values of the data presented in Figure 30. Epochs of Jupiter-CM conjunctions are indicated by black triangles. Open circles mark second harmonics of conjunction cycles. The respective epochs coincide with extrema in the rainfall variation.

The JU-CM-CS effects seem to have left their mark still in other climatic features. The longest records of ice in the western North Atlantic are derived from the yearly counts of the number of icebergs that pass south of latitude 48° N to affect the shipping lanes.[104] These counts are quoted in terms of the Smith-index which provides a scale from −5 to +5. The time series covers the period 1880 to 1976. As the counts refer to higher latitudes, the position of the crucial epochs in the sine wave should show no phase shift. This turns out to be true. The test of both groups, processed in the same way as the German, England and Wales, and U.S. rainfall data, yields the following result: $n_1 = 56$; $\bar{x}_1 = 5.32$; $s_1 = 7.17$. $n_2 = 40$; $\bar{x}_2 = 2.68$; $s_2 = 3.37$. t (df=84) = 2.41; P = 0.009. The rejection of the null hypothesis is again justified at a high level of significance.

Temperature opens a further field of replication. F. Baur[105] established a time series of yearly temperature averages (°C) based on the respective means of the stations Utrecht-de Bilt, Potsdam, Basle, and Vienna. With extensions taken from the "Berliner Wetterkarte", the series covers the period 1851–1983. The sine wave method, as applied to the central European rainfall data, gives the following values: $n_1 = 77$; $\bar{x}_1 = 0.463$; $s_1 = 0.619$. $n_2 = 55$; $\bar{x}_2 = 0.217$; $s_2 = 0.3$. t (df=118) = 3; $P < 0.002$. This result is again highly significant. Yearly mean temperatures in central England for the period 1851 – 1976[106] offer occasion for another replication. The result is significant, but less striking: $n_1 = 69$; $\bar{x}_1 = 0.293$; $s_1 = 0.382$. $n_2 = 56$; $\bar{x}_2 = 0.196$; $s_2 = 0.274$. t (df=123) = 1.65; $P = 0.05$. As was to be expected, there are no indications of a phase shift. Phases π radians (180°) point to series of years showing little contrast in temperature, whereas JU-CM-CS epochs are characterized by sequences of alternately hot and cold years. An analysis of annual average temperatures of the Northern Hemisphere for the period 1850 — 1978 yielded no significant difference of the means of groups formed with respect to epochs of JU- CM-CS events. This may be due to phase differences in different geographical latitudes that cancel out.

These are the first results in the field of solar-terrestrial relations regarding weather which cover large areas and long periods consistently. Moreover, they are accessible to prediction because they are based on configurations of cosmic bodies in the solar system that can be computed. The results of this new kind of interdisciplinary approach, which integrates astrological views and modern science, should be intriguing enough to induce experts in the different fields involved to follow the trace outlined in this study.

XIII. PYTHAGOREAN HARMONY

One of the first interdisciplinary approaches to a holistic understanding of our world was that of Pythagoras and his disciples. They created the theory of the functional significance of numbers in the objective world and in music. Their famed dictum "all is number" meant that all existing entities can be ultimately reduced to number relationships that do not only link mathematics to music theory, but also to acoustics, geometry, and astronomy. Even the dependence of the dynamics of world structure on the interaction of pairs of opposites, the first of which is the even-odd polarity essential to numbers, emerges from these number relationships.[107] Pythagoras would have been happy to learn of attractors opposite in character that are created by simple feed back cycles of numbers and form tenuous boundaries, dynamic sites of instability and creativity.

Pythagorean thinking deeply influenced the development of classical Greek philosophy and medieval European thought, especially the astrological belief that the number harmony of the universe affects everything including terrestrial affairs in their relation to space-time configurations of cosmic bodies. Men were intrigued by the precision of those number relationships between musical harmonies, that deeply touch man's soul, and prosaic arithmetical ratios of integers. This connection was first demonstrated by Pythagoras himself in the sixth century B.C. In his famous experiment a stretched string on a monochord was divided by simple arithmetical ratios as 1/2, 2/3, 3/4, 4/5, 5/6 and plucked. It was a Eureka moment when he discovered that the respective partitions of the string create the consonant intervals in harmony.

One tone is not yet music. One might say it is only a promise of music. The promise is fulfilled, and music comes into being, only when tone follows upon tone. Strictly speaking, therefore, the basic elements of music are not the individual tones, but the individual tone to tone moves. Each of these moves spans a certain pitch distance. The pitch distance between two tones is called an interval. If the basic elements of a melody are the individual moves, melody is a succession of intervals rather than of tones.[108] Intervals can be consonant or dissonant. It was Pythagoras' great discovery to see that the ratios of the first small integers up to six give birth to consonant intervals; the smaller these integers, the more complete the resonance. A string divided in the ratio 1 : 2 yields the octave (C-C') of its fundamental note, an equisonance. The ratio 2 : 3 – the entire length of the string to two thirds of its length – yields the fifth (C-G), 3 : 4 the fourth (C-F), 4 : 5 the major third (C-E), 5 : 6 the minor third (E-G), and 3 : 5 the major sixth (C-A). The pairs of notes given in brackets are examples of the respective consonances.

The minor sixth created by the ratio 5 : 8 seems to go beyond the limit six. But eight, the only integer greater than 6, is only the third power of 2 which is a member of the senarius of consonant numbers; eight is created by an octave operation which gives birth to absolutely equisonant tones. All authorities agree that besides the equisonant octave there are no other consonant intervals than the third, the fourth, the fifth and the sixth.[109] If more than two notes are to be consonant, each pair of them must also be consonant. As mentioned already, the most complete consonance within the range of an octave is the

major perfect chord C-E-G = 4:5:6 that unites the major third and the fifth to the fundamental note. These concepts of harmony, harmonic intervals and chords are not an arbitrary invention. The consonant intervals are formed in nature by the first terms in the series of overtones or harmonics. The harmonic series was unknown in the age of Pythagoras. It was discovered by Marin Mersenne in 1636, and the inherent law of nature was found by Joseph Sauveur in 1702. When there is a musical sound, there is always in addition a series of harmonics that relate the fundamental tone to an infinity of overtones which influence the quality of the fundamental. The overtones up to the sixth harmonic represent the consonant intervals: the octave, the fifth, the fourth, the major third, the minor third, and the sixth.

XIV. ENERGY DISPLAY IN SOLAR ERUPTIONS "SET TO MUSIC"

Now we are prepared to focus again and with more attention to detail on the art of "composing" predictions of energetic solar eruptions. Most features of Figure 32 are known to the reader already. They were presented in Figure 21 that shows the angular acceleration *dω/dt* of the vector of the tidal forces of Venus, Earth, and Jupiter. The cyclic pattern created by boundary transitions from positive to negative values, or inversely, correlates with proton events (*P*) and X-ray bursts ≥ X3 (*X*) observed in 1982. This year was only an example of the general pattern of this kind of cycles. 1982 was, however, a year with exceptionally intense eruptional activity. In the preceding years the Sun produced less intense eruptions, even though there were active phases in the *dω/dt* cycles as well as in 1982 and in spite of the fact that the 11-year sunspot cycle reached a high maximum in 1979/1980.

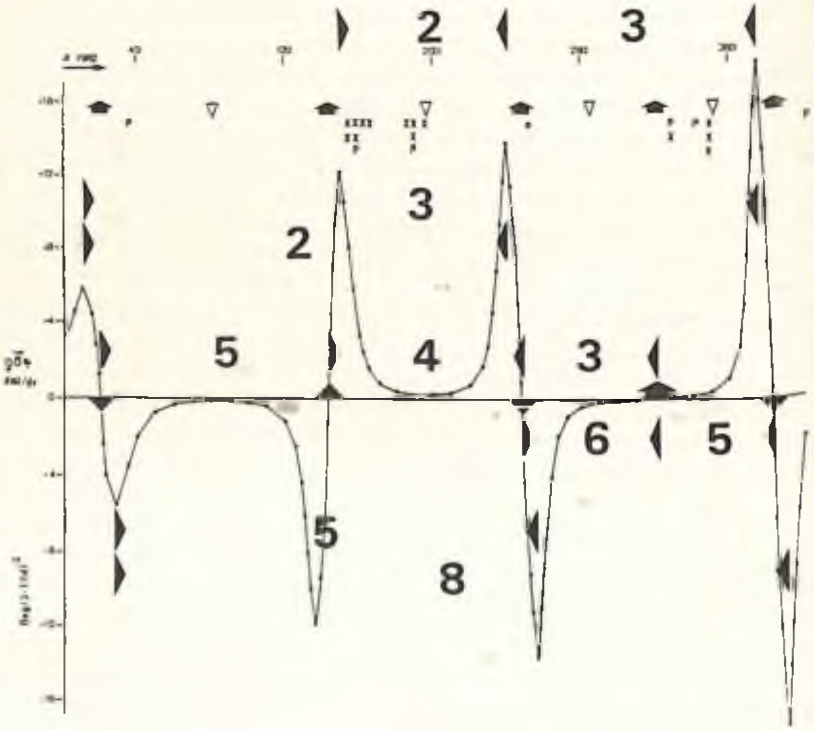

Figure 32: Role of Pythagorean harmony in "composing" predictions of energetic solar eruptions. A wealth of consonant intervals (2 : 3, fifth; 3 : 4, fourth; 4 : 5, major third; 5 : 6, minor third; 5 : 8, minor sixth), designated by vertical triangles and large numbers, points to eruptions of exceptional intensity. Flares that emerge in active phases of cycles related to the angular acceleration of the composed vector of the tidal forces of Venus, Earth, and Jupiter, as explained with respect to Figure 21, display unusual energy when the extrema of the angular acceleration appear at intervals that are together consonant intervals in musical harmony.

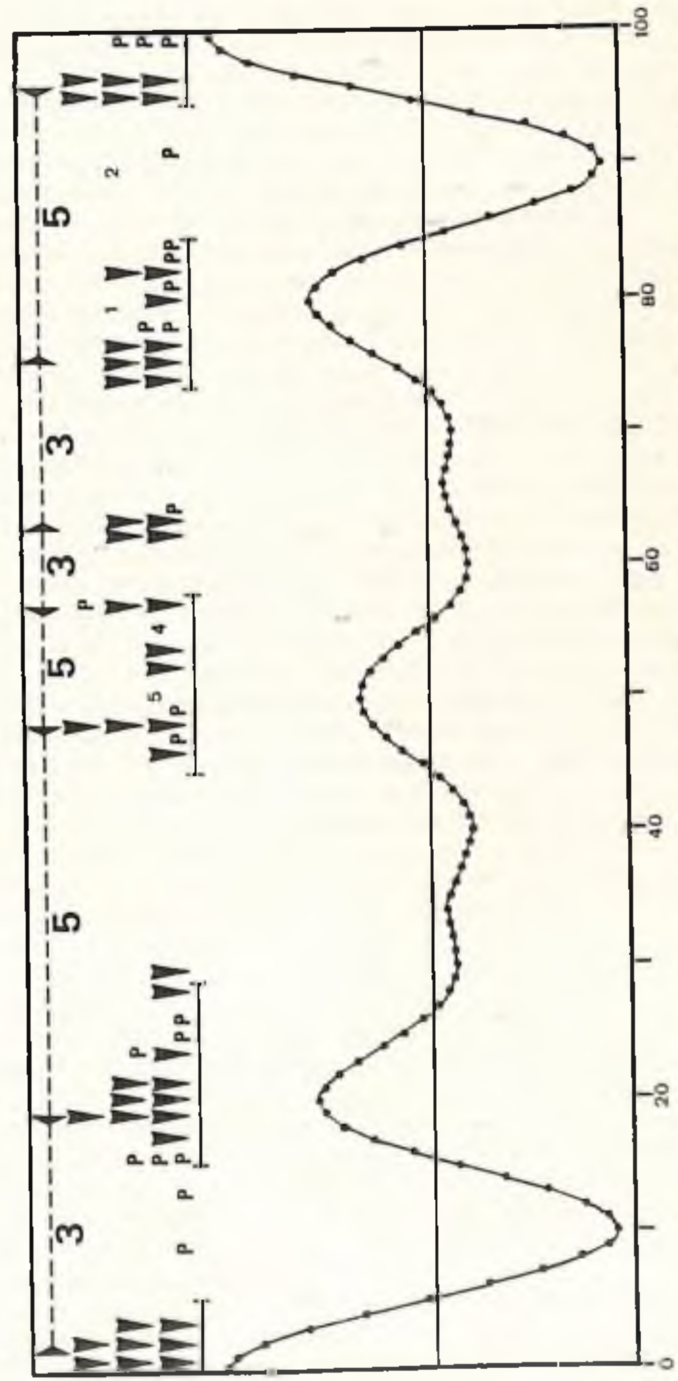

Figure 33: The prototypal pattern of a composite wave formed by the superimpositions of the fourth, fifth, and sixth harmonics of cycles of Jupiter-CM conjunctions, as explained in relation to Figure 26. The distribution of highly energetic X-ray flares and proton events, as explained with respect to Figure 26, is not only related to the major perfect chord. It also follows the ratio of the major sixth (3 : 5), indicated by vertical triangles and large numbers, as well as the major third (4 : 5) and the octave (1 : 2) indicated by small numbers between groups of arrow-heads.

Figure 32 explains why in 1982 the active phases in the *dω/dt* cycles displayed eruptions of such high intensity. Contrary to former years, zero phases and extrema of the curve of the angular acceleration of the composed vector of the tidal forces of Venus, Earth, and Jupiter formed just in 1982 a wealth of consonant intervals of musical harmony. Vertical flat triangles in Figure 32 indicate the limits of the respective intervals. At the top two fifths (2 : 3) are formed by the positive extrema in the curve. In the middle, around the time axis, the zero phases appear just at such distances that they represent a fourth (3 : 4), a major third (4 : 5), and a minor third (5 : 6). Eventually, three of the four negative extrema form a minor sixth (5 : 8). Such connection of an accumulation of consonant intervals and strong solar activity is a common feature. Only when the 11-year sunspot cycle is in its deepest valley, is there no effect because of the lack of an energy potential that could be tapped.

Figure 33 repeats the former presentation of the prototypal pattern of a composite wave formed by the superimposition of the fourth, fifth, and sixth harmonics of JU-CM-CS cycles of any length. The positive phases coincide with clusters of solar cosmic ray events (*P*), observed from 1942 to 1969, and flare-generated *X*-ray bursts ⩾ X4, indicated by arrow heads, registered from 1970 through 1987. It has been stressed in the explanation of Figure 26 that the ratio 4 : 5 : 6 of the composed harmonics is representative of the major perfect chord. Figure 33 shows in addition that the centroids of clusters of highly energetic events mark intervals of the major sixth (3 : 5) rather precisely. This is indicated by vertical flat triangles and large numbers on top of the plot. Furthermore, the octave (1 : 2) and the major third (4 : 5) form substructures that are indicated on the right of Figure 33 by small numbers between the arrow heads. As the prototypal pattern in Figure 33 presents a synopsis of the most energetic category of solar eruptions recorded for the past 45 years, it corroborates the hypothesis that consonant intervals play an important role with respect to the Sun's eruptional activity.

XV. HARMONICAL CONSONANCES IN SOLAR CYCLES COVERING THOUSANDS OF YEARS

Another confirmation of this hypothesis are the connections presented in Figure 34 that cover thousands of years. It has been shown in Figure 19 that consecutive impulses of the torque IOT in the Sun's motion about CM, when taken to constitute a smoothed time series, form a wave-pattern the positive and negative extrema ($\pm A_s$) of which coincide with maxima in the secular sunspot cycle. This Gleissberg cycle, with a mean period of 83 years, which modulates the intensity of the 11-year sunspot cycle, is in turn modulated by a supersecular sunspot cycle with a mean period of about 400 years. The Maunder Minimum of sunspot activity in the 17th century and a supersecular maximum in the 12th century are features of this supersecular cycle. It seems to be related to the energy in the secular wave presented in Figure 19.

This energy may be measured by squared values of the secular extrema $\pm A_s$. When these values are taken to form another smoothed time series, a supersecular wave emerges as plotted in Figure 34.[110] It runs parallel with the supersecular sunspot cycle. Its mean period is 391 years, but it varies from 166 to 665 years. Each dot in the plot indicates the epoch of a secular extremum ($\pm A_s$). These epochs are numbered from −64 to +28 and range from 5259 B.C. to 2347 A.D. Black triangles indicate maxima in the correlated supersecular sunspot curve and white triangles minima. The medieval maximum, which was together a climate optimum (O), the Spoerer Minimum (S), and the Maunder Minimum (M) are marked by respective abbreviations. The extrema in the supersecular wave properly reflect all marked peaks and troughs in the supersecular sunspot curve derived from radiocarbon data by Damon and Eddy.[111]

Phase jumps are a common feature of all kinds of cyclic time series observed in Nature. Diverse examples of phase jumps in series of short-term cycles have been presented above. The energy wave in Figure 34 is an intriguing example of phase change in series of long-term cycles. The dashed horizontal lines mark two quantitative thresholds. When the energy in the wave transgresses the upper line, or falls beneath the lower line, a phase jump emerges in the correlated supersecular cycle of sunspot activity. At the crucial phases, set off in Figure 34 by dotted vertical lines, the extrema change sign; a preceding supersecular maximum is not followed by a minimum, but by another maximum, or a minimum by a further minimum. More details of these connections have been given in special publications. One of the consequences that can be derived from the energy wave is the forecast of an imminent supersecular sunspot minimum around 2030 A.D. The dotted vertical line quite on the right of Figure 34 points to the epoch of a phase change such that the supersecular Maunder Minimum (M) will be followed by another supersecular minimum about 2030.

Intriguingly, the intervals in the energy wave that separate consecutive phase jumps, too, show a relationship with consonant intervals. These intervals, marked by the vertical dotted lines and vertical flat triangles, represent the major sixth (3 : 5) and the minor sixth (5 : 8). The pattern that combines the major with the minor sixth seems to be a permanent feature, a

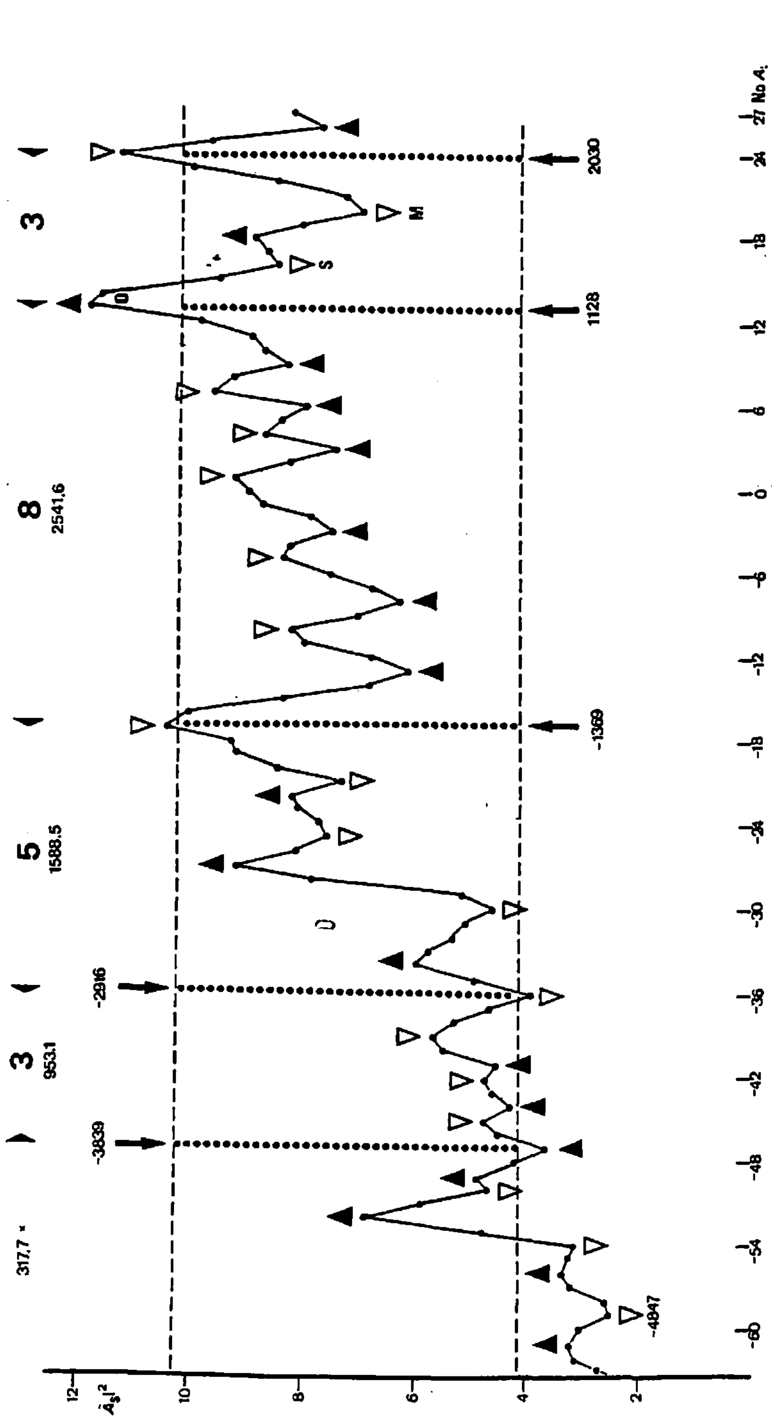

Figure 34: Combination of the consonant intervals major sixth (3 : 5) and minor sixth (5 : 8) emerging in solar system processes covering thousands of years. The intervals are indicated by vertical triangles and great numbers. The curve represents the supersecular variation of the energy in the secular torque wave, part of which was shown in Figure 19. The energy is proportional to squared values of the extrema in the secular torque wave (A_s^2). Points in the curve represent epochs of extrema A, numbers −64 to +28 (5259 B.C. to A.D 2347). The mean length of the cycle is 391 years. Black triangles point at maxima in the corresponding supersecular sunspot cycle; open triangles indicate minima. When the energy goes beyond quantitative thresholds, indicated by hatched horizontal lines, a phase jump occurs in the correlated supersecular sunspot cycle. These critical phases are marked by vertical dotted lines. A new phase jump is imminent about 2030. It points to a supersecular minimum, comparable with the Egyptian minimum (E) around 1369 B.C., a prolonged period of distinct cooling and glacier advance. The proportion 3 : 5 : 8, representing the major and minor sixth, just marks the intervals that separate those rare phase jumps set off by vertical dotted lines. The 317.7-year period of the triple conjunction of Jupiter, Saturn, and Uranus is, too, involved in this connection as indicated by small numbers beneath the great numbers at the top.

new start of which can be identified beyond the phase jump in 1128, the epoch of the medieval optimum (O). The consonant intervals are designated by large numbers on top of Figure 34. The smaller numbers underneath point to a connection with the period of the triple conjunction of Jupiter, Saturn, and Uranus, mentioned in the introductory part. This period of 317.7 years, which is related to the Sun's activity and terrestrial climate in Precambrium, also shows a connection with the consonant intervals investigated here. The threefold, fivefold, and eightfold values of the period of the triple conjunction, namely 953, 1589, and 2542 years, properly reflect the actual intervals between consecutive phase jumps. These actual values seem to oscillate about the values derived from multiples of the period of the triple conjunction of Jupiter, Saturn, and Uranus. As has been pointed out in the beginning with respect to the Elatina cycle, the period of conjunctions of Jupiter and Saturn and important torque cycles are involved, too, because they are commensurable with the period of the triple conjunction. Reference is made to the corresponding details.

XVI REALISATIONS OF MUSICAL CONSONANCES IN TERRESTIAL CYCLES

Just that interval of the sixth (5 : 8) as defined in Figure 34 by the phase jumps in 2916 B.C., 1369 B.C, and 1128 A.D, is reflected, too, in terrestrial data that show a relation to the supersecular sunspot cycle. Figure 35, after H. H. Lamb,[112] shows 20-year averages in the growth rings of Bristlecone pine trees near the upper tree line in the White Mountains, California, from 3431 B.C. The variations in the ring widths at this height may be taken as indicating variations of summer warmth or its seasonal duration. The data were supplied by V. C. La Marche at the Laboratory of Tree Ring Research, University of Arizona. The arrows point to the respective epochs of phase jumps in the supersecular energy wave. It is obvious that just the periods around these epochs are characterized by the greatest variations in the ring widths that reach 34/100 mm to 39/100 mm, whereas in the long periods between these three phases of exceptional change the ring widths vary by less than half of this range. This coincidence of outstanding features in the supersecular energy wave and the time series of growth rings of trees, matching the consonant interval of the minor sixth (5 : 8) in both cases, is a solid indication that we are dealing with a real relationship.

Figure 36 after Rhodes W. Fairbridge[113] contributes to this growing body of circumstantial evidence. In the Hudson Bay, Canada, beach ridge formations have been preserved as a long series of almost continuous "staircases" from top to bottom of ancient strandlines in an area of maximum postglacial uplift. As Fairbridge put it, "we have been able to walk back so-to-speak through time, ascending the stair-treads, a few meters at a time, from the present beach to the level dated about 8300 years B.P., the marine limit, the time of the postglacial marine invasion of the Hudson Bay." Fairbridge assumes that critical periods of storminess, when local sea level was raised above its usual average stand, may have been an important factor in the building of beach ridges. The irregular curve in Figure 36 is a plot of the moving average of the measured beach de-levelings. Each dot represents one of the individual beach ridge formations. The measured data cover more than 8000 years before the period 1975 (B.P.).

In the plot of Figure 36 only the data back to about 6000 B.P. are given, because the calculation of phase jumps in the supersecular energy wave does not go beyond this range. The fat arrows mark the epochs of phase jumps in the energy wave that are indicated by vertical dotted lines in Figure 34. If these epochs coincide with supersecular maxima in Figure 34, the respective arrows in Figure 36 point upwards, while they point downwards when the epochs indicate supersecular minima in sunspot activity. The respective arrows properly fit the most prominent ups and downs in the curve that reflect the differences in the beach de-levelings measured on the ordinate axis by rates of emergence in cm/yr. The trend is designated by a dashed line. Both of the two greatest negative deviations from the trend properly fit the phase jump minima in 2916 B.C (4892 B.P.) and 1369 B.C (3345 B.P.) while the most

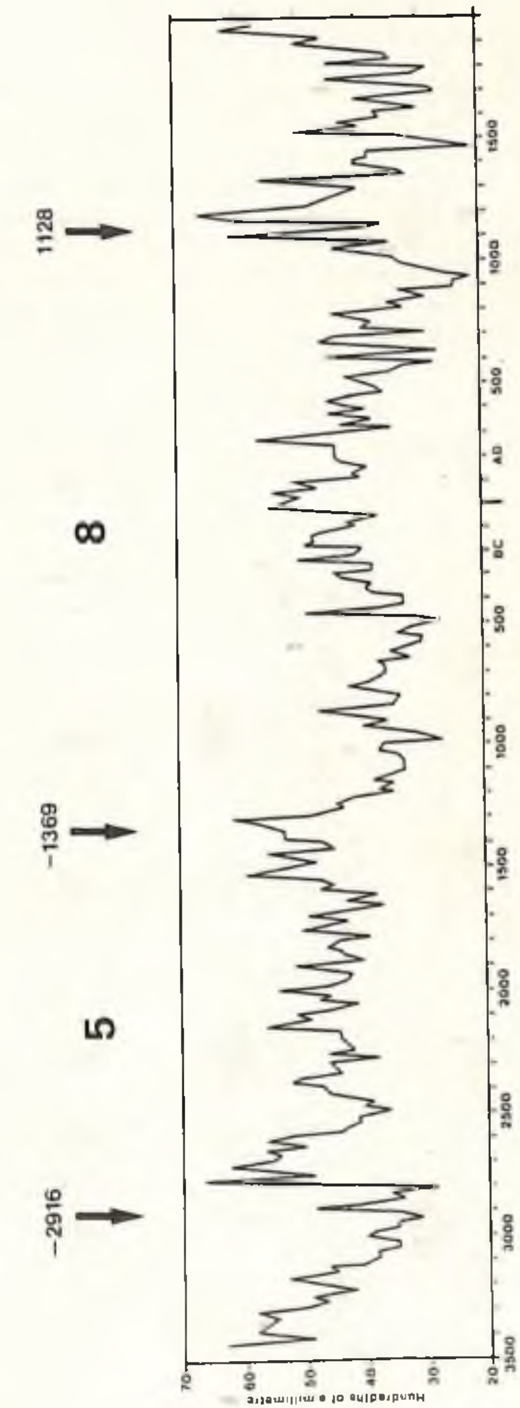

Figure 35: This plot after H. H. Lamb shows 20-year averages in the growth rings of Bristlecone pine trees near the upper tree line in White Mountains, California, from 3431 B.C. Arrows point at the respective epochs of phase jumps in the supersecular energy wave. These epochs, separated by intervals conforming with the ratio 5 : 8 of the minor sixth, coincide with the greatest variations in the tree ring widths.

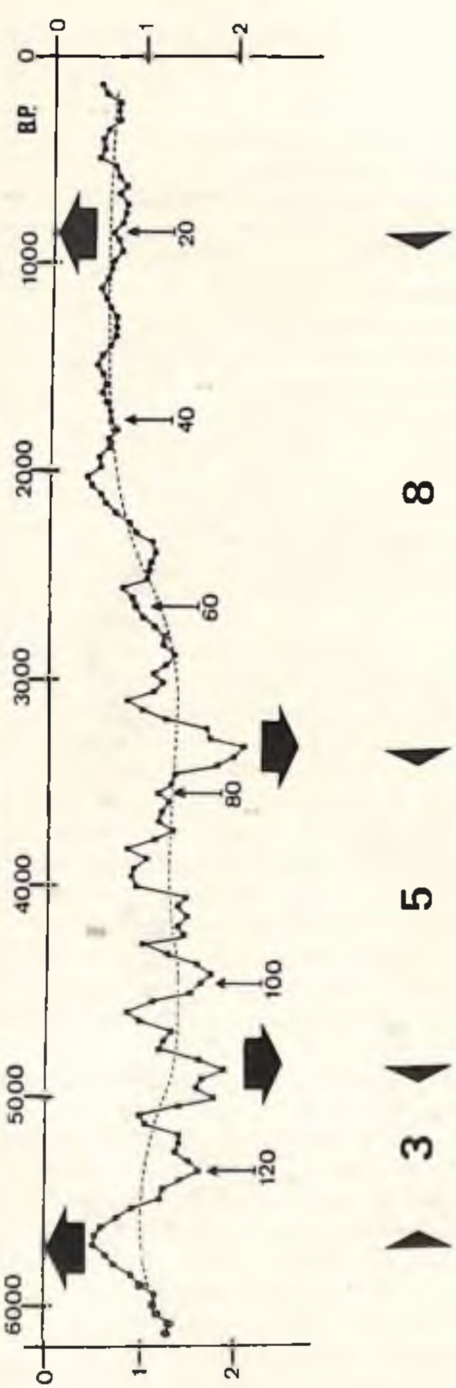

Figure 36: Beach ridge formations in the Hudson Bay, Canada, after R. W. Fairbridge, a long series of almost continuous "staircases" from top to bottom of ancient strand lines in an area of maximum postglacial uplift, covering more than 6000 years before the period 1975 (B.P.). The pattern of this series seems to reflect critical periods of storminess. The figures beneath small pointers indicate the numbering of individual "staircases". Fat arrows mark the epochs of phase jumps in the energy wave indicated in Figure 34 by vertical dotted lines. They properly fit the most prominent ups and downs in the curve which repeat the proportions of the major and minor sixths (3 : 5 : 8), also present in the energy wave and the related supersecular sunspot cycle.

prominent positive deviations coincide with the phase jump maxima in the secular wave about 3839 B.C. (5815 B.P.) and 1128 A.D. (847 B.P.). In the period of rather flat oscillations around the trend about 847 B.P. on the right of the plot this is not as clearly visible as in the period about 5815 B.P with its strong positive deviation from the trend. It is obvious, however, that all of the fat arrows in Figure 36 point to maxima of curvature or turning points in the trend line. The arrow at the phase jump epoch 1128 A.D. (847 B.P.) is no exception; it indicates a crest turning point as well as the other arrow pointing upwards at the epoch 3839 B.C. (5815 B.P.). Consistently, the major and minor sixths (3 : 5 and 5 : 8) appear as well as with respect to the phase jumps in the supersecular energy wave. These consonant intervals are set off in Figure 36 by vertical flat triangles and numbers designating the respective ratios of the intervals.

XVII. EPILOGUE

Cycles are at the core of all connections presented here. So let us complete a cycle in returning to the beginning where it has been shown that a simple mathematical feed-back cycle, a model of the fundamental functions of cycles, creates pre-images of polar tension, called attractors, and instable, but creative boundaries between the domains of competing attractors of opposite quality. These boundaries give birth to a wealth of explicit structures, an incredible variety of Julia sets, one of which was presented in Figure 3. Adrien Douady[114] has given an apt description of their various forms: "Some are a fatty cloud, others are a skinny bush of brambles, some look like the sparks which float in the air after a firework has gone off. One has the shape of a rabbit, lots of them have sea-horse tails. . .".

But from the mathematical feed-back cycles also emerges a core entity called Mandelbrot set *M* which regulates the incidence of the different forms of Julia sets. Peitgen and Richter[115] compare its function with that of the genome, the entire set of hereditary factors contained in a haploid number of chromosomes of an individual: "There is one constant in the diversity of motives and their variation in the morphology of the Julia sets: the Mandelbrot set itself, which appears again and again in different sizes but always in the same form. One has to think of the genetic organisation in higher organisms: each cell contains the complete genome, the totality of all forms of expression, but at any point in the organism only a small selection actually is expressed."

Similar thoughts occurred to Adrien Douady,[116] an authority on the analysis of the Mandelbrot set: "We can think of the iteration process defined by the formula $z_{n+1}=z_n^2+c$ as an extraordinary efficient way to develop the information contained in the data (the value of c for a Julia set, and the window for a detail of the Mandelbrot set), acting as a key. This phenomenon of developing information is also striking in biology: a transcription of all the genetic DNA of a human being (or any vertebrate) would take a hundred pages or so. Compare this with a treatise on anatomy, to which you should add one on endocrinology and one on innate behaviour! Imagine scientists faced with the collections of Julia sets without knowing where they come from; would they not do just what zoologists did in the 19th century: define phyla, classes, orders and genera, give a description of the specific features attached to each term of classification, and so on? Let us be clear: I am not claiming that Julia sets can provide a model for any biological phenomenon, but they are a striking example of how a very simple dynamical system can develop the small information contained in a key, and produce various highly organized structures."

According to J. H. Hubbard, the Mandelbrot set is "the most complicated object in mathematics."[117] It can be defined as the set of all complex numbers of c for which the size of $z^2 + c$ is finite even after an indefinitely number of iterations. The mathematical feed-back cycle, described by words in the introductory part and defined by a formula in the Douady quotation ($z_{n+1}=z_n^2+c$; given a number z_0 take its square and add a constant c to get z_1; then repeat to get z_2, z_3, and so on), produces the Mandelbrot set when the complex number z is always made zero and different values of c are selected.

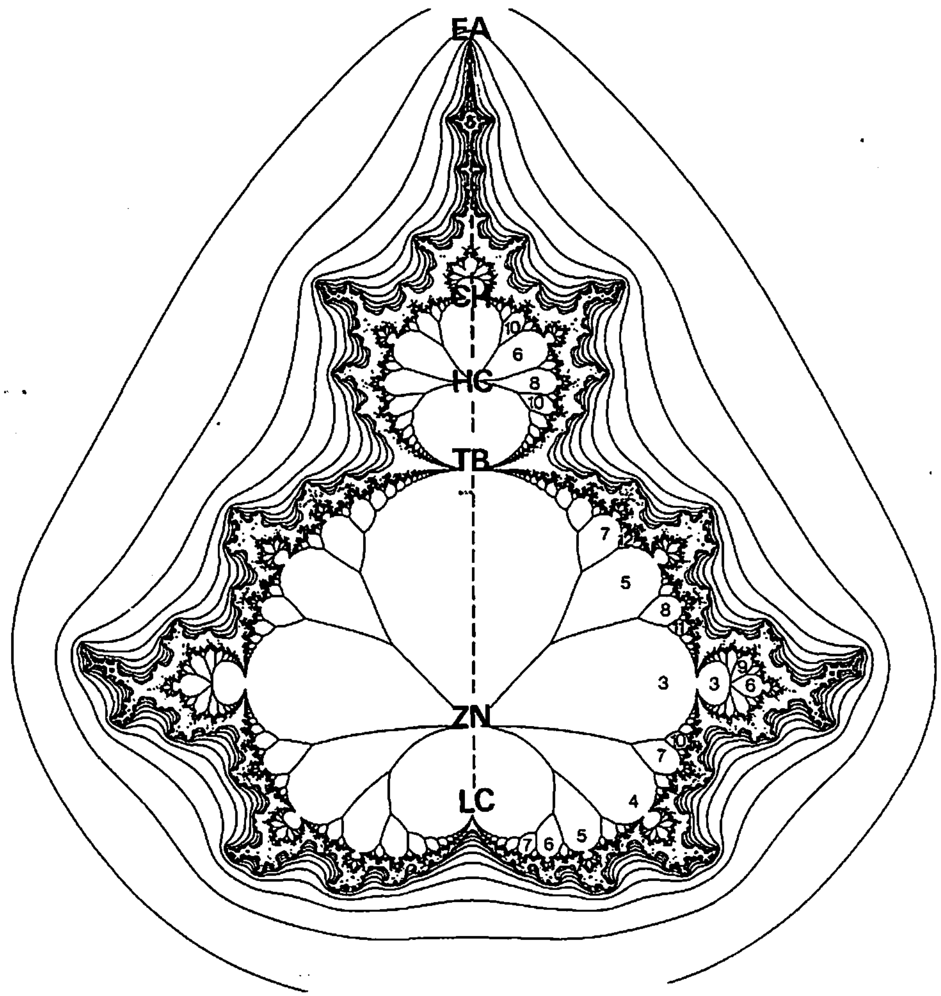

Figure 37: Representation of the Mandelbrot set after Peitgen and Richter. The impression that it rests on harmony, even better conveyed by Figure 4, is confirmed by rational analysis. It reflects in double version all known consonant intervals, the major perfect chord, and also the combination of the major and minor sixth 3 : 5 : 8 found in the supersecular torque- and sunspot cycle, as well as in tree ring widths and beach de-levelings. The intervals are measured along the "spine", marked by a dashed line, ranging from the libido centre (LC) to the end of antenna (EA). The zero navel (ZN), top of body (TB), head centre (HC) and crown of head (CH), are distributed such that respective intervals form all acknowledged harmonical proportions. The acronyms allude to Peitgen and Richter's "apple man anatomy" and might stimulate imagination beyond the number relationships involved.

Figure 4 is the result of such process. Julia sets are created when c remains fixed and z varies beginning with a special initial value z_0. Julia sets are legion; for each fixed value of c used in the iteration formula, a new and different Julia set develops. Here the control function of the Mandelbrot set comes in. The position of c in the complex plane relative to the Mandelbrot set M decides on the form of the Julia sets. They are connected structures if c is from within M, and broken into infinitely many pieces if c lies outside M. Most interesting is the boundary of M. When c crosses the boundary, associated Julia sets will be subject to an explosion that decomposes them into a cloud of points, called Fatou dust. This fractal dust gets thinner and thinner the farther c is from the Mandelbrot set M. Thus, crossing the boundary of M functions like a mathematical phase transition for Julia sets, as Peitgen and Richter[118] put it.

The reader should hold in mind that all these fascinating qualities emerge from simple feed-back cycles that can be found, too, in the relative motion of cosmic bodies in the solar system. Beyond the mathematical complexity of the Mandelbrot set its aesthetic appeal should not be forgotten. The mathematicians Philip J. Davis and Reuben Hersh[119] have stated: "Blindness to the aesthetic element in mathematics is widespread and can account for a feeling that mathematics is as dry as dust, as exciting as a telephone book, as remote as the laws of infangthief of fifteenth century Scotland. Contrariwise, appreciation of this element makes the subject live in a wonderful manner and burn as no other creation of the human mind seems to do."

This is the proper attitude to look at Figure 4 again. The picture, when looked at in a holistic way, conveys the impression of harmony and creativity. It could serve as a powerful emblem of these fundamental qualities. Even the self-collectedness and sitting posture of meditating man seems to be embodied in the pictorial representation of M. This impression is deepened by the antenna above the "head" of the "apple man". It is seen on close inspection that it carries many little copies of the larger M. They sit there like pearls on a string, and further smaller ones sit between the larger ones, and so on and on forever. One relatively large miniature Mandelbrot on the antenna is visible in Figure 4. This productive abundance which contributes to the impression of creativity is not limited to the antenna. There is a wealth of sprouting miniature Mandelbrots everywhere; they grow out of the cardioid-shaped main body as well as out of the head disk and satellite disks. Buds give birth to buds that give birth to buds and so on without end. This image applies to the growth of ideas as well as to bodily propagation.

The pictorial impression that the Mandelbrot set rests on harmony is confirmed by rational analysis. As shown at the Sixth London Astrology Research Conference in 1987,[120] the proportions of the pictorial representation of the Mandelbrot set reflect all known consonant intervals, the major perfect chord, and also the combination of major and minor sixth 3 : 5 : 8 which has been found in the energy wave related to the supersecular sunspot cycle as well as in tree ring widths and beach de-levelings. The harmonic ratios of the intervals in question may be taken from Figure 37 after Peitgen and Richter.[121] Its original destination was to present results from some ongoing research on M. The numbers on the right of the plot are related to this research and may

be neglected in our context though they attest to the deep interest mathematicians have in bringing to light structures hidden in M.

The intervals are measured along the spine of the "apple man" that is marked in Figure 37 by a dashed line. This ranges from the cusp of the cardioid-shaped main body to the end point of the antenna. According to a theorem by A. Douady and J. H. Hubbard, the Mandelbrot set is connected, and the antenna, too, is contained in M.[122] The spine is no arbitrary choice. In the complex plane that the Mandelbrot set inhabits, the real part of complex numbers is represented by an axis of coordinates, a section of which is the spine. The origin of the complex plane is that point in Figure 37 where those fine lines in the main body intersect. This zero point, the natural centre of the cardioid-shaped main body, is marked by ZN (zero navel). This acronym alludes to the "apple man anatomy", as well as five others. Interestingly, ZN coincides with the Hara point of spiritual tradition in Japan.

The cusp below the zero point, designated by LC (libido centre), is at the point 0.25 on the real part axis. In the large disc, tangent to the cardioid body, the fine lines, a result of mathematical analysis as well as those in the main body, intersect at the centre HC (head centre) at the point – 1 on the axis designating the real parts. The points TB (top of body) at – 0.75 and CH (crown of head) at – 1.25 designate boundary positions the structural importance of which is evident. EA (end of antenna) indicates the upper point reached by the representation of the Mandelbrot set in Figure 4. The overall distance LC – EA is 2.25. Unity on the real part axis is equal to ZN – HC, the interval that separates head centre and zero navel. LC – TB, the height of the main body, too, is equal to 1. The third distance that is equal to unity is HC – EA, the interval that separates head centre and end of antenna. All of the three distances LC – ZN, TB – HC, and HC – CH are equal to 0.25, and both ZN – TB and CH – EA equal three times 0.25. Thus, it is no surprise that the "apple man's" proportions, measured along the spine, show a wealth of consonant intervals and harmonies:

Octave (1 : 2)	→	(TB1 – CH)	:	(LC – TB)	and	(HC – EA)	:	(ZN – EA)
Fifth (2 : 3)	→	(TB – CH)	:	(ZN – TB)	and	(TB – CH)	:	(CH – EA)
Fourth (3 : 4)	→	(ZN – TB)	:	(LC – TB)	and	(ZN – TB)	:	(ZN – HC)
Major third (4 : 5)	→	(LC – TB)	:	(LC – HC)	and	(HC – EA)	:	(LC – HC)
Minor third (5 : 6)	→	(ZN – CH)	:	(LC – CH)	and	(LC – HC)	:	(LC – CH)
Major sixth (3 : 5)	→	(ZN – TB)	:	(ZN – CH)	and	(CH – EA)	:	(TB – EA)
Minor sixth (5 : 8)	→	(ZN – CH)	:	(ZN – EA)	and	(TB – EA)	:	(ZN – EA)

There are always at least two forms of the respective interval that visually, too, make sense and appeal to imagination. The first realisation of the octave, for instance, relates the height of the "head" to that of the main body. The reader may delve into these appealing relationships by himself with the aid of Figure 37. The most harmonious chord is also present in two forms:

Major perfect chord (4 : 5 : 6) → (LC – TB) : (LC – HC) : (LC – CH)
(ZN – HC) : (ZN – CH) : (LC – CH)

The visualisation of these proportions again yields intriguing relationships that stimulate imagination. The best way to tune in, however, is to listen to the major perfect chord struck on a monochord or another instrument. The combination of the major and minor sixth is, as announced above, also related to the proportions of the "apple man":

$$3:5:8 \rightarrow \quad (ZN-TB):(ZN-CH):(ZN-EA)$$

This is all the more important as the Mandelbrot set is no arbitrary invention of the human mind, but a structure found in Nature, as the physicist and mathematician Gert Eilenberger[123] put it: "It is not our sensory and perceptual activity that forces Nature into a strait-jacket of mathematics, it is Nature, which, in the process of our evolutionary development, has impressed mathematics into our reason as a real, existing structure, inherent to herself. Less abstractly: the ape, from which we are descended, had to have a very accurate idea of the geometry of space actually existing if he were not to fall out of his tree and break his neck. Similarly, one can argue that the evolution of our abilities for abstraction and manipulation of logical symbols must be oriented on actually existent structures in the real world."

The Mandelbrot set, seen as a pre-image, embraces a wide range of phenomena that seem to be the common morphological root of most diverse processes in microcosmos and macrocosmos: control of the growth of highly organized structures by the development of relatively simple key information; realization of consonances, resonances, and harmony in accordance with balanced harmonious proportions inherent in the set; expression of primordial cyclic functions that create polar tension and instability and conditions favourable to creativity in boundary regions between the realms of attractors of different quality. The most fundamental morphological features, however, seem to be those feed-back cycles that create polarities, conditions of instability and creativity, Mandelbrot- and Julia sets, and that mesh of harmonically interwoven oscillations which connects the revolutions of the giant planets with the Sun's irregular swing about the centre of mass, the Sun's rotation, secular and supersecular sunspot cycles, energetic solar eruptions, geomagnetic storms, climatic change, rainfall and temperature, abundance in wildlife, economic cycles, and human creativity.

Thus, our new multidisciplinary approach, together based on wide astrological views and on recent scientific knowledge from so diverse fields as mathematics, astronomy, geophysics, climatology, meteorology, biology, economy, and psychology, has yielded unexpected holistic results that confirm in detail the unity of the universe which is generally proven by the violation of Bell's inequality. As Peitgen and Richter[124] aptly say: "It is no longer sufficient to discover basic laws and understand how the world works "in principle". It becomes more and more important to figure out the patterns through which these principles show themselves in reality. More than just fundamental laws are operating in what actually is."

TABLE

Epochs of JU-CM-CS events 1800 – 2000:1998.56

(g)	22	July	1998	1998.56	(c)	20	April	1990	1990.30
(g)	31	Oct.	1982	1982.83	(c)	24	June	1974	1974.48
(g)	9	Jan.	1970	1970.02	(c)	20	Oct.	1967	1967.80
(g)	13	Aug.	1959	1959.62	(c)	16	May	1951	1951.37
(g)	15	April	1942	1942.29	(c)	1	May	1930	1930.33
(g)	25	Oct.	1920	1920.82	(c)	18	Jan.	1912	1912.05
(g)	8	Oct.	1901	1901.77	(c)	2	March	1891	1891.17
(g)	20	Nov.	1881	1881.89	(c)	11	April	1873	1873.28
(g)	16	March	1859	1859.21	(c)	26	Nov.	1850	1850.90
(g)	5	March	1843	1843.18	(c)	22	Nov.	1834	1834.89
(g)	9	Sept.	1819	1819.69	(c)	3	June	1811	1811.42
(g)	14	Sept.	1803	1803.70					

Epochs of second harmonics of JU-CM-CS cycles:

1994.43	1986.57	1978.66	1972.25
1968.91	1963.71	1955.50	1946.83
1936.31	1925.58	1916.44	1906.91
1896.47	1886.53	1877.59	1866.25
1855.06	1847.04	1839.04	1827.29
1815.56	1807.56		

REFERENCES

1) Einstein, Podolsky, and Rosen (1935); Bell (1965; 1976); d' Espagnat (1979); Jammer (1980); Aspect *et al.* (1981); Zukav (1979); Selleri (1984); Krueger (1984); Gardner (1986) (*See Glossary*)
2) d'Espagnat (1979) p.140; Stapp (1975; 1977; 1979); Sarfatti (1977); Selleri (1984) pp. 139, 140 (*See Glossary*)
3) Landscheidt (1987 b)
4) Aspect *et al.* (1981); Freedman and Clauser (1972); Bruno *et al.* (1977); Bertolini *et al.* (1981); Jammer (1980) p. 516; d'Espagnat (1979) pp. 136, 137
5) Gingerich (1982) p. 124
6) Brewster (1855) Vol. 2, pp. 371, 372
7) Rattensi (1972)
8) Jantsch (1984) pp 34–36
9) Prigogine *et al.* (1983); Glansdorff and Prigogine (1971)
10) Hofstadter (1979) p. 27
11) Peitgen and Richter (1986) p. 84
12) Peitgen and Richter (1986) p. 10
13) Colour picture of the Mandelbrot set created by Peitgen and Richter; a black and white version is to be found in Peitgen and Richter (1986) p. 78
14) Poincaré (1889); Poincaré (1892) Vol. 1, p.253 and Chapter V, entitled "Nonexistence of Uniform Integrals"; see also Ekeland (1984)
15) Haken (1978) Preface to the First Edition
16) Krueger (1984) p. 144
17) Landscheidt (1976; 1980; 1981 a; 1981 b; 1983; 1984 a; 1984 b; 1984 c; 1984 d; 1986 a; 1986 b; 1986 c; 1987 a; 1987 c; 1988)
18) Dewey (1973) p. 25
19) Haken (1981) p. 127
20) Dewey (1973) p. 27
21) McLeod (1985) p. 4599
22) Dewey (1973) p. 95
23) Dewey (1973) p. 119
23a) The forecast of the top turning point 1987.3 and the bottom epoch 1990 in the course of international stock prices was first published January 9, 1986, in a lecture presented at the astronomical Olbers-Gesellschaft, Bremen: Zyklen solarer Energieausbrüche: Entdeckung, irdische Auswirkungen, Vorhersage
24) Dewey (1973) p. 71
25) Williams *et al.* (1985); Williams (1986)
25a) Eysenck (1981) pp. 11–14
26) Dean (1986) p. 170
26a) Correlation (1981) p. 3
27) Landscheidt (1976; 1980; 1981 a; 1981 b; 1983; 1984 a; 1984 b; 1984 c; 1984 d; 1986 a; 1986 b; 1986 c; 1987 a; 1987 c; 1988)
28) Dean (1977) p. 508
29) Dean (1983)
30) Woehl *et al.* (1986)
31) Woehl (1986) p. 585
32) Recely *et al.* (1984)
33) EOS (1986) p. 537
34) Landscheidt (1984 b) pp. 105–114
35) Landscheidt (1987 b) pp. 113–118
36) Burton *et al.* (1973)
36a) Armstrong *et al.* (1983) p. 75

37) Landscheidt (1986 c) p. 195; Kreplin *et al.* (1977)
38) Mayaud (1973); Mayaud *et al.* (1977)
39) Krishna (1967)
40) Bucke (1969) pp. 332, 351
41) Kollerstrom (1986)
42) Personal communication by Suitbert Ertel
42a) Seymour (1986) pp. 2–3, 10–13
43) Koestler (1967) pp. 216, 217
44) Segrè (1984) p. 190
45) von Klitzing (1985); Halperin (1986)
46) Landscheidt (1984 a; 1986 c)
47) Blackman and Tukey (1959)
48) Mitchell (1966)
49) Panofsky and Brier (1958)
50) Burg (1968, 1972, 1975)
51) Junk (1982) p. 39
52) Stuart *et al.* (1971)
53) Cajori (1934)
54) Zehnder (1923)
55) Jose (1965)
56) Landscheidt (1976; 1980; 1981 a; 1981 b; 1983; 1984 a; 1984 b; 1984 c; 1984 d; 1986 a; 1986 b; 1986 c; 1986 d; 1987 a; 1987 c; 1988)
57) Landscheidt (1981 a) p. 8; (1983) p. 294
58) Blizard (1982) p. 896
59) Brier (1979)
60) Landscheidt (1983) p. 298
61) Gleissberg (1975)
62) Gleissberg (1958)
63) Landscheidt (1983) p. 302
64) Landscheidt (1983) p. 304
65) Landscheidt (1986 b) pp. 54–56
66) Landscheidt (1984 c) p. 28; (1986 a) p. 83
67) Landscheidt (1984 c) p. 29; (1986 a) pp. 83–85
68) Oepik (1972)
69) Blizard (1965); Švestka (1968); Landscheidt (1983; 1984 a; 1984 b; 1984 c; 1986 a; 1988)
70) Landscheidt (1976) pp. 12–13
71) Eddy *et al.* (1977)
72) Howard (1975)
73) Dicke (1964)
74) Howard (1984); Howard *et al.* (1983)
75) Feynman *et al.* (1966) pp. 50-4
76) Warrain (1942) p. 79; Haase (1976) pp. 38, 39
77) Bucha (1983) p. 21
78) Gosling *et al.* (1977)
79) Sazonov (1965)
80) Mustel (1966)
81) Beynon and Winstanley (1969)
82) Stolov and Shapiro (1974)
83) Sidorenkov (1974)
84) Cobb (1967)
85) Mustel (1977)
86) King (1974)
87) Roberts and Olson (1973)

88) Prohaska and Willett (1983)
89) Sazonov (1974)
90) King (1974)
91) Neubauer (1983)
92) Schneider and Mass (1975)
93) Landscheidt (1987 c)
94) Wilcox (1975)
95) EOS (1985) p. 441
96) Mayaud (1977) p. 102
97) Reiter (1983)
98) Duetsch (1974). Figure 29 was adapted from a plot by H. U. Duetsch. Eidgenoessische Technische Hochschule, Zuerich, in Rowland (1978)
99) Baur (1975)
100) Lamb (1977) pp. 621–625
101) Lamb (1977) pp. 625–628
102) Lamb (1977) p. 631
103) Mooley and Parthasarathy (1984)
104) Lamb (1977) pp. 580–581
105) Baur (1975)
106) Manley (1974) pp. 389–405; Lamb (1977) pp. 574–576
107) Thesleff (1977)
108) Zuckerkandl (1971) p. 64
109) Rameau (1971) p. XLI
110) Landscheidt (1983) pp. 300–303
111) Damon (1977); Eddy (1977) p. 67
112) Lamb (1982) p. 133
113) Fairbridge (1981) p. 134
114) Douady (1986) p. 161
115) Peitgen and Richter (1986) p. 17
116) Douady (1986) pp. 172, 173
117) Dewdney (1985) p. 12
118) Peitgen and Richter (1986) p. 12
119) Peitgen and Richter (1986) p. 21
120) Landscheidt (1987 a)
121) Peitgen and Richter (1986) p. 61
122) Peitgen and Richter (1986) p. 15; Douady (1986) p. 162
123) Eilenberger (1986) p. 178
124) Peitgen and Richter (1986) p. 1

Bibliography of quoted authors

Armstrong, T. P., Brungardt, C., and Meyer, J. E. (1983): Satellite Observations of Interplanetary and Polar Cap Solar Particle Fluxes from 1963 to the Present, in McCormac (1983) pp. 71 – 79.

Aspect, A., Grangier, P., and Roger, G. (1981): Experimental Test of Realistic Local Theories via Bell's Theorem, Phys. Rev. Lett. 47, 460.

Baur, F. (1975): Abweichungen der Monatsmittel der Temperatur Mitteleuropas und des Niederschlags in Deutschland, Beilage zur Berliner Wetterkarte des Instituts fuer Meteorologie der Freien Universitaet Berlin vom 24. 6. 1975.

Bell, J. S. (1965): Physics 1, 195.

Bell, J. S. (1976): Epistemological Letters (March 1976).

Bertolini, G., Diana, E., and Scotti, A. (1981): Nuovo Cim. 63 B, 651.

Beynon, W. J. G. and Winstanley, E. H. (1969): Geomagnetic Disturbance and the Troposphere, Nature 222, 1262 – 1263.

Blackman, R. B. and Tukey, J. W. (1959): The Measurement of Power Spectra, Dover Publications, New York.

Blizard, J. B. (1965): Predictions of Solar Flares Months in Advance, Astron. J. 70, 667.

Blizard, J. B. (1982): Solar Motion and Solar Activity, Bull. Am. Astron. Soc. 13, 896.

Brewster, D. (1855): Memoirs of the Life, Writings, and Discoveries of Sir Isaac Newton, Vol. 2, 371 – 372, Boston.

Brier, G. W. (1979): Use of Difference Equation Methods for Predicting Sunspot Numbers, in McCormac and Seliga (1979) pp. 209 – 214.

Bruno, M., d'Agostino, M., and Maroni, C. (1977): Nuovo Cim. 40 B, 142.

Bucha, V. (1983): Direct Relations between Solar Activity and Atmospheric Circulation, its Effect on Changes of Weather and Climate, Studia Geoph. et Geod. 27, 19 – 45.

Bucke, R. M. (1969): Cosmic Consciousness, Dutton, New York.

Bürg, J. P. (1968): A New Analysis Technique for Time Series Data, paper presented at NATO Advanced Institute for Signal Processing, Enschede.

Burg, J. P. (1972): The Relationship between Maximum Entropy and Maximum Likelihood Spectra, Geophysics 37, 375 –376.

Burg, J. P. (1975): Maximum Entropy Analysis, Ph.D. thesis, Stanford University, Palo Alto.

Burton, N., Hart, P., and Laughlin, J., eds. (1973) The Asian Journal of Thomas Merton, New York.

Cajori, F. (1934): Newton's Principia, University of California Press, San Francisco, Book III, Proposition XIII.

Cobb, W. E. (1967): Evidence of Solar Influence on the Atmosphere Electric Elements at Mauna Loa Observatory, Mon. Weather Rev. 95, 905 – 911.

Damon, P. E. (1977): Solar Induced Variations of Energetic Particles at One AU, in White (1977) pp. 429 – 445.

Dean, G. (1977): Recent Advances in Natal Astrology, Analogic, Subiaco.

Dean, G. (1983): Shortwave Radio Propagation: Non–Correlation with Planetary Positions, Correlation Vol. 3, No. 1, 4 – 36.

Dean, G. (1986): Does Astrology Need to Be True?, The Skeptical Inquirer 11, 166 – 184.

d'Espagnat, B. (1979): The Quantum Theory and Reality, Scient. American 241, 128 – 140.

Dewdney, A. K. (1985): A Computer Microscope Zooms in for a Look at the Most Complex Object in Mathematics, Scient. American 253, 8 – 12.

Dewey, E. R. (1973): Cycles, Manor Books, New York.

Dicke, R. H. (1964): The Sun's Rotation and Relativity, Nature, 202, 432 – 435.

Douady, A. (1986): Julia Sets and the Mandelbrot Set, in Peitgen and Richter (1986), pp. 161 – 173.

Drodzdov, O. A. and Vorob'eva, eds. (1974): General and Synoptic Climatology, Trudy, Vyp. 316, Leningrad, Glavnaja Geofiziceskaja Observatorija, pp. 35 – 42.

Duetsch, H. U. (1974): The Ozone Distribution in the Atmosphere, Can. J. Chem. 52, 1491 – 1504.

Eddy, J. A. (1977): Historical Evidence for the Existence of the Solar Cycle, in White (1977) pp. 51 – 71.

Eddy, J. A., Gilman, P. A., and Trotter, D. E. (1977): Anomalous Solar Rotation in the Early 17th Century, Science 198, 824 – 829.

Eilenberger, G. (1986): Freedom, Science, and Aesthetics, in Peitgen and Richter (1986) pp. 175 – 180.

Einstein, A., Podolsky, B., and Rosen, N. (1935): Can Quantum Mechanical Description of Reality be Considered Complete? Phys. Rev. 47, 777.

Ekeland, I. (1984): Le calcul, l'imprévu, Editions du Seuil, Paris.

EOS (1985): Transactions, American Geophysical Union.

EOS (1986): Transactions, American Geophysical Union.

Eysenck, H. (1981): The Importance of Methodology in Astrological Research, Correlation 1, 1, 11 – 14.

Fairbridge, R. W. (1981): Holocene Sea–Level Oscillations, in: Koenigsson, L. K. and Paabo, K., eds., In Florilegium Florinis Dedicatum, Striae 14, 131 – 139, Uppsala.

Feynman, R. P., Leighton, R. B., and Sands, M. (1966): The Feynman Lectures on Physics, Vol. 1, Addison–Wesley, Reading.

Freedman, S. J. and Clauser, J. F. (1972): Phys. Rev. Lett. 28, 938.

Gardner, M. (1986): The EPR Paradox and Rupert Sheldrake, The Skeptical Inquirer 11, 128 – 131.

Gingerich, O. (1982): The Galileo Affair, Scient. American 247, 118 – 128.

Glansdorff, P. and Prigogine, I. (1971): Thermodynamic Theory of Structure, Stability, and Fluctuations, New York.

Gleissberg, W. (1958) The 80–Year Sunspot Cycle, J. Brit. Astron. Ass. 68, 150.

Gleissberg, W. (1975) Gibt es in der Sonnenfleckenhaeufigkeit eine 179–jaehrige Wiederholungstendenz, Veroeffentlichungen des Astronomischen Instituts der Universitaet Frankfurt, No. 57.

Gosling, J. T., Asbridge, J. R., and Bame, S. J. (1977): An Unusual Aspect of Solar Wind Speed Variations during Solar Cycle 20, J. Geophys. Res. 82, 3311 – 3314.

Haase, R. (1976): Der messbare Einklang – Grundzuege einer empirischen Weltharmonik, Ernst Klett Verlag, Stuttgart.

Haken, H. (1978): Synergetics, Springer Verlag, Berlin, Heidelberg, New York.

Haken, H. (1981): Erfolgsgeheimnisse der Natur, Deutsche Verlagsanstalt, Stuttgart.

Halperin, B. I. (1986): The Quantized Hall Effect, Scient. American 254, 40 – 47.

Hofstadter, D. R. (1979): Goedel, Escher, Bach: an Eternal Golden Braid, Basic Books, New York.

Howard, R. (1975): The Rotation of the Sun, Scient. American 232, 106 – 114.

Howard, R. (1984): Solar Rotation, Ann. Rev. Astron. Astrophys. 22, 131 – 155.

Howard, R., Adkins, J. M., Boyden, T. A., Cragg, T. A., Gregory, T. S., LaBonte B. J., Padilla, S. P., and Webster, L. (1983): Solar Rotation Results at Mount Wilson, Solar Physics, 321 – 338.

Jammer, M. (1980): Le paradoxe d'Einstein–Podolsky–Rosen, La Recherche 11, 510 – 519.

Jantsch, E. (1984): Die Selbstorganisation des Universums, Deutscher Taschenbuch Verlag, Carl Hanser Verlag, Muenchen. Edition in English: The Self–Organizing Universe, New York 1980.

Jose, P. D. (1965): Sun's Motion and Sunspots, Astron. J. 70, 193 – 200.

Junk, H. P. (1982): Die Maximum–Entropie–Spektral–Analyse (MESA) und ihre Anwendung auf meteorologische Zeitreihen, Diplomarbeit des meteorologischen Instituts der Universitaet Bonn.

King, J. W. (1974): Weather and the Earth's Magnetic Field, Nature 247, 131 – 134.

Koestler, A. (1967): The Act of Creation, Laurel Edition, New York.

Kollerstrom, N. (1986): The Eureka Moment, paper presented at the 5th International Astrological Research Conference, London, November 22 – 23, 1986.

Kreplin, R. W., Dere, K. P., Horan, D. M., and Meekins, J. F (1977): The Solar Spectrum Below 10 Å, in White (1977) pp. 287 – 312.

Krishna, G. (1967): Kundalini, The Evolutionary Energy in Man, Ramadhar and Hopman, New Delhi and Zuerich.

Krueger, F. R. (1984): Physik und Evolution, Verlag Paul Parey, Berlin and Hamburg.

Lamb, H. H. (1977): Climate Present, Past, and Future, Vol. 2: Climatic History and the Future, Methuen, London.

Lamb, H. H. (1982): Climate History and the Modern World, Methuen, London and New York.

Landscheidt, T. (1976): Beziehungen zwischen der Sonnenaktivitaet und dem Massenzentrum des Sonnensystems, Nachrichten der Olbers–Gesellschaft 100, 2 – 19.

Landscheidt, T. (1980): Saekularer Tiefpunkt der Sonnenaktivitaet, Ursache einer Kaelteperiode um das Jahr 2000?, Jahrb. d. Wittheit zu Bremen 24, 189 – 220.

Landscheidt, T. (1981 a): Swinging Sun, 79–Year Cycle, and Climatic Change, J. interdisc. Cycle Res. 12, 3 – 19.

Landscheidt, T. (1981 b): Long Range Prediction of Energetic Solar Eruptions and their Terrestrial Effects, paper presented at the Second International Astrological Research Conference, London, November 28 – 29, 1981 (Correlation 1, 2, 3).

Landscheidt, T. (1983): Solar Oscillations, Sunspot Cycles, and Climatic Change, in McCormac (1983) pp. 293 – 308.

Landscheidt, T. (1984 a): Cycles of Solar Flares and Weather, in Moerner and Karlèn (1984) pp. 473 – 481.

Landscheidt, T. (1984 b): Funktionen kosmischer Organismen: Schwingungen der Sonne und irdische Resonanzen, in Resch (1984) pp. 37 – 130.

Landscheidt, T. (1984 c): Prediction of Energetic Solar Eruptions and their Terrestrial Effects by Constellations of Planets, Astrology'84, The National Astrological Society, New York, pp. 25 – 35.

Landscheidt, T. (1984 d): Decipherment of the Rosetta Stone of Planetary Functions in the Solar System, paper presented at the 4th International Astrological Research Conference, London, October 27 – 28, 1984.

Landscheidt, T. (1986 a): Long Range Forecast of Energetic X-Ray Bursts Based on Cycles of Flares, in Simon, Heckman, and Shea (1986) pp. 81 – 89.

Landscheidt, T. (1986 b): Long Range Forecast of Sunspot Cycles, in Simon, Heckman, and Shea (1986) pp. 48 – 57.

Landscheidt, T. (1986 c): Cyclic Distribution of Energetic X–Ray Flares, Solar Physics 107, 195 – 199.

Landscheidt, T. (1986 d): Modulation of the Sun's Rotation, Energetic Solar Eruptions, Geomagnetic Storms, Weather, Abundance of Wild Life, and Economic Cycles by Conjunctions of Sun, Jupiter, and the Center of Mass of the Solar System, paper presented at the 5th International Astrological Research Conference, London, November 22 – 23, 1986.

Landscheidt, T. (1987 a): Foundations of Astrology in the Third Millenium, paper presented at the 6th International Astrological Research Conference, London, November 20 – 22, 1987.

Landscheidt, T. (1987 b): Wir sind Kinder des Lichts – Kosmisches Bewusstsein als Quelle der Lebensbejahung, Verlag Herder Freiburg, Basel, Wien.

Landscheidt, T. (1987c): Long Range Forecasts of Solar Cycles and Climatic Change, in Rampino, Sanders, Newman, and Koenigsson (1987) pp. 421 – 445.

Landscheidt, T. (1988): Solar Rotation, Impulses of the Torque in the Sun's Motion, and Climatic Variation, Climatic Change 12, 265–295.

Manley, G. (1974): Central England Temperatures, Monthly Means 1659 to 1973, Quart. J. Roy. Met. Soc. 100, 389 – 405.

Mayaud, P. N. (1973): A Hundred Year Series of Geomagnetic Data 1868 – 1967, IAGA Bulletin No. 33, IUGG Publication Office, Paris.

Mayaud, P. N. and Romana A. (1977): Supplementary Geomagnetic Data 1957 – 1975, IAGA Bulletin No. 39, IUGG Publication Office, Paris.

McCormac, B. M., ed. (1983): Weather and Climate Responses to Solar Variations, Colorado Associated University Press, Boulder, Colorado.

McCormac, B. M. and Seliga, T. A., eds. (1979): Solar–Terrestrial Influences on Weather and Climate, Reidel, Dordrecht, Boston, London.

Moerner, N. A. and Karlèn, W., eds. (1984): Climatic Changes on a Yearly to Millenial Basis, Reidel, Dordrecht, Boston, London.

McLeod, M. G. (1985): On the Geomagnetic Jerk of 1969, J. Geophys. Res. 90, 4597 – 4610.

Mitchell, J. M. (1966): Climatic Change, World Meteorolog. Org. Publ. No. 195, Geneva.

Mooley, D. A. and Parthasarathy, B. (1984): Fluctuations in All-India Summer Monsoon Rainfall 1871 – 1978, Climatic Change 6, 287 – 301.

Mustel, E. R. (1966): The Influence of Solar Activity on the Troposphere in the Polar Cap Regions, Soviet Astronomy – AJ 10, 288 – 294.

Mustel, E. R. (1977): Solar Activity and the Troposphere, Translation from Russian, available from NTIS, Springfield, VA 22151, 25 – 52.

Neubauer, L. (1983): The Sun–Weather Connection – Sudden Stratospheric Warmings Correlated with Sudden Commencements and Solar Proton Events, in McCormac (1983) pp. 395 – 397.

Oepik, E. (1972): Planetary Tides and Sunspots, Irish Astron. J. 10, 298.

Panofsky, H. A. and Brier, G. W. (1958): Some Applications of Statistics of Meteorology, The Pennsylvania State University, University Park, Pennsylvania.

Peitgen, H. O. and Richter, P. H. (1986): The Beauty of Fractals – Images of Complex Dynamical Systems, Springer Verlag Berlin, Heidelberg, New York, Tokyo.

Poincaré, H. (1889): Sur le problème des trois corps et les équations de la dynamique.

Poincaré, H. (1892): Méthodes nouvelles de la mécanique céleste, Vol. 1, Chapter 5, G. Villars, Paris, and Dover Publications, New York.

Prigogine, I. and Stengers, I. (1983): Dialog mit der Natur, Piper Verlag, Muenchen and Zuerich.

Prohaska, J. T. and Willett, H. C. (1983): Dominant Modes of Relationships between U.S. Temperature and Geomagnetic Activity, in McCormac (1983) pp. 489 – 494.

Rameau, J. P. (1971): Treatise on Harmony, Dover Publications, New York.

Rampino, M. R., Sanders, J. E., Newman, W. S., and Koenigsson, L. K., eds. (1987): Climate History, Periodicity, and Predictability, van Nostrand Reinhold Company, New York.

Rattensi, P. M. (1972): Science, Medicine, and Society in the Renaissance, London.

Recely, F. and Harvey, K. L. (1986): He I 10830 Observations of Flare Generated Coronal Holes, in Simon, Heckman, and Shea (1986) pp. 204 – 211.

Reiter, R. (1983): Modification of the Stratospheric Ozone Profile after Acute Solar Events, in McCormac (1983) pp. 95 – 116.

Resch, A., ed. (1984): Geheime Maechte, Resch Verlag Innsbruck.

Roberts, W. and Olson, R. H. (1973): J. atmos. Sci. 30, 135.

Rowland, F. S. (1978): Stratospheric Ozone – Earth's Fragile Shield, 1979 Yearbook of Science and the Future, Encyclopaedia Britannica, University of Chicago.

Sarfatti, J. (1977): The Case for Superluminal Information Transfer, MIT Technology Review, No. 5.

Sazonov, B. I. (1965): On the Solar–Troposphere Relation, Astron. Zhurnal 42, 653 – 655.

Sazonov, B. I. (1974): Circulation in the Troposphere and Anomaly in the Terrestrial Magnetic Field, in Drodzdov and Vorob'eva (1974) pp. 35 – 42.

Schneider, S. H. and Mass, C. (1975): Volcanic Dust, Sunspots, and Temperature Trends, Science 180, 741 – 746.

Segrè, E. (1984): Die grossen Physiker und ihre Entdeckungen, Piper Verlag, Muenchen, Zuerich.

Selleri, F. (1984): Die Debatte um die Quantentheorie, Verlag Vieweg, Braunschweig, Wiesbaden.

Seymour, P. A. H. (1986): A Causal Mechanism for Gauquelin's Planetary Effect, published by the author, Mannamead, Plymouth.

Sidorenkov, N. S. (1974): Solar Corpuscular Fluxes and Weather on Earth, Moscow Akademija Nauk, Priroda 3, 14 – 23.

Simon, P. A., Heckman, G., and Shea, M. A., eds. (1986): Solar–Terrestrial Predictions: Proceedings of a Workshop at Meudon, France, June 18 – 22, 1984, National Oceanic and Atmospheric Administration, Boulder, Colorado.

Stapp, H. P. (1975): Bell's Theorem and World Process, Nuovo Cimento, No. 29 B.

Stapp, H. P. (1977): Theory of Reality, Foundations of Physics 7, 317.

Stapp, H. P. (1979): Foundations of Physics 9, 1.

Stolov, H. L. and Shapiro, R. (1974): Investigation of the Responses of the General Circulation at 700 mb to Solar Geomagnetic Disturbance, J. Geophys. Res. 79, 2161 – 2170.

Stuart, W. F., Sherwood, V., and MacIntosh, S. M. (1971): Pure Appl. Geophys. 92, 150.

Švestka, Z. (1968): On Long–Term Forecasting of Proton Flares, Solar Physics 4, 18 – 29.

Thesleff, H. (1977): Pythagoreanism, Encyclopaedia Britannica, Macropaedia 15, 322 – 326.

von Klitzing, K. (1985): Mit Kurven im Kopf das Unerwartete gefunden, Bild der Wissenschaft No. 12, 124 – 134.

Warrain, F. (1942): Essai sur Harmonices mundi ou musique du monde de Johann Kepler, Vol. 2, Paris.

White, O. R., ed. (1977): The Solar Output and its Variation, Colorado Associated University Press, Boulder, Colorado.

Wilcox, J. M. (1975): Solar Activity and the Weather, J. Atmosph. Terr. Phys. 37, 237 – 256.

Williams, G. E. (1986): The Solar Cycle in Precambrian Time, Scient. American 255, 80 – 89.

Williams, G. E. and Sonett, C. P. (1985): Solar Signature in Sedimentary Cycles from the Late Precambrian Elatina Formation, Australia, Nature 318, 523 – 527.

Woehl, H. and Landscheidt, T. (1986): Solares Aktivitaetsminimum erst 1989/90?, Sterne und Weltraum 25, 584 – 585.

Zehnder, L. (1923): Die zyklische Sonnenbahn als Ursache der Sonnenfleckenperiode, Halle an der Saale.

Zuckerkandl, V. (1971): The Sense of Music, Princeton University Press, Princeton.

Zukav, G. (1979): The Dancing Wu Li Masters – An Overview of the New Physics, William Morrow, New York.

Glossary:

***am*:** Annual mean of Mayaud's index *aa* of geomagnetic activity.

Å: Unit of wavelength for electromagnetic radiation covering visible light and X-rays, named after the Swedish physicist A. J. Ångström: 10^{-10} m.

Angular acceleration: Time rate of change of the angular velocity, the angular displacement of an object or a vector.

Angular momentum: Property that characterizes the rotary motion of an object. The Earth has orbital angular momentum by reason of its annual revolution about the Sun and spin angular momentum because of its daily rotation on its axis. Angular momentum is a vector quantity that requires the specification of both a magnitude and a direction. This quantity measures the intensity of rotational motion and is equal to the product of the angular velocity of a rotating object and its moment of inertia with respect to the rotation axis.

Autocorrelation function: The plot of the autocorrelation coefficient as a function of different lags in a time series. The autocorrelation coefficient measures the correlation between successive data of the time series. The statistical autocorrelation analysis can be used as a means to detect cyclic features within a time series.

Bell's theorem: In 1964 John S. Bell showed mathetically that the tenets of theories based on separability impose a limit on the extent of correlation of a pait of distant particles (see Einstein-Rosen-Podolsky paradox). The limit is expressed in the form of an inequality that can be proved by means of the mathematical theory of sets. This Bell inequality constitutes a precise prediction of the outcome of an experiment on condition that Einstein separability is valid. The rules of quantum mechanics can be employed to predict the quantum results of the same experiment which differ by 40%. Actual experiments carried out from 1972 violate the Bell inequality based on the principle of separability. They precisely confirm the prediction of quantum mechanics, a comprehensive theory describing a universe governed by the principle of inseparability and nonlocality (for details see references 1–2, especially B. d'Espagnat, 1979: The Quantum Theory and Reality, Scient. American 241, 128–140).

Carrington rotation: R. C. Carrington, who is famous for his discovery that the Sun rotates faster at the equator than near the poles, defined the heliographic longitude of the central point of the solar disk. This longitude is measured from the solar meridian that passed through the ascending node of the solar equator on the ecliptic on January 1, 1854, at Greenwich mean noon. Carrington's zero meridian passed the ascending node 12 hours earlier. Carrington rotations are numbered in relation to these coordinates. No. 1 commenced on November 9, 1853. The dates of commencement of current rotation numbers are given in astronomical yearbooks and ephemerides.

C-conjunctions: JU-CM-CSc events.

Chi-square test: see Pearson-test.

CM: Center of mass of the solar system, also called barycentre. Forces external to the solar system produce an acceleration of this centre just as though the whole mass of Sun and planets were concentrated there. The Sun's position relative to CM depends practically on the masses and the varying distances and directions of the giant planets Jupiter, Saturn, Uranus, and Neptune; the effect of the inner planets and of Pluto's tiny mass is negligible. Constellations of the outer planets regulate the Sun's orbital motion about CM. The Sun's centre CS and CM nearly coincide when Jupiter is in opposition to Saturn, Uranus, and Neptune, whereas the two centres reach their greatest distance when all of the giant planets are conjunct. Most of the time CM is outside the Sun's body.

Cosine wave: A curve described by the equation $y = \cos x$, the ordinate being equal to the cosine of the abscissa. The cosine wave reaches its maximum at 0°, its minimum at 180° (π radians), and zero values at 90° ($\pi/2$ radians) and 270° ($3\pi/2$ radians).

Cross correlation function: Statistical analysis of the correlation of two time series involving lags as applied in autocorrelation analysis.

CS: The Sun's geometric centre.

dB: Decibel, a unit of power ratio, proportional to the common logarithm of the intensities of two sources.

Dobson unit: Unit measuring the level of ozone concentration in the atmosphere.

***dω/dt*-cycle:** 3.36-month cycle in energetic solar flares related to cyclic variations in the angular acceleration of the vector of the tidal forces of Venus, Earth, and Jupiter.

Einstein-Rosen-Podolsky paradox: Albert Einstein throughout his life remained dissatisfied with the probabilistic nature of the interpretations, generally given to quantum mechanics, which he thought incompatible with the locality principle, also called separability, inherent in his theory of relativity. In 1935 he and two young colleagues, Boris Podolsky and Nathan Rosen, devised a thought experiment, aimed to cast special doubt on quantum mechanics. They argued that this theory, based on nonlocality and inseparability, was incomplete because it does not explain how two particles, once related by interaction, can remain correlated over vast distances without being causally connected.

Filter coefficient: Determines the length of a prediction-error filter of the estimate of covariances in an autoregressive process related to informational entropy. It shows a vague resemblance to the function of lags in the autocorrelation function (Vide N. Andersen, On the calculation of filter coefficients for maximum entropy spectral analysis, Geophysics 39 (1974), 69 - 72).

Fisher-Behrens formula: This algorithm has to be applied in the t-test of the difference between means if the variance in the test groups shows a significant difference:

$$t = \frac{\bar{x}_1 - \bar{x}_2}{\sqrt{\frac{s_1^2}{n_1} + \frac{s_2^2}{n_2}}}$$

The number of the degrees of freedom (df) results from:

$$df = \frac{\left(\frac{s_1^2}{n_1} + \frac{s_2^2}{n_2}\right)^2}{\frac{\left(\frac{s_1^2}{n_1}\right)^2}{n_1+1} + \frac{\left(\frac{s_2^2}{n_2}\right)^2}{n_2+1}} - 2$$

Forbush decrease: A decrease in the level of galactic cosmic ray reception on Earth caused by major solar flares.

Gaussian low pass filter: A special techniqûe of data smoothing related to the Gaussian distribution (Vide H. A. Panofsky and G. W. Brier, Some applications of statistics to meteorology, Pennsylvania State University, University Park, 1958).

G-conjunctions: JU-CM-CSg events.

Gleissberg-cycle: Secular cycle of sunspot activity that exhibits an average periodicity of about 80 years.

IOT: Impulse of the torque in the Sun's orbital motion about the centre of mass CM of the planetary system. The intensity of IOT is measured by the change in angular momentum effected by the impulse. This is why IOT are also called time integral of the torque. Strong IOT are initiated by JU-CM-CS events that occur when the centre of mass CM, the Sun's centre CS, and Jupiter are in line.

IUWDS: International Ursigram and World Days Service founded in 1962 by the International Astronomical Union (IAU), the Union Radio Scientifique Internationale (URSI), and the International Union of Geodesy and Geophysics (IUGG). Ursigrams spread diverse solar-terrestrial data gathered by more than 140 institutes all over the world.

JU-CM-CS: Heliocentric constellation that is formed when the centre of mass of the solar system (CM), the Sun's centre (CS), and the planet Jupiter are in line. JU-CM-CS events initiate impulses of the torque (IOT) in the Sun's orbital motion about CM that release energetic solar eruptions and connected terrestrial events.

JU-CM-CSc: JU-CM-CS event that is accompanied with a sharp increase in orbital angular momentum and centrifugal motion of the Sun away from CM.

JU-CM-CSg: JU-CM-CS event that goes along with a steep decrease in orbital angular momentum and centripetal motion of the Sun toward CM due to prevailing gravitation.

Major instability event: The centre of mass of the solar system keeps staying in or near the Sun's surface for several years; a phase of instability in solar activity and its terrestrial response ensues from this solar system constellation.

Markov type persistence: Distribution of data that reflects the pattern of a Markov chain, named after the Russian mathematician A. A. Markov. Markov chains appear in sequences of random events in which the probability of each event depends on the distribution of previous data.

Maunder Minimum: A period of very weak sunspot activity in the 17th century that seems to be connected with the climatic period of the so-called Little Ice Age.

MEM: Maximum entropy method of spectral variance analysis which shows much higher resolution than earlier methods, especially at lower frequencies. It is based on the density of informational entropy related to the autocovariance function of a time series.

MeV: Million electron-volt.

Minor instability event: Term that points to the boundary quality of JU-CM-CS events.

Orbital momentum: Angular momentum of the Sun's motion about CM.

Pearson-test: Chi-square test for the significance of the deviation of observed frequencies from expected frequencies.

Pi radians: Phase angle of 180° expressed in radians.

Pi/2 radians: Phase angle of 90° expressed in radians.

Polar cap absorption (PCA): An ionospheric phenomenon evidenced by enhanced absorption of radio waves in the polar regions. PCA are released by solar proton events.

Proton event: A sudden increase in the number of solar protons of very high energy detected at the Earth after an energetic solar eruption.

Radiosonde flights: Sounding balloon which ascends to high altitudes, carrying meteorological equipment which modulates radio signals transmitted back to equipment on Earth.

Running variance: The well-known smoothing technique of running means over two, three, or more consecutive readings with equal or different weights is applied to variance, the square of the standard deviation.

Secular cycle of sunspot activity: Vide Gleissberg-cycle.

Secular torque cycle: Torque cycle in the Sun's motion about CM that is related to the secular sunspot cycle.

Spectral analysis: Statistical methods (Fourier analysis, autocorrelation function, cross correlation function, power spectrum, maximum entropy spectrum) for disclosing cyclic patterns in time series of data. The results of such analysis are presented in the form of spectra in the frequency or time domain.

Spectral peak: Peak in a spectrum resulting from spectral analysis that points to the frequency or the period of a cycle hidden in the data.

Supersecular sunspot cycle: Cycle of sunspot activity that exhibits an average periodicity of about 400 years.

Tidal cycle: Vide *dω/dt*-cycle.

Torque: Torque bears the same relationship to rotation as force does to linear movement. It could be called "rotary force" because it is the tendency of a force to rotate the body to which it is applied about a point or an axis. Torque produces rotation or revolution the effectiveness of which is measured by the vector product of the force and the perpendicular distance from the line of action of the force to the axis of rotation. The time rate of change of the angular momentum of a rotating body is equal to the torque of the force applied to it.

Torque cycles: Quasi cycles of different periods that are related to impulses of the torque (IOT) in the Sun's revolution about the centre of mass of the solar system (CM).

***t*-test:** Student's test of the significance of experimental data.

Variance: Average of the squares of the deviations of a number of observations of a quantity from their mean value.

***X*-ray bursts:** Flare-generated emission of energetic *X*-rays. The *X*-ray classification of solar flares is a better index of the geophysical significance of flares than the older optical groups of importance 1 to 4.

INDEX

SUN-EARTH-MAN

The world's climate

Stock market movements

Ozone levels

Moments of mystical insights

Periods of creative inspiration

all these phenomena and many more, are shown by Dr. Landscheidt's meticulous research to move in tune with the planetary harmonies of our solar system. His findings, supported by his successful forecasts, will be of deep interest both to the layman and to anthropologists, astrologers, biologists, ecologists, economists, historians, meteorologists, psychologists, sociologists and indeed students in almost every area of study.

Dr Theodor Landscheidt, Director of the Schroeter Institute for Research in Cycles of Solar Activity, is a modern Kepler, a rare combination of scientist and mystic who is equally at home in pure research and in Pythagorean speculation. He recently retired from his post as a West German High Court judge in order to continue his research on a full-time basis.

(A fuller account of Dr. Landscheidt's life and work is given in the book)

ISBN 1-871989-00-0